FACULDADE DE ENGENHARIA DA UNIVERSIDADE DO PORTO

Cutting tool for forest vegetation applicable to robots

Ricardo Gomes de Carvalho

Master's Degree in Mechanical Engineering

Supervisor: Doctor Eng. Filipe Baptista Neves dos Santos

Second Supervisor: Professor António Torres Marques

Porto, 2023

© Ricardo Gomes de Carvalho, 2023

Cutting tool for forest vegetation applicable to robots

Ricardo Gomes de Carvalho

Master's Degree in Mechanical Engineering

Porto, 2023

Abstract

There is an ever growing concern with the Portuguese Forest, due to its high value. Forest fires lead do the destruction of natural resources and have plagued Portugal for many years, with fires like in Pedrogão Grande wasting land, houses and killing people. One of the ways of preventing wildfires and its spread comes from preventive silviculture, the act of cutting the overgrowth of the forest that could cause its spread. It is natural that there are solutions being developed in order to automate such tasks.

By combining the above mentioned reasons with the ever growing technological progress being made, one such solution is being developed by the Robotics and IoT Laboratory for Agriculture and Forest for Intelligent Precision at INESC TEC. The presented dissertation is done to create a cutting tool for a forest robot like the one being developed.

In present days most of the work is done by motorized hand tools, like brush cutters or chainsaws, or heavy machinery, like agricultural vehicles adapted for forest use. While there are already some solutions regarding remotely operated machines, which can reduce the amount of workers and reduce work-related injuries, robot solutions for different forestry can still be considered scarce.

A mechanical project for a cutting tool was made based on circular disks rotating with free rotating blades at the edges of it, together with a supporting structure donned of a height regulating mechanism. The necessary components were designed or chosen, dimensioned and its assembly was made on a CAD software. A material selection was made in important components. Cost analysis and validations regarding critical components were made.

Resumo

Existe uma preocupação cada vez maior com a Floresta Portuguesa devido ao seu alto valor económico e social. Os incêndios florestais levam à destruição de recursos naturais e têm assolado Portugal por muitos anos, com incêndios como o de Pedrogão Grande causando a perda de terras, casas e vidas humanas. Uma das formas de prevenir incêndios florestais e a sua propagação vem da silvicultura preventiva, o ato de cortar o crescimento excessivo da floresta que pode contribuir para a sua propagação. É então natural que estejam a ser desenvolvidas soluções para automatizar estas tarefas.

Ao combinar as razões mencionadas acima com o progresso tecnológico em constante crescimento, uma dessas soluções está a ser desenvolvida pelo Laboratório de Robótica e IoT para Agricultura e Floresta Inteligente do INESC TEC. A dissertação apresentada tem como objetivo criar uma ferramenta de corte para um robô florestal como o está em desenvolvimento.

Hoje em dia, a maior parte do trabalho é feito por ferramentas motorizadas manuais, como motorroçadoras ou motosseras, ou por maquinaria pesada adaptada da agricultura. Já existem algumas soluções relacionadas com máquinas operadas remotamente, que podem reduzir a quantidade de trabalhadores e diminuir acidentes de trabalho. Também já existem algumas soluções robóticas em diferentes situações florestais, embora ainda sejam escassas.

Um projeto mecânico para uma ferramenta de corte foi desenvolvido com base em discos rotativos com lâminas dotadas de um grau de liberade montadas na sua extremidade. Os componentes necessários foram projetados ou escolhidos, dimensionados e sua montagem foi realizada num software de CAD. Uma seleção de materiais foi feita em componentes importantes. Foi feita uma análise de custos assim como validação de partes críticas.

Aknowledgement

First and foremost, I would like to show my appreciation for the Faculty of Engineering for all the moments that it offered me throughout these five years of my academic journey. As everything in life, there were joyous moments and less than great moments while studying in this prestigious institution, however all of those experiences molded myself into a greater person, able to tackle everything in life with a smile on my face and an attitude to never give up.

A genuine thank you to my supervisors, Doctor Filipe Santos and Professor António Torres Marques, for their ever concern on the development of this dissertation and all the support given throughout this thesis. A sincere thank you to Engineer Humberto Rocha from INESC TEC as well for his eagerness to help in all aspects of the thesis, always being available to give his opinion and for his unwavering support to help me create something to be proud of.

To all the teachers who accompanied my growth as a person, all while teaching me the ways to be a proper engineer. Your teachings reached me and your dedication to provide students with the tools they need to either enter the job market or pursue an academic career set an example that I hope to carry throughout my life. I hope that if I ever am in the same situation I can convey all these teachings to the younger generation.

A big thank you is not enough to show one's gratitude to every individual I came across during my passage in Engineering and had the gratefulness to call friends. This journey that a person is living would a completely different, sad and monotonous adventure were you not there to help me when I was down, to cheer when everything was fine and to be one of the most important pillars in my life. Whether these friendships came about during studious ventures, academic traditions or in the student's association, older or younger, a special place in my heart is reserved for you.

To my parents, my source of drive to be someone in life and make them proud, for being the pillars that supported me throughout my whole life and for never giving up on me, there are no words of appreciation to demonstrate it. Thank you.

Lastly, to my grandparents for which, even though not all are around anymore, they always believed in me and made sure that nothing was ever missing from my life. I just wish you were here to witness what I did.

My deepest gratitude to everyone.

Ricardo Carvalho

"Don't be afraid of going slow, just be afraid of stopping/standing still."

Chinese Proverb

Contents

Abstract i

Resumo iii

1 Introduction 1
- 1.1 Current Context . . . 1
  - 1.1.1 Portuguese Forest . . . 1
  - 1.1.2 The use of a robot . . . 5
- 1.2 Goals of the Dissertation . . . 5
- 1.3 Structure of the Dissertation . . . 5

2 Bibliographic Review 6
- 2.1 Preventive Silviculture and Forestry . . . 6
- 2.2 Commercial Solutions . . . 7
- 2.3 Forest Robots . . . 9
  - 2.3.1 MowIT . . . 10
- 2.4 Cutting Solutions . . . 11
  - 2.4.1 Motorized Mechanical Machines . . . 11
  - 2.4.2 Cutting Solutions on Commercial Solutions and Forest Robots . . . 13
- 2.5 Material Selection and Product Design . . . 14

3 Mechanical Design 17
- 3.1 Introduction . . . 17
- 3.2 Requirements . . . 17
- 3.3 Subsystems and their Interactions . . . 18
- 3.4 Cutting Solution . . . 19
  - 3.4.1 Design Inspiration . . . 19
  - 3.4.2 Layout and Considerations . . . 22
  - 3.4.3 Blade Design . . . 22
  - 3.4.4 Blade Material Selection . . . 24
  - 3.4.5 Shaft . . . 26
  - 3.4.6 Holding Disks . . . 27
  - 3.4.7 Subsystem Bolting . . . 29
  - 3.4.8 Bushing and Washers Material Selection . . . 30
  - 3.4.9 Cutting Subsystem Overview . . . 32
- 3.5 Motor Drive . . . 33
  - 3.5.1 Motor Selection . . . 33
  - 3.5.2 Motor Working Point . . . 34

3.5.3 Motor Drive Overview . . . 35
3.6 Mechanical Transmission . . . 35
3.6.1 Cutting Disposition . . . 36
3.6.2 Transmission . . . 38
3.6.3 Belt Drive . . . 38
3.6.4 Pulley Assembly . . . 40
3.6.5 Power Delivery Overview . . . 42
3.7 Supporting Structure . . . 43
3.7.1 Structural Inspiration . . . 43
3.7.2 Materials Chosen . . . 45
3.7.3 Enclosure . . . 45
3.7.4 Connection to Robot . . . 46
3.7.5 Lifting Mechanism . . . 53
3.7.6 Motor Plate . . . 55
3.7.7 Bearing Units . . . 57
3.7.8 Supporting Structure Overview . . . 60
3.8 Design Overview . . . 60

4 Design Validation **62**
4.1 Cutting Solution . . . 62
4.1.1 Number of Blades . . . 62
4.1.2 Rotating Blades Validation . . . 63
4.1.3 Shaft Fatigue . . . 64
4.2 Supporting Structure . . . 69
4.2.1 Bearing Unit . . . 69
4.2.2 Weight Validation . . . 70
4.3 Cost of Production . . . 76
4.4 Specification Discussion . . . 77

5 Conclusion e Future Works **78**
5.1 Conclusion . . . 78
5.2 Future Works . . . 79

References **81**

A US20080307763A1 Patent **86**

B AISI 1045 Medium Carbon Steel **90**

C Granta EduPack Material Selection Charts **94**
C.1 Bushing and Washers' Material Selection . . . 94

D HPM3000B - High Power BLDC Motor **98**
D.1 HPM3000 (3KW) Motor Performance Curve (48V) . . . 98
D.2 HPM3000 (3KW) Motor Performance Data (48V) . . . 100

E Timing Belt **102**
E.1 Optibelt CAP 6.5 calculation . . . 102
E.2 Optibelt OMEGA HP Technical Sheet . . . 106

F Thomson Linear Electrak GX Actuator **108**

G SKF Y-bearing Unit **112**
G.1 SKF FYTB 20 TF specification 112
G.2 SKF ECY 204 specification 119

H Mechanical Drawing of the tool **123**
H.1 Cutting Tool 123
H.2 Cutting Solution 140

I Cost Analysis **148**

List of Figures

1.1 Distribution of total areas by forest species in Mainland Portugal in 2015 [2] . . . 1
1.2 A Cork Oak tree [5] . . . 2
1.3 Burnt area in Mainland Portugal per year, from 2000 to 2021 [7] . . . 3
1.4 Example of a flyer distributed to the population in 2021 [10] . . . 4

2.1 Some examples of robots sold at McConnel Limited [22] . . . 8
2.2 Two models built by Greeb Climber . . . 8
2.3 Two models built by Energreen . . . 8
2.4 Multiscope Forester Brushcutter by Milrem Robotics [28] . . . 10
2.5 INESC TEC's MowIT . . . 11
2.6 Some machines built by different brands . . . 12
2.7 Three types of blades recommended by *Stihl* for bushes and thin trees [35] . . . 12
2.8 Other types of blades that can also be used . . . 13
2.9 Head 100 Cutting Head for the RoboMINI [25] . . . 13
2.10 Cutter Bar for the RoboMINI [25] . . . 14
2.11 Young's Modulus vs Density Materials Chart, created using CES EduPack 2019, ANSYS Granta © 2020 Granta Design [40] . . . 15
2.12 Strength vs Relative Cost per Unit Volume Materials Chart, created using CES EduPack 2019, ANSYS Granta © 2020 Granta Design [40] . . . 16

3.1 How the different subsystems interacts with each other . . . 19
3.2 Patent's Scheme [41] . . . 20
3.3 Tuff Kutt [42] . . . 21
3.4 Six-leaf Cutter sold by Tenyu Tools [43] . . . 21
3.5 Stihl GrassCut 230-4 grass-cutting blade [46] . . . 23
3.6 Blade Design . . . 23
3.7 Shaft Design . . . 27
3.8 Holding Disks . . . 28
3.9 Section view of the blade mounted to the disks . . . 29
3.10 CAD view of the blade assembled to the disks . . . 30
3.11 Layout without blade and disks . . . 30
3.12 Cutting Solution subsystem . . . 33
3.13 3KW BLDC Motor from Golden Motor [56] . . . 34
3.14 Performance Curve of the motor. Red line indicates the working point. . . . 35
3.15 MowIT's visual dimension representation . . . 36
3.16 Inverted triangle setup . . . 37
3.17 Pulley Layout (dimensions are not to scale) . . . 39
3.18 Assembly without the pulley . . . 41

3.19 Assembly with the pulley . . . 41
3.20 Detail of the new motor's keyway . . . 42
3.21 Pulley assembly in the motor . . . 42
3.22 Loose inspirations for the structural design . . . 44
3.23 2D sketch of an outline for the supporting structure (not to scale) . . . 44
3.24 Section View of the bolting connection . . . 45
3.25 Enclosure, the box and lid bolted on each other . . . 46
3.26 Position for the mounting brackets . . . 47
3.27 Mounting Bracket component . . . 48
3.28 Weld details for the bracket . . . 49
3.29 Isometric view of the mounting bracket with the clevis pin and spring cotter applied to it . . . 50
3.30 Side view of the top connecting rod with the eye bolts applied . . . 50
3.31 Isometric view of one side rod with the elastic ring cutouts . . . 50
3.32 Two views of the appendage . . . 51
3.33 Trapezium component in different perspectives . . . 52
3.34 Isometric view of the mounting bracket . . . 53
3.35 Side view with clevis pin mounted to the hole and secured by an elastic ring . . . 53
3.36 Securing component with identifying numbers . . . 54
3.37 Securing component mounted on the connecting rod . . . 54
3.38 Lifting Mechanism . . . 55
3.39 Motor plate from the top . . . 56
3.40 Motor mounted on the plate . . . 56
3.41 Motor and plate mounted on the lid component . . . 56
3.42 Detail of the short space between the shaft and the motor's position . . . 58
3.43 Sectioned front view of the bearing unit assembly with the cutting solution . . . 59
3.44 Supporting Structure final view . . . 60
3.45 Render figure of the cutting tool . . . 61
3.46 Assembly without the lid component to show interior . . . 61

4.1 2D problem of the shaft . . . 65
4.2 Bending moment diagram . . . 65
4.3 Stress values throughout time in a pure bending situation . . . 66
4.4 The two considered groupings . . . 70
4.5 2D sketch of the simplified problem . . . 72
4.6 Beam 1-2 represented . . . 72
4.7 Beam 3-4 represented . . . 73
4.8 Bending diagram for Beam 1-2 . . . 74

C.1 Hardness - Vickers vs Machinability Ashby Chart, created using ANSYS EduPack 2023 . . . 95
C.2 Detailed View of the Hardness - Vickers vs Machinability Ashby Chart, created using ANSYS EduPack 2023 . . . 95
C.3 Density vs Price Ashby Chart, created using ANSYS EduPack 2023 . . . 96
C.4 Density vs Price Ashby Chart without low lubricating oil durability, created using ANSYS EduPack 2023 . . . 96
C.5 Range of property values on different material families [53] . . . 97
C.6 Density vs Price Ashby Chart with polymer thermal conductivity values as filter, created using ANSYS EduPack 2023 . . . 97

List of Tables

2.1 Differences between Robots and Remotely-operated Machines [adapted from 17,18] 7

3.1 Advantages and disadvantages of two common cutting solutions [13] 20
3.2 Husqvarna model's maximum output shaft speed [33] 22
3.3 Some relevant properties of C45 steel [45] 22
3.4 Blade's Dimensions 24
3.5 Composition and application of six different tool steels [48] 26
3.6 Some properties of W1 tool steel and O1 tool steel [53] 26
3.7 Shaft's Dimensions 26
3.8 Disk's Dimensions 27
3.9 Normalized components involved in the connection 29
3.10 Normalized components involved in one blade connection. Each cutting subsystem contains four of these connections. 30
3.11 Comparison of some specifications between POM+PTFE and PEEK+PTFE [53,54] 32
3.12 Motor Characteristics [56] 34
3.13 Engine Values at 8.9 Nm 35
3.14 MowIT's Relevant Dimensions given by the CAD model 36
3.15 Dimensions used in Figure 3.16 37
3.16 Advantages and disadvantages of different drives [57] 38
3.17 Components suggested by Optibelt's software, for the motor working point . . . 40
3.18 Relevant values taken from Optibelt's software (available in Appendix E) 40
3.19 Material Properties of AISI 304 [53] 45
3.20 Normalized components involved in the bolting in the enclosure 46
3.21 Connecting rod specifications 48
3.22 Total number of normalized components involved in the connection 52
3.23 Electrak GX specifications [61] 53
3.24 Total number of Normalized components involved in the lifting mechanism . . . 55
3.25 Normalized components for adjusting the motor position and motor fixation . . . 57
3.26 The three choices remaining 58
3.27 Standard components involved with the bearing units 59

4.1 MowIT's maximum linear speed 63
4.2 Beam Dimensions 65
4.3 Reaction forces at the supports 65
4.4 Maximum and minimum values for bending moment and shear forces 65
4.5 Values of a and b for machined shafts [64] 67
4.6 Calculation data for SKF FYTB 20 TF bearing unit [62] 69
4.7 Mass of the considered system 71

4.8 Relevant Dimensions for Figure 4.5 72
4.9 Forces in the static problem 74
4.10 Torque and speed comparison between Husqvarna 336FR [67] and the cutting subsystem. 77

I.1 Cost of standardized components and branded components, in euros. Prices from Norelem unless specified on Observations column 149

Abbreviatons and Symbols

AC	Alternate Current
AI	Artificial Intelligence
AISI-SAE	American Iron and Steel Institute - Society of Automotive Engineers
BLDC	Brushless Direct Current
CAD	Computer Aided-Design
DIN	Deutsches Institut für Normung
DC	Direct Current
HSS	High-Speed Steel
INEGI	*Instituto de Ciência e Inovação em Engenharia Mecânica e Engenharia Industrial*
INESC TEC	Institute for Systems and Computer Engineering, Technology and Science
IoT	Internet of Things
ISO	International Organization for Standardization
MIG	Metal Inert Gas
PEEK	Polyether ether ketone
POM	Polyoxymethylene
PTFE	Polytetrafluoroethylene
TIG	Tungsten Inert Gas
UGV	Unmanned Ground Vehicle
ZIF	*Zona de Intervenção Florestal* (Forest Intervention Zone)

d	Diameter - mm
i	Drive Ratio
k	Average Wear Rate - m^3 / Nm
l	Length - meter
n	Rotational Speed of Frequency - rotations per minute
ω	Angular Velocity - rad/s
P	Power - kilowatt
S	*clip* - mm
M_b	Bending Moment - Nm
M_t	Torque - Nm
T	Period - s
v	Speed - m/s

Chapter 1

Introduction

1.1 Current Context

1.1.1 Portuguese Forest

The Portuguese Forest has been steadily growing its area around the years. Between 2010 and 2015, its area increased by sixty thousand hectares, something that had not been observed since 1995. In total, it occupies around 3.2 million hectares, representing 36% of the area of the country. This area is mainly populated with eucalyptus, oak and pine species, as visible in Figure 1.1.Naturally, it leads to opportunities of investment in the forest, such as the paper industry and furniture. [1]

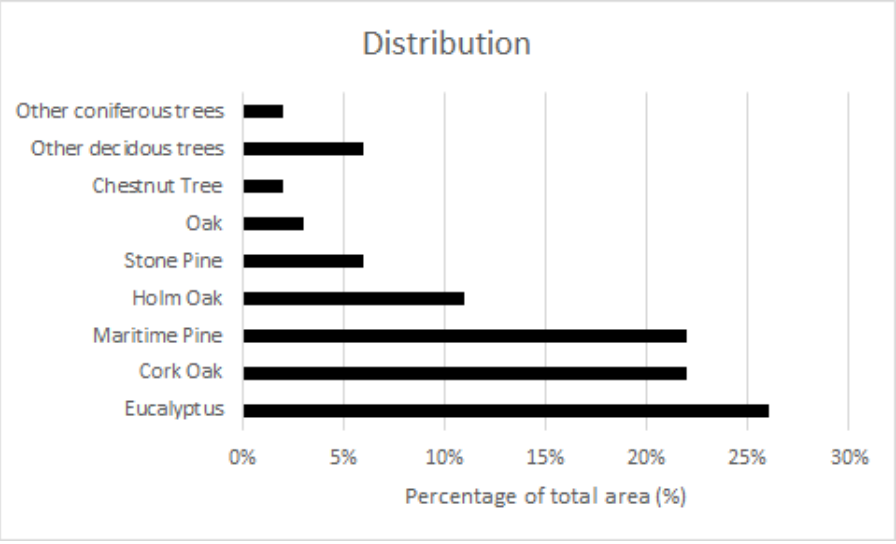

Figure 1.1: Distribution of total areas by forest species in Mainland Portugal in 2015 [2]

Another characteristic of the Portuguese Forest landscape is who owns it, as the percentage of privately owned forest amounts to 84% [1]. In 2004, the Portuguese Forest owners could be divided into four groups.

- Non-industrial private owners who own about 80% of pine forests, primarily in the north and center of the country.
- Non-industrial private owners that own the vast majority of cork oak forests, located in the south of Portugal.
- Central Government Forest Services who take charge in maintaining public forests as well as some communal forests, which are comprised of mostly maritime pine.
- Industrial private owners in the paper and pulp industries who own about 28% of the eucalyptus forests.

These practices are important, as high temperatures and low humidity are perfect factors to trigger a fire.

If the forest is left unkempt however, this can become a liability. As the natural course of nature occurs, bushes, small trees, fern and fast-growing species, denominated as forest undergrowth, grows and permeates the ground, becoming the source of the fire [3]. This raises more concern in wilder and disorganised areas, just like the north and center regions owned by non-industrial private owners, as these areas not having industrial value, might lead to less maintenance [3].

When a forest fire happens, the natural resources used in the various industries are wasted, lives are put to danger fighting the fires and the loss of natural habitats for different species of living beings that inhabit the forest, by altering food, water and habitat situations [4]. Some of the trees that burn are beings which have grown up throughout decades, like the Cork Oak tree (Figure 1.2) which can live up to 500 years [5], and the same amount of time will be needed in order to new trees to be grown in the affected areas, decreasing the value of these natural resources.

Figure 1.2: A Cork Oak tree [5]

Portugal has been dealing with forest fires throughout the years, and giant fires, like what happened in Pedrogão Grande in 2017, with 66 people who died and over 50 thousand hectares of land burnt (Figure 1.3) in 2017 [6], made the ever growing concern with the maintenance of

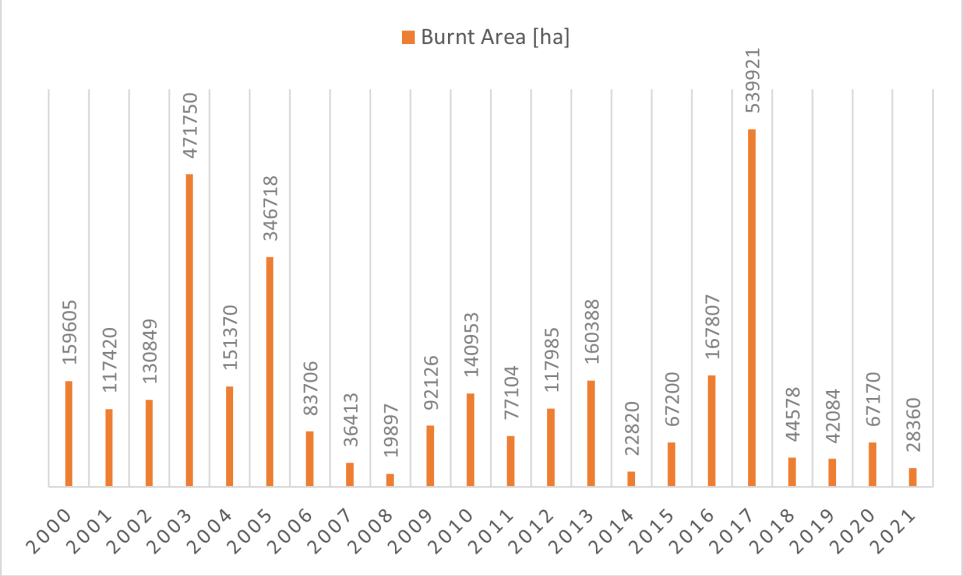

Figure 1.3: Burnt area in Mainland Portugal per year, from 2000 to 2021 [7]

the Portuguese Forest increase even more. With these concerns in mind, it is natural that ways to prevent these situations are constantly being devised.

There are different ways that a forest can be maintained, such as:

- better patrolling of the risk areas
- educate the population to discourage risky behaviour during the critical periods (Figure 1.4)
- cleaning the forest undergrowth [3]
- encourage forest land owners to join Forest Intervention Zones (ZIF) [8]
- implement laws that require the land owners to maintain their properties and clean them when deemed necessary, if it is not something that is already done. (For example the Integrated Management System for Rural Fires [9])

As 84% of forest property is privately owned [1], some of the measures can prove to be extremely helpful preventing wildfires. The creation of ZIF's enable small land owners to join and together more easily manage their territory in a joint effort, helping prevent forest fires from occuring,

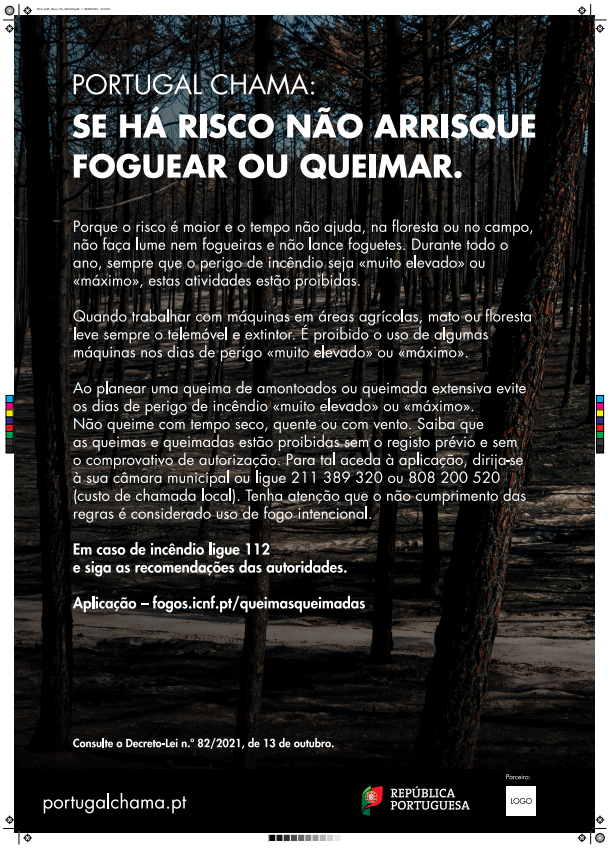

Figure 1.4: Example of a flyer distributed to the population in 2021 [10]

1.1.2 The use of a robot

A robot is a machine that can perform a complicated series of tasks automatically [11]. This can in fact help humans to achieve efficiency levels never attained before, by creating robots responsible for different tasks which can accomplish it safely.

Despite the use of robots in other areas, such as the automobile industry and the agricultural sector, there is a lack of robotics in forest applications available or being developed, specially compared with agricultural applications, an area related to the forest. This can be related to higher complexity of the environment, with variables such as:

- temperature variation,
- variations in humidity,
- extremely irregular terrain

that are detrimental to the development of such technologies [12].

1.2 Goals of the Dissertation

With everything stated before, a dissertation was proposed to create a cutting tool that would be applied to a forest robot for undergrowth cleaning, able to cut trees up to 50 mm of diameter and energetically efficient.

This dissertation has the following objectives:

- Examine current preventive silviculture solutions available in the market;
- Examine current preventive silviculture solutions being researched;
- Examine cutting solutions for forest undergrowth;
- Creation of a mechanical project for a cutting tool for a forest robot along with a material selection.

1.3 Structure of the Dissertation

This dissertation starts with an introduction where the topic of the Portuguese forest is addressed, along with forest fires and methods for its prevention and maintenance of forests.

Along with the introduction, this dissertation contains 4 more chapters. In Chapter 2, preventive silviculture and its practice are explained, along with different methods available to use. A research on cutting solutions as well as a brief explanation on material selection and product design is made. In Chapter 3, the mechanical project of the cutting tool is devised and shown. In Chapter 4, some validations regarding choices made in the previous chapter are made. In Chapter 5 the main conclusions are drawn and future works are explained.

Chapter 2

Bibliographic Review

To clear forest undergrowth, there are some methods which are used quite frequently during forest cleaning operations. These come commonly in the form of moto-manual work, with the use of chainsaws, clearing saws and brush cutters, mechanical methods, with the use of mobile industrial machines like tractors, the use of controlled fire or agroforestry practice.

As mentioned in Chapter 1.1.2, there has not been as much research through forest robotics compared to agricultural robotics. In spite of this, there are ventures into this area of robotics and even some commercial solutions.

2.1 Preventive Silviculture and Forestry

Preventive silviculture can be entailed as the planned installation and management of forest plantations, taking into account the degree of flammability of various vegetation kinds and diversifying both the structure and composition of the forest. Making routes, water stations, and firebreaks are all included in these acts [8]. By doing this, it is possible to prevent the spread of destruction or possibly manage the fuel that can trigger a fire, as well as create points where firefighting is possible.

In the recent years, most of the forest cleaning and silviculture work is still being done with the use chainsaws, brush cutters and clearing saws [3, 13]. While these methods can be enough when working in small scale and plain areas, when dealing with large-scale areas and sloped and irregular terrain it can become very time consuming, inefficient and even become dangerous for the user [14]. There are many instances of diseases that originate from the prolonged use of these machines, such as hearing losses, carpal tunnel syndrome and musculoskeletal disorders, as well as injuries such as falls derived from the weight of the machine together with the steepness of the terrain or even injuries directly dealt by the heads of the machines [13, 15, 16].

When certain conditions are met, heavier machinery can be used for forest cleaning. Usually the areas where heavier machinery is used are commercially developed forests, as small private owners might not have the means to implement it. It comes in the form of agricultural vehicles, like

tractors, with attachments to be used in forestry operations. For these to be used, the conditions required are the following:

- big enough clearance for the machines to operate,
- specialized labor workers to operate these machines,
- safety conditions are maintained.

2.2 Commercial Solutions

Firstly, a separation must be done to differentiate between a robot and a remote-operated machine, as there are some key differences. Like seen in Table 2.1, one of the main points that differentiates a robot from a remote-operated machine is the fact that the robot can operate autonomously without human intervention.

Table 2.1: Differences between Robots and Remotely-operated Machines [adapted from 17, 18]

Robots	Remotely-operated Machines
Can carry out tasks or groups of tasks that have been pre-programmed in them	Controlled by users or external devices
Are self-governing and can make decisions without an external input	When accidents are involved, human lives can be at danger
Can operate independently and perform tasks without human intervention	Require human intervention to operate
More complex, intelligent, and interactive than their remotely operated machine counterparts	Usually have a less complex structure
When designed correctly, can operate far more efficiently than human operated machines	More prone to problems due to misuse of the machine
Can be affected by bugs and cause critical failure in their functioning	

There are many advantages of remotely operated machines over the use of heavy and hand-operated machinery. The smaller scale of remotely operated machines allows for an easier entry and locomotion in smaller terrains, something not possible with heavy machinery. In terrain where heavy machinery can't operate hand-operated machinery, like brush cutters, handled by operators need to be used. By using something remotely operated, unlike with brush cutters, the operator does not need to handle directly the tool, meaning that he can distance himself out of harm's way, turning the act of cleaning the forest turf into a less dangerous activity to the involved party.

There are some solutions available for commercial use on forest maintenance available in the market at the moment and come in the form of remotely-operated vehicles. The vast majority of them use internal combustion engines (either a gasoline or a diesel engine) to power a hydraulic pump that controls the tracks and attached tools, and a radio controller to operate the machine, requiring the presence of an operator, responsible for guiding the machine. In Figures 2.2a and 2.3b an operator can be seen controlling the machine. Such machines were found while researching for the dissertation, such as the robots for forest cleaning made by McConnel Limited (Figure 2.1), Green Climber (Figure 2.2) or Almovi (Figure 2.3). In Portugal, Green Climber products are being sold by Maquiloendro [19] and Energreen products by Almovi [20]. In a previous thesis, Diogo Vieira had gathered a list of some commercially available vehicles, along with a survey with the desired requirements a land owner would need, and devised a mechanical project for a remotely controlled vehicle for for forest cleaning [13]. Daniel Moleiro in his thesis also retrofitted a brush cutter into a remotely operated machine to make use of existing machines owned by land owners [21].

Figure 2.1: Some examples of robots sold at McConnel Limited [22]

(a) LV600, built by Green Climber [23]

(b) LV300 Pro, built by Green Climber [24]

Figure 2.2: Two models built by Greeb Climber

(a) RoboEVO, sold by Energreen [20]

(b) RoboMINI, built by Energreen [25]

Figure 2.3: Two models built by Energreen

2.3 Forest Robots

The next step after a remotely operated forest vehicle would be a forest robot. Grabbing most of the advantages of the remote machine, such as its more versatile size, and improving upon them, it is possible to create a Unmanned Ground Vehicle (UGV) with high capabilities.

With the joint use of Internet of Things (IoT), Artificial Intelligence (AI) and Robotics, Forest 4.0 can be achieved. By digitizing the forest, it becomes far easier to survey, manage and maintain large areas of land [26]. By assuring that the robots can work autonomously, the need for an operator decreases, as human intervention will be mainly used for robot maintenance and transport and enables the use of robots with different purposes working in tandem and perform various tasks simultaneously and cooperatively at the fields. These "robot swarms", can then monitor the forest, which increase the chances of early wildfire detection; create an inventory of existing trees to further increase the digitization and management of the forest; plant, prune or harvest trees and clean undergrowth, contributing to preventative silviculture practices; intervene early on wildfires with water or retarding agents in the case that a wildfire actually breaks out by acting autonomously using the input received from its surroundings and joint coordination between each other, which can lead to scalability.

One robot that can do silviculture operations is the Multiscope Forester Brushcutter, built by Milrem Robotics, a military sector company (Figure 2.4). It uses a caterpillar system to move and is modular. This means that it shares the same platform as its planter counterpart, the Multiscope Forester Planter [27]. Like the Multiscope Forester Planter, the Brushcutter model is being developed as a hybrid system, enabling the owner of the robot to operate it remotely, follow the user, waypoint navigation or even swarming [28]. This company also builds robots for fire suppresion situations (like to Multiscope Rescue Transport [29]) and all of the mentioned robots are equiped with hybrid power solutions, having a diesel engine, an electric generator and battery-equipped and being able to operate both with the engine or electrically.

Figure 2.4: Multiscope Forester Brushcutter by Milrem Robotics [28]

2.3.1 MowIT

A robot which can be used for autonomous forest undergrowth cleaning being developed is the MowIT (Figure 2.5). Developed by the Robotics and IoT Laboratory for Agriculture and Forest for Intelligent Precision at INESC TEC, it is a fully electrical model, designed to be completely autonomous and applied in vineyards or forests. It can be used for forest management and on steep hills, with its sensor system that contributes to an autonomous operation of the machinery.

One clear advantage of the electrical solution made by INESC TEC can be noted by the use of electricity itself. Contrary to its internal combustion competitors, it does not cause environmental pollution because of its combustion byproducts, like spilling from the refuelling or any leaks that the robot might have. The robot can also do fine adjustments in the locomotion speed and power distribution and increase the efficiency of power consumption. Its size allows for better navigation across forests and vineyards.

With the use of artificial intelligence and sensors, the robot can pass through the trails between the trees and identify different elements, knowing it would avoid obstacles or elements that would not be desirable to cut, such as trees and rocks, and cut grass and turf, for example.

Figure 2.5: INESC TEC's MowIT

2.4 Cutting Solutions

Existing cutting solutions exist throughout the different means they are applied to.

2.4.1 Motorized Mechanical Machines

Current applications of motorized mechanical machines use clearing saws and brush cutters to cut undergrowth, each being applied according to what is being cut. Brush cutters are considered lighter solutions, more appropriate for domestic use. They are mostly used for weeds, grass and bushes. They can, however, be fitted with some heavier duty attachments, like knife blades to be able to cut some thicker or woodier targets. On the other hand clearing saws are heavier machines, designed for more professional use cases. Even though there are some battery powered solutions, most of the machines found used internal combustion engines to power the machine heads. They usually come with harnesses and double handle style to provide a better stability and reduce arm fatigue to the operator when handling the machine for long periods of time. Like with bush cutters, it also has interchangeable heads, being able to adapt which tool is more appropriate for each situation [30, 31].

Such machines are sold by companies, such as Stihl (Figure 2.6a), Husqvarna (Figure 2.6b) and Echo (Figure 2.6c), with varying specifications. Both Stihl's and Echo's models depicted in the figures use an internal combustion engine as its power source, while the Husqvarva model

is electrically powered. However, these three brands offer both electrically powered and gaoline powered solutions.

(a) *Stihl* FS 561 C-EM [32]

(b) Husqvarna 535iFR [33]

(c) Echo Tools CLS-520ES [34]

Figure 2.6: Some machines built by different brands

There are different types of attachments that can be applied to these machines, according to the situation. According to *Stihl*, to clear bushes and thin trees, saw blades are recommended, such as:

- chisel-tooth circular saw blades (Figure 2.7a),
- scratcher-tooth circular saw blades (Figure 2.7b),
- carbide tipped circular saw blades (Figure 2.7c).

(a) Chisel-tooth circular saw blades

(b) Scratcher-tooth circular saw blades

(c) Carbide tipped circular saw blades

Figure 2.7: Three types of blades recommended by *Stihl* for bushes and thin trees [35]

Other solutions available as well are brush knives (Figure 2.8a), grass cutting blades (Figure 2.8b), suitable for thinner undergrowth and nettle or chainsaw toothed blades (Figure 2.8c), more suitable for thicker undergrowth and trees.

(a) Brush knives [36] (b) Grass cutting blades [35] (c) Chainsaw tooth blades [37]

Figure 2.8: Other types of blades that can also be used

2.4.2 Cutting Solutions on Commercial Solutions and Forest Robots

Current remotely commercial solutions that were observed showed the vast majority of them used a rotating drum solution, either set up with hammer flail drums or knife drums, all moved by a hydraulic pump powered by its combustion engine. This is visible in the machines built by Energreen (Figures 2.3 and 2.9), McConnel Limited (Figure 2.1) and Green Climber (Figure 2.2). More specifically, it is possible to observe the Head 100 (Figure 2.9), a forestry head that can be attached to Energreen's RoboMINI which can come equipped with either hammer flails or Y shaped knives, but also the Head 130, Forestry 130 T, Forestry 130 H which can be attached to the RobotEVO and the Head 155 together with the before mentioned heads for the RobotEVO can be applied to the RobotFiFTI, a bigger counterpart in Energreen's lineup [25].

(a) Head 100 (b) Head 100 in action

Figure 2.9: Head 100 Cutting Head for the RoboMINI [25]

Some other alternatives were found in some solutions applied to current robot or remotely operated applications. Such as disc cutters and trimming solutions. Both MowIT's and MultiScope Forester Brushcutter use a trimmer setup. Energreen's RoboMINI has a Cutter Bar attachment

that can be applied and both RoboEVO and RoboFiFTI have a cutter bar setup, although slightly different than the one used on RoboMINI. In Diogo Vieira's thesis, the solution used circular saws generally used in clearing saws in a triangular positioning to achieve the desired cutting result [13].

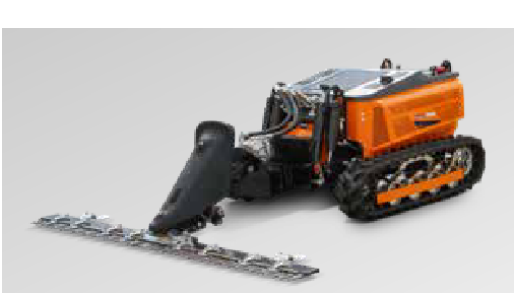

(a) Cutter Bar

(b) Cutter Bar in action

Figure 2.10: Cutter Bar for the RoboMINI [25]

2.5 Material Selection and Product Design

Material selection and product design often come hand in hand with each other. By designing a product, an idea is transformed into something that can be manufactured. While in the process of designing, both the shape of the product and the materials used on it are closely related. The material can be chosen by design restrictions, or the design can originate from material constraints.

As design is an iterative process, when creating a new product, some base points need to be established. These come in the form of the initial idea and the requirements it will have. These dictate what the product will need in accordance to its desired function. Based on the requirements, it is possible to convert them into specifications, actual values that can be measured and compared against each other. By having the specifications, the conceptual phase starts, where the implementation of the specifications and requirements that the product has to fulfill are turned into actual ideas. From these ideas the most innovative is then selected, and analysis will be done to create the concept of the product. This concept then will be implemented into product design, leading into prototyping, benchmarking and detailed drawings for production are done . To create a new product, not always the idea has to be created from scratch. *Variant design* comes as the process of design where there is a change in the scale of a product but without changing its functions [38, 39].

Along the years, the amount of materials that can be used for engineering purposes has increased, with new materials surging every year with increasingly more interesting properties associated. This has increased the complexity of choosing a material for a design, making it a far more difficult task compared to many years ago [39]. Material selection charts are used to plot different materials against each other, with one property in each axis and scaled on logarithmic scales, forming ellipses from their range in each property, where materials from the same group are grouped together [40]. In Figures 2.11 and Figure 2.12, these materials charts can be observed

with different properties used as plotting axis. While this grouping can be done when dealing with a material choice that has very few constraints, when dealing with more complex situations, computer-aided tools, such as CES material and selection software (now ANSYS Granta Edupack [1]) are a must [39]. It integrates a database with a variety of properties for different materials, stored in a range of admissible values along with unstructured data, such as figures, text and references to further help in the material selection process. It allows the plotting of such properties into materials selection charts, along with a filtering option to further refine the results. It also possesses different levels, where the variety of the materials shown increases when going down in the hierarchical chain of the group of materials.

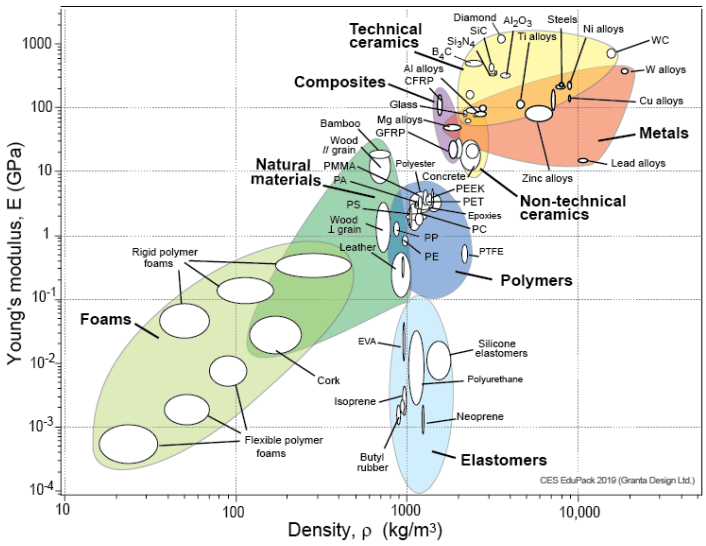

Figure 2.11: Young's Modulus vs Density Materials Chart, created using CES EduPack 2019, ANSYS Granta © 2020 Granta Design [40]

[1] ANSYS, Inc., Cambridge, UK (https://www.ansys.com/products/materials)

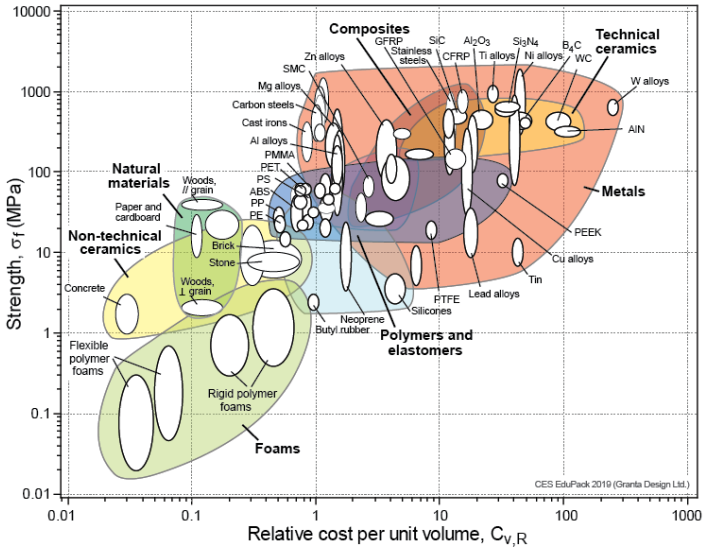

Figure 2.12: Strength vs Relative Cost per Unit Volume Materials Chart, created using CES EduPack 2019, ANSYS Granta © 2020 Granta Design [40]

Chapter 3

Mechanical Design

3.1 Introduction

The present chapter explains the design process behind the creation of the tool. Firstly, an analysis of the requirements the tool would need to comply with was done. Then, a breakdown of what a cutting tool would be comprised of in terms of sub-systems is done, conceptualizing the different problems that would be necessary to tackle during the chapter.

Afterwards, taking into account what was learned in the previous chapter, together with some inspiration during the design phase, a conceptual idea of the desired design is created. An explanation of the different design choices involved in the creation a subsystem, accompanied by the the standardized components used that are used in conjunction with the creation of designed parts, is followed. In this part, relevant components that are used and how each component interacts with each other are also explained. Lastly an overview of that subsystem is shown.

To complete the chapter and the design phase, an assembly overview is done, showing all the subsystems mounted together. In Appendix H a mechanical drawing of the solution is shown.

3.2 Requirements

As a first step, some requirements for the tool had to be designated. Understanding which points to focus on at the beginning of the project would prove useful in tackling more demanding parts in the tool designing and conceptualization. They are the following:

- The tool would have to be energetically efficient, as it would be applied to an electrical robot using batteries for energy.
- The tool would need to be able to cut trees up to 50 millimeters in diameter.
- It would need to be able to withstand prolonged use.
- It needed to be easily assembled and able to be mounted on different robots.
- With easy and reduced maintenance.

In spite of the mention that one of the requirements is to be able to be mounted on different robots, for the purpose of this dissertation, the designing of the tool was mainly focused on applying it to the MowIT robot that was mentioned in Chapter 2.3.1.

3.3 Subsystems and their Interactions

There are some components that a cutting solution would most definitely require. By breaking down the tool into a set of smaller subsystems, each with its own requirements and how they interact between each other, a conceptualization of a solution can be acquired in a more organic way. Thus, the main subsystems that would require attention as well as some requirements would then be:

- **Cutting Solution:** the cutting solution itself is the most important subsystem of the cutting tool. It is responsible for the act of cutting the undergrowth. It needs to be durable enough to be used without replacement, light enough to be applied to the robot and be efficient enough to be powered by an electrical solution. The cutting rate also needs to be ascertained, as a slow cutting rate will mean that the cutting speed of the machine will be lower, lowering the efficiency of the cutting process.
- **Motor Drive:** to power the cutting solution, a motor is needed. The motor needs to have the required specifications that the tool might need, however the choice of the motor can also be affected by external factors such as the ones available at INESC TEC's laboratory.
- **Mechanical Transmission:** it is necessary to deliver power to the cutting solution for it to work so the means to achieve it need to be thought of. The mechanical transmission subsystem might need to multiply or decrease the speed of the motor in order to achieve the desired cutting speed and keep the motor working at a healthy power consumption. Depending on the cutting solution, it may also be responsible for the cutting width of the mowing implement and the number of cutting solutions are deployed.
- **Supporting Structure:** the supporting structure is responsible for holding all the before mentioned subsystems in place, as well as provide the correct geometric relations between everything and is responsible for connecting the solution to the robot as well. As such, it is required to be structurally sound.

Figure 3.1 shows, schematically, how each mentioned subsystem interacts with each other in a more graphical way. For example, even though the cutting solution is powered by the motor drive, this is not done directly, being aided by the mechanical transmission subsystem to deliver the required power to the solution. Incidentally, all of these subsystems are held in place by the supporting structure. This shows that all of the subsystems are interconnected between each other and shows that the failure of one subsystem means that the whole tool will be rendered useless.

In addition, by creating this scheme, ideas on each sub component that encompasses the whole tool could be idealized more easily and contribute to the end goal.

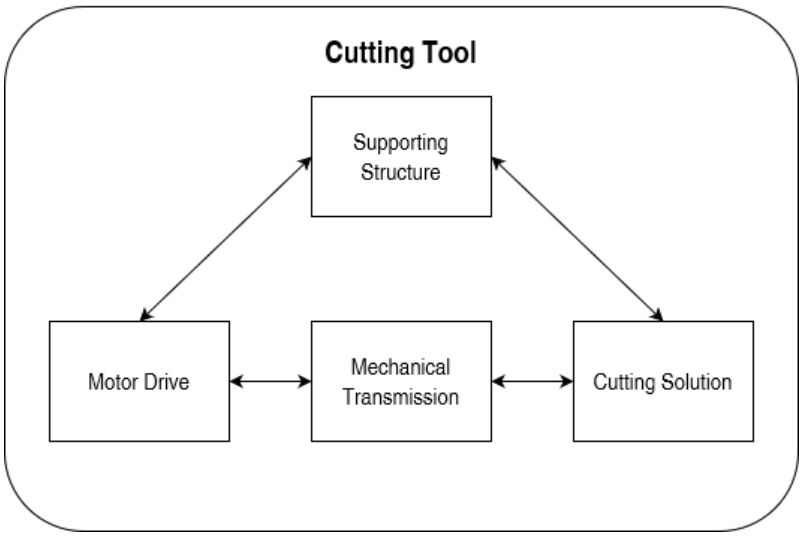

Figure 3.1: How the different subsystems interacts with each other

The subsystems and its respective components were designed on the 3D CAD software *Fusion 360*® from Autodesk® [1], a versatile CAD tool, the normalized and branded components were imported using parts4cad *Insert a manufacturer part* feature on *Fusion 360* when available and the manufacturer chosen for the standardized parts was Fabory [2]. MowIT's CAD model, as well as some dimensions were made available to the author by INESC TEC's lab.

3.4 Cutting Solution

As the whole system is comprised of different subsystems, the cutting solution is also made up of various components that together enable the tool to cut material.

For this subsystem, the design needs to possess the ability to cut up vegetation, as well as allow an interaction with the power delivery system to receive the power coming from the motor drive.

3.4.1 Design Inspiration

To create a cutting solution, firstly a research was made into already existing design approaches, in tools observed on the market, previous thesis and research. This was made in Chapter 2.4 and helped discard some approaches right away.

A common approach that was found, as previously stated, was the use of drum solutions. While there are advantages to the use of drums solutions, the disadvantages will outweigh the advantages for this particular application. The slower times of acceleration and deceleration, derived from its higher inertia associated with drums setup, could lead to a higher consumption of

[1] Autodesk® Fusion 360®, version 2.0.16985, San Rafael, CA, US https://www.autodesk.pt/products/fusion-360/overview

[2] https://www.fabory.com/pt

energy when stopping the system. In Table 3.1 it is possible to observe some of advantages and disadvantages both of these types of systems possess.

Table 3.1: Advantages and disadvantages of two common cutting solutions [13]

Rotary Drum	
Advantages	**Disadvantages**
Breaks down vegetation Easier waste management Safety Can destroy almost all types of vegetation Does not leave tree stumps	Heavier More complex Higher cost Requires a very powerful drive motor
Circular Blades	
Advantages	**Disadvantages**
Affordable Simple Good cutting for all types of vegetation Interchangeable blades	Leaves tree stumps Blade can break on stones

Drum solution was discarded during initial considerations, in favor of circular blades for their lower complexity and lower associated cost, through a qualitative analysis of both options.

Rotary options, such as the ones found in brush cutters and clearing saws came into mind as possibly using less power, as there was a wide variety of existing machines operated by a person that were handheld and in some cases electrically powered, proving that smaller devices could deliver similar results. During this step, a cutting tool to be applied on a brush cutter which was designed and patented came into talk. This was a solution which used a rotating disc (Component 1) with blades donned of a rotational degree of freedom on its rotational axis (Component 2) (Figure 3.2) [41].

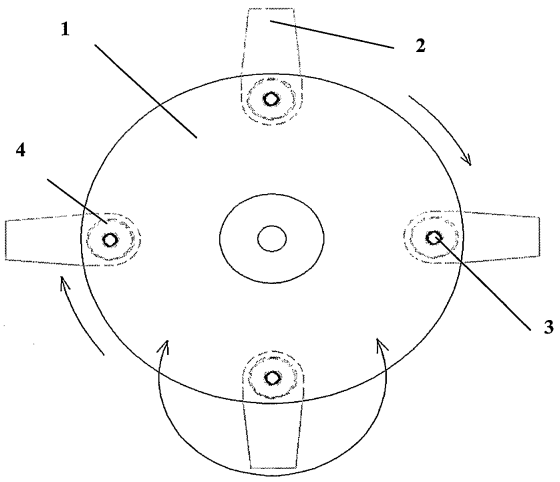

Figure 3.2: Patent's Scheme [41]

This design could have some pros, like mitigation of some of the impact that a blade would get by hitting on a hard material. This in turn could prolong the lifespan of the blades, as the blade could maintain its sharpness for longer. It could also reduce the burden on the engine, as after the impact it would not need as much torque to go back to the speed it had before. Further confirmation that this type of solution could prove to be useful came by a tech report written by the United States' Department of Agriculture's Forest Service evaluated a similar tool, by the name TUFF KUTT (Figure 3.3), which provided favourable results with this design choice [42].

Figure 3.3: Tuff Kutt [42]

To note that Tenyu Tools also commercializes a similar type of tool, but donned of six blades [43].

Figure 3.4: Six-leaf Cutter sold by Tenyu Tools [43]

3.4.2 Layout and Considerations

There were some choices that needed to be made during the design process regarding the layout. The main components that would be a part of the tool are:

- the blades;
- the top and bottom holding disks, responsible for aligning the blades;
- a shaft responsible for receiving the power of the motor to turn the disks;
- a bushing that would hold in place the blades to the plates, all while allowing them to rotate and have the desired degree of freedom.

The subsystem would then be divided in two halves. The upper half would receive the power delivered from the motor as well as hold the bottom half, which would, in turn, house all the components related with the cutting aspect of the subsystem.

The chosen layout was a four-blade system with a cross (+) configuration of the blades, just like the patent's scheme in Figure 3.2. A rotational speed also needed to be chosen, in order to progress with the design. As the patent's original purpose was to be applied to a brush cutter, it was decided to choose the speed at the cutting head of a commercially available brush cutter. As neither Stihl nor Echo's models have this parameter in their model's specification sheets, the Husqvarna 535iFR brush cutter shown in Chapter 2.4.1, Figure 2.6b was selected as a basis for this parameter. The value is as shown in Table 3.2.

For the majority of components, C45 steel (also known as AISI 1045) was chosen for being a really versatile construction material, with good weldability and mechanical properties [44, 45] and a widespread use of this material in the industry, possibly saving some costs in non critical components. In Table 3.3 relevant mechanical properties of C45 steel are shown.

Table 3.2: Husqvarna model's maximum output shaft speed [33]

Maximum output shaft speed
8200 rpm

Table 3.3: Some relevant properties of C45 steel [45]

Denomination	**Young's Modulus (GPa)**	**Density (kg/m3)**	**Hardness - Vickers (HV)**	**Ultimate Tensile Strength (MPa)**	**Yield Strength (MPa)**
C45	200	7870	170	565	310

3.4.3 Blade Design

The design of the blades took inspiration from some different sources. The main basis came from the patent´s design, however, some other sources were considered. Further confirmation for the thinning of the tip of the blade and the blade finishing on a non rounded edge instead of a

pointed tip took inspiration on the Stihl BrushCut brush knife - 3 blades (Figure 2.8a) and Stihl GrassCut 230-4 grass-cutting blade (Figure 3.5) attachments, respectively.

Figure 3.5: Stihl GrassCut 230-4 grass-cutting blade [46]

The blades have an angular double bladed design, with a hole at one side to enable the free rotating movement on its axis. The blade edge's length was selected arbitrarily in an earlier phase, suffering some slight modifications to allow the blade to do a full revolution along the freedom axis in the cutting solution subsystem. A double blade design was chosen as it would allow either bidirectional rotational movement to be used whenever required, or if the use scenario would only be unidirectional, it could allow the blades to be flipped and use the other blade's edgem prolonging the life of the component. The blade is milled into shape and a hole is drilled in it freedom axis. The blade is then sharpened for optimal cutting conditions. In Figure 3.6 a visual representation of the designed blades can be seen and in Table 3.4, some important dimensions are displayed.

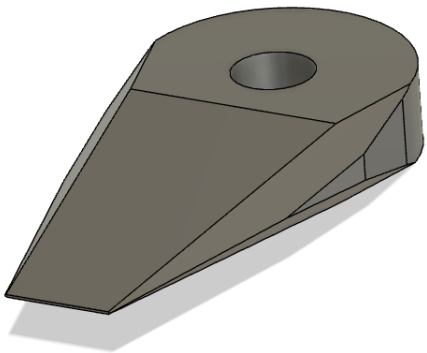

Figure 3.6: Blade Design

Table 3.4: Blade's Dimensions

Height (mm)	**Edge Length (mm)**	**Projected Edge Length (mm)**	**Hole Diameter (mm)**
15	45.6	44.2	15.5

3.4.4 Blade Material Selection

As one of the main components of the mowing implement, the blades were considered a critical component, as such, a more thoughtful approach would then be used for the material selection of the blade. For this some requirements were established:

- the blades would need to be hard enough to cut through the vegetation;
- the blades should have relatively high wear resistance to maximize their lifespan;
- they need to be able to be sharpened.

To further help in choosing a material, existing cutting solutions were observed. A general trend showed that in most commercial products for brush cutters the material of the blades would not be disclosed. Blades, like the one shown in Figure 3.5, or TUFF KUTT (Figure 3.5) simply refer to the material as steel, whereas the brush knife on Figure 2.8a refers to it as *special steel*. Chainsaw tooth brushes like in Figure 2.8c from Forester say that they are carbide tipped. This can be seen as confidentiality against competition.

Some attachments for Energreen remotely operated machines make mention of tungsten carbide tipped blades. Remotely operated machines by other manufacturers shown in Chapter 2.4.2 and robots mentioned do not refer to any material regarding their cutting tools.

Krilek et all. [47] make reference that from the two circular saw blades tested for wood cutting, one was made out of HSS (high-speed steel) carbon tool steel 75CR1 (DIN 1.2003) and the other out of steel with sinterized carbide (SC) tips soldered on to the body of the saw. While the clearing saw was used for cutting of wood and not undergrowth, this proved to be an insight into possible materials for the blades. By searching for the keyword "blade" in the search function of Granta EduPack[3] at Level 2, tungsten carbide and white cast iron were the materials shown.

Tool steels are a type of steel that are used mostly for manufacturing of tools to be used on mechanical forming or object measuring. The name actually encompasses a wide variety of classes of steel derived from the diversity of problems in this area. Although it is quite a big subgroup of materials, they all possess some common characteristics, such as:

- high hardness values, with resistance to deformation in mechanical forming operations;
- high resistance to wear, specially friction based wear;

[3] ANSYS® Granta EduPack 2023 R1, version 23.1.1, Inc., Cambridge, UK (https://www.ansys.com/products/materials))

- high toughness values, holding against high tensions without rupture, together with a good resistance to shock.
- good machinability
- good mechanical properties even at higher temperatures;
- good compatibility with quenching, enabling the obtainment of high and homogeneous hardness without excessive deformations.

All these characteristics result from a high percentage of carbon, usually over 0.6%, and the presence of carbide forming elements, such as tungsten, molybdenum or vanadium, chromium, cobalt, manganese or silicon [48].

High-speed steel, is a type of tool steel used primarily to produce cutting tools for machining processes. It possesses high carbon content and a big amount of carbide forming elements, that give this type of steel great wear resisting behaviour [49]. It can be used in the fabrication of machining tools, for operations such as drilling, reaming, tapping and dieing, forming, broaching and milling as they can be easily shaped in their soft or hardened state [50].

Tungsten carbide, a technical ceramic, is a really stiff, hard and wear resisting material that can be pressed, sintered and grinded into shape, and then brazed or soldered to a blade made of cheaper steel. With this method a blade can achieve high levels of hardness and wear resistance at lower costs. It is the predominant tool material for making cutting, drilling, and fabrication tools, having surpassed the use of HSS steel a few years ago, being the material used in 70% of the tools, as opposed to 20% made out of HSS. It is also widely used in the rock-drilling industry [51].

White cast iron is casted and then cooled at a high cooling rate, preventing the formation of graphite. Because of this, they are hard and brittle, possess high compressive strength and resistance to abrasion. However, they possess low machinability, needing to be cast into shape [52].

As white cast iron presented low machinability and brittleness, this material was discarded in an initial phase in favour of more friendly solutions to use machining processes to create the tool. Tungsten carbide tips on a blade with the design chosen would carry a higher degree of complexity, related to the processes of sintering the tips and either brazing or soldering them to a blade to create an edge. Tool steel was therefore the material of choice. In Table 3.5 a list of six important tool steels, using the American Iron and Steel Institute - Society of Automotive Engineers (AISI-SAE) classification, along with their applications was taken from the book "Materiais de Construção" [48].

By observing Table 3.5, the most interesting materials to consider would be O1 and W1 tool steel. According to AISI-SAE denomination, "O" stands for cold working and "W" for water quenching. In Table 3.6 some properties for both materials are shown. It is visible that while O1 tool steel presents itself with higher average values for hardness and for its yield strength, W1 tool steel possesses a slightly lower average price per kilogram and a higher average value for both toughness and fracture toughness. A higher toughness and fracture toughness can mean a

Table 3.5: Composition and application of six different tool steels [48]

AISI Designation	Composition in mass percentage						Applications
	Carbon	Chromium	Nickel	Molybdenum	Tungsten	Vanadium	
M1	0.85	3.75	0.30	8.70	1.75	1.20	Drills, saws, lathe tools
A2	1.00	5.15	0.30	1.15	-	0.35	Punches, engraving tools
D2	1.50	12	0.30	0.95	-	1.10	Cutlery, extraction tools
O1	0.95	0.50	0.30	-	0.50	0.30	Cutting blades, cutting tools
S1	0.50	1.40	0.30	0.50	2.25	0.25	Tube cutters, tools for concrete
W1	1.10	0.15	0.20	0.10	0.15	0.10	Blacksmith tools, wood cutting tools

longer lifespan for the blade by being able to absorb more energy before it fractures, and after fracture have a slower propagation of the fracture. The lower price of W1 can prove advantageous in higher scale production and while it possesses a lower hardness compared to O1 tool steel, the target of the blade will be plant derived and not metal, where a higher hardness is essential. For these reasons, W1 tool steel was chosen for the material of the blades.

Table 3.6: Some properties of W1 tool steel and O1 tool steel [53]

AISI	Young's Modulus (GPa)	Density (g/m^3)	Hardness - Vickers (HV)	Fracture Toughness ($MPa.m^{0.5}$)	Toughness (kJ/m^2)	Yield Strength (MPa)	Price (€/kg)
W1	204-214	7773-7923	520-820	32.4-33.5	4.99-5.41	1000-1060	2.91-3.27
O1	185-195	7780-7930	660-770	19.3-22.1	1.97-2.57	1800-2140	3.16-3.54

3.4.5 Shaft

The shaft component is a cylindrical shaft with a flange at the bottom (Figure 3.7). It is responsible for receiving the power delivered by the mechanical transmission subsystem so that the Cutting Solution subsystem can rotate and do its desired function. The shaft has a diameter of 20h6 mm and a height of 180 mm, and possesses a flange of diameter 60 mm and a thickness of 2.5 mm. The shafts diameter chosen was the same diameter as the shaft from the electric motor that is chosen in Chapter 3.5.1 for simplicity purposes. The thickness of the flange chosen was the thickness of the sheet metal used in other components of the project. The shaft is manufactured with a spindle as welding could warp and not maintain its straightness. The diameter of the flange was chosen to accommodate the size of the nuts and washer that will hold the bottom half of the subsystem to the flange. It also possesses four clearance holes to allow the passing of screws to tighten both halves of the subsystem and a key-way to receive a parallel key. The dimensions of the key-way were chosen in accordance to ISO/R 773 for parallel keys for the specified diameter.

Table 3.7: Shaft's Dimensions

Cylinder Diameter (mm)	Flange Diameter (mm)	Flange Thickness (mm)	Holes Diameter (mm)	Shaft height (mm)
20	60	2.5	8.25	180

Figure 3.7: Shaft Design

3.4.6 Holding Disks

Holding disks were designed to hold the blades in their places, while receiving the power required to rotate from the connection to the shaft. The design of the disk is present in Figure 3.8.The two disks have the same dimensions and are relevant dimensions are represented in Table 3.8. They also impose the distance between the blades and the total cutting diameter came at 394 mm, taking into account the length of the blade protruding from the disk.

Table 3.8: Disk's Dimensions

Outer Diameter (mm)	**Inner Diameter (mm)**	**Disk Thickness (mm)**	**Distance between Plates (mm)**
270	60	5	20

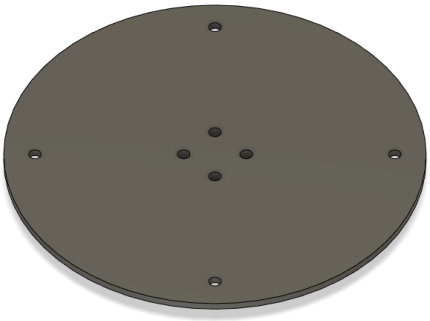

(a) Top holding disk: view from above

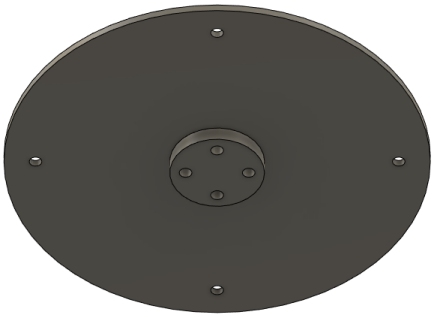

(b) Top holding disk: view from below

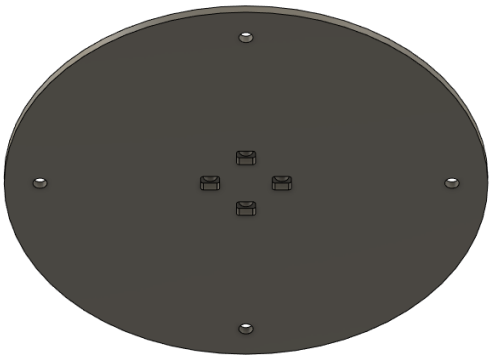

(c) Bottom holding disk: view from below

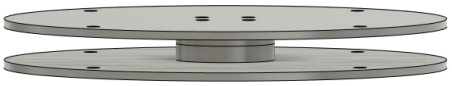

(d) Both holding disks connected

Figure 3.8: Holding Disks

3.4.7 Subsystem Bolting

The connection between the shaft and the disks is made by four DIN 982 hexagon nuts of prevailing torque type, with non-metallic inserts, tightened to four DIN 603 square cup neck bolts in a plus disposition. Between the bolt, the nut and the disks there are two DIN 7089 washers on each side, making it a total number of eight washers. Prevailing torque type nuts and square cup neck bolts were chosen to mitigate any loosening that may happen during the rotation of the cutting solution and to have a more flush surface, respectively. The holes to accommodate the DIN 603 square cup neck bolts can be observed in Figure 3.8d.

In Table 3.9 a list of standard components and the quantity used is shown.

Table 3.9: Normalized components involved in the connection

Quantity	Designation
4	Cup square neck bolt DIN 603 M8x45-8.8
4	Hexagon nut DIN 982-M8-8
8	Washer ISO 7089-8-200HV

For the blade fixation, an ISO 4014 hexagon head bolt is bolted to a DIN 982 hexagon nut and two ISO 7089 washers are used to alleviate the pressure applied by the bolt connection. The blade is mounted by having the bolt pass through the blade's hole and the blade is between the two disks, as seen in Figure 3.9, where component marked by 1 is the blade and the component passed by a center line is the bolt. To ensure a proper functioning of the principle behind this cutting tool, it is important to assure that the blades can rotate freely around its rotational freedom axis. For this, a bushing is inserted in the connection between the bolt and the blade, component 1 in Figure 3.9. To avoid contact between the blade and the disks two washers are also inserted, one between the top disk and the blade and the other between the blade and the bottom disk, copmonents marked with 3 in Figure 3.9. A 0.5 mm gap is left to allow the rotation of the blade and the washers have an external diameter of 40 mm to cover the the area until the border of the holding disks. The layout with and without the blade and disks can be observed in Figures 3.10 and 3.11. As with the bolting between the shaft and the disks, this is assembled four times in a "cross" (+) layout, aligned with the previous bolt connection. In Table 3.10 the list of standard components and their quantity is represented.

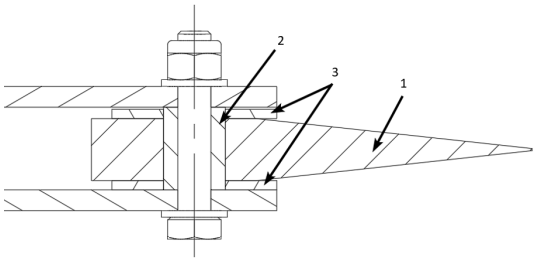

Figure 3.9: Section view of the blade mounted to the disks

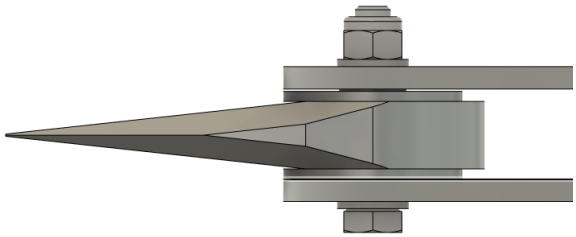

Figure 3.10: CAD view of the blade assembled to the disks

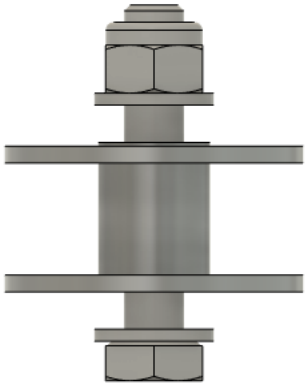

Figure 3.11: Layout without blade and disks

Table 3.10: Normalized components involved in one blade connection. Each cutting subsystem contains four of these connections.

Quantity	Designation
4	Hexagon Bolt ISO 4014 M8x45-8.8
4	Hexagon Nut DIN 982-M8-8
8	Washer ISO 7089-8-200HV

3.4.8 Bushing and Washers Material Selection

A material selection process was done with the aid of the software Granta EduPack 2023 R1 [4] for the bushing and the washer components from the previous chapter. The list of requirements that both the bushing and the washer component would have are as follow:

1. Have a high degree of machinability, for an easy manufacturing process;

[4] ANSYS® Granta EduPack 2023 R1, version 23.1.1, Inc., Cambridge, UK (https://www.ansys.com/products/materials))

2. Hard enough to not be too wearing against steel;
3. Not too dense, to minimize weight at the border of the tool;
4. Low cost;
5. Be resistant in rural areas and with lubricating oil;
6. Low friction coefficient with steel.

Refer to Appendix C for all the charts used in this selection.

A preliminary materials selection chart (also known as Ashby charts) was done with the first two requirements the component woud need. For this, machinability was plotted on the X-axis and the hardness, in Vickers in the Y-axis was generated, as seen in Figure C.1. A high hardness was needed but machinability would also be a big factor in creating the components, so an area selection on the chart was made on the top right corner, as seen in Figure C.2, trying to maximize hardness and machinability, as they can be two conflicting properties. To further reduce the number of options, a second Ashby chart was generated. Weight could play a factor on the acceleration of the disk, while price is usually a concern, so the chart generated used the price as the Y-axis and the density as the X-axis, respectively, fulfilling points number 3 and 4, with the results are shown in Figure C.3. In this phase, it is already possible to observe that there are materials that might meet most of the criteria chosen, such as some natural materials, polymers, metals and alloys, composites, non technical ceramics, one foam material and one elastomer. On the third stage of the selection, all materials with unacceptable or limited use durability with lubricating oil and less than excellent durability in rural areas were removed, using a filter on the software, removing some polymers, a natural material, the elastomer, steel and cast iron, fulfilling point number 5 this way. To fulfill point number 6, the range of values for specific heat capacity and thermal conductivity were observed, and it was noted that polymers could be a good choice for the type of material chosen regarding their good thermal properties. These ranges of values can be seen in Figure C.5. In a last phase of selection on EduPack, density was still plotted against price, however, a limiting filter was applied, for the thermal conductivity property which excluded any materials with values outside of polymers' value range. In Figure C.6 this last Ashby chart is as shown.

As it was not possible to filter materials according to friction coefficients on *Granta Edupack*, a research was done on polymer behaviour against steel. In Reference 54, measurements for friction coefficient and wear behaviour were done on different polymers, and in composite materials with the same polymers as the base, but with Polytetrafluoroethylene (PTFE) filling or PTFE filling plus glass fibre. The measurements were taken on twenty hour tests in both air and water environments. For the twenty hour tests done in air, Polyoxymethylene (POM) with PTFE filling proved to have a low friction coefficient throughout its thermal range as well as good values for the average value of specific wear rate, k, the rate at which the material loses volume per unit force per unit distance when in a motion against another body, together with Polyether ether ketone (PEEK) also filled with PTFE. PEEK with PTFE filling was the compound material that had the best results in this

work and was also one of the materials considered by the Granta EduPack material selection process, in its polymer form. By observing Table 3.11, the results for the friction coefficient and specific wear rate are shown together with the price of their polymer form without the PTFE filling. It is observed that the price difference between both materials is quite substantial. This can also be observed in Figure C.6, where there are bubbles indicating POM, PEEK and PTFE and the vertically distance between each other is quite apparent. Thus, choosing POM as the material for the bushing component and the washer components.

Table 3.11: Comparison of some specifications between POM+PTFE and PEEK+PTFE [53, 54]

Material	**POM+PTFE**	**PEEK+PTFE**
Equilibrium values of the friction coefficient	0.22	0.19
***k* values**	$0.4 \cdot 10^{-15}$ m^3 N^{-1} m^{-1}	$0.6 \cdot 10^{-15}$ m^3 N^{-1} m^{-1}
Price (without PTFE filling)	2.09-2.13 €/kg	80.40-89.10 €/kg

POM with PTFE filling is a polymeric compound, with a polymeric base and a solid additive that creates a separate phase in the composite. PTFE filling is a particular filling and greatly reduces the properties related to friction all while maintaining the mechanical properties related to POM, which are far superior to PTFE, which possesses particularly low wear resistance for example. As PTFE is a soft material, a low amount of filler is needed, as it will spread out across the polymer surface during the use [55].

3.4.9 Cutting Subsystem Overview

The cutting solution obtained is then an altered rotary disc based solution, where instead of being an actual disk cutting the vegetation, two disks hold a set of four blades which are responsible for the cutting action. A distinguishing factor from this solution comes in the form of polymer based composite bushings and washers in contact with some surfaces of the blades, giving the solution a free rotating ability on its axis. This could prove to be fortuitous in the case that the blade hits something harder, allowing the blades to retract and prolong the life of the blades' edge.

In Figure 3.12 the assembled cutting solution can be observed.

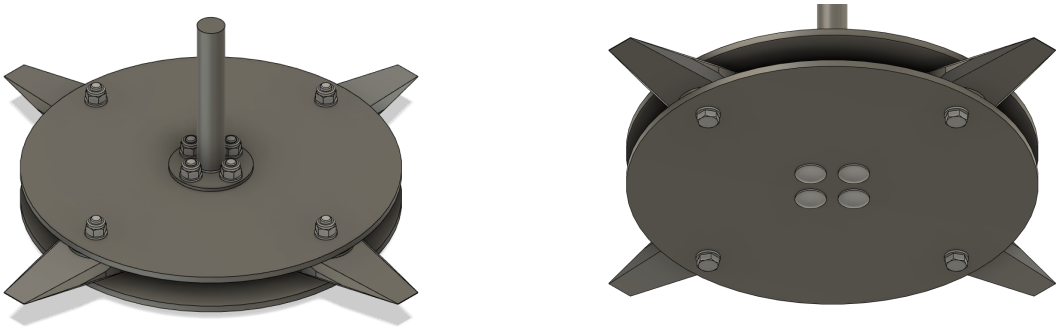

(a) Solution from above

(b) Solution from below

Figure 3.12: Cutting Solution subsystem

3.5 Motor Drive

The motor drive is an essential subsystem for the cutting tool. It is responsible for giving power to the cutting subsystem and ensuring that there is enough power in the system to allow the cut.

3.5.1 Motor Selection

Another distinguishing factor observed on attachments that would be used in remotely operated machines and robots is that many used an hydraulic approach to power it. For the tool that will be designed in this dissertation, an electrical approach will be used. A hydraulic approach if not maintained properly can also lead to leakages, which can be harmful even with the use of bio-friendly oils, while being less efficient and associated losses compared to the electrical motor. It also would not be realistic to install a hydraulic pump to an entirely electrical robot, which would add a degree of complexity to the design which was not desirable. It will use a Direct Current (DC) motor due to limitations on the power delivery coming from the UGV as it is using VARTA Easy Blade battery packs as the power storage unit means that the output of power comes in Direct Current. This discards the option of using three-phase motor, as it would require Alternate Current (AC) to operate and to provide AC, it would require to install an inverter to convert DC to AC, which in turn could also add a lot of complexity, weight to the solution and higher power consumption. DC brushed motors were also discarded due to their higher maintenance needs regarding cleaning and replacement of the brushes.

Despite these setbacks the use of an electrical motor allows for a much more precise control of the speed of the tool, increasing the power efficiency as well as cut efficiency itself.

Another important fact comes from the choice of motor being limited by what was available at INESC TEC's laboratory, where the alternatives that could be chosen were between an unnamed BLDC motor traditionally used in CNC spindles or a 3 kilowatt BLDC motor from Golden

Motor, shown in Figure 3.13. The choice prevailed with the use of the 3 kW motor, as the the specifications of the motor were known and the assembly would be easier.

The CAD files for the motor were downloaded from the Golden Motor website as a *.step* file and imported to *Fusion 360*.

In Table 3.12 the list of characteristics of the motor are listed and in Appendix D the performance curve and data is shown. The motor is the 48 V air-cooled version, as the batteries used on the robot also held this voltage.

Figure 3.13: 3KW BLDC Motor from Golden Motor [56]

Table 3.12: Motor Characteristics [56]

Model	HPM3000B - High Power BLDC Motor
Voltages	48/72 V
Rated power	2-3 kW
Peak power	6 kW
Speed	3000-5000 rpm
Rated torque	10 Nm
Peak torque	25 Nm
Efficiency	>90%
Dimensions	18 cm diameter 12.5 cm height
Weight	7.3 kg (air c.), 8kg (water c.)
Cooling	air or liquid cooling
Output Shaft diameter	20 mm

3.5.2 Motor Working Point

To determine some aspects in subsequent sections of the project, a working state had to be chosen. While this did not mean that the motor would always be running in this state, it meant that values for motor speed and power output could be used for calculations. The point chosen was at 8.9 Nm of torque. The value was chosen by observing the working curve shown in Figure

3.13, found in the motor data and choosing a point that would hold a high efficiency value, still not consuming the maximum power available, which would increase the energy consumption, but hold a high motor speed. The exact values at this working point were taken from the performance data table also found in the motor data for more concrete values that were not visible in the curve.

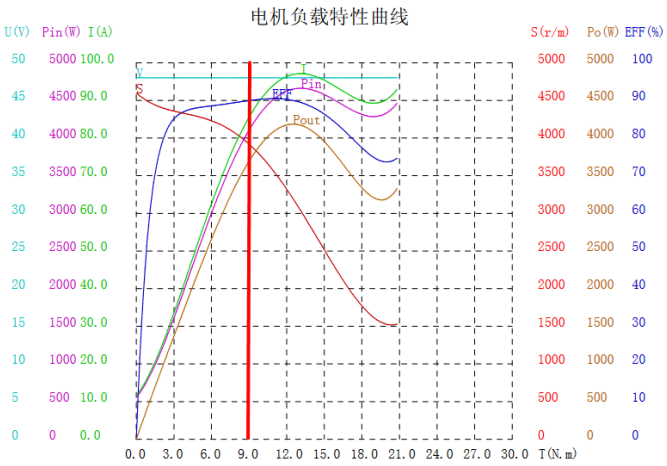

Figure 3.14: Performance Curve of the motor. Red line indicates the working point.

Table 3.13: Engine Values at 8.9 Nm

U (V)	48.0
I (A)	87.20
P_{in} (W)	4186
T (Nm)	8.9
N (rpm)	4017
P_{out} (W)	3773
$\eta(\%)$	90.1

3.5.3 Motor Drive Overview

As the choice for the motor to be applied was limited to two options by INESC TEC's lab, the motor that suited more the needs of the project was a 3 kW BLDC motor by Golden Motor. As the motor was an implied condition, it meant that the adjustment regarding the desired functioning speed and torque would have to be controlled by the mechanical transmission subsystem.

3.6 Mechanical Transmission

The mechanical transmission subsystem, besides converting the speed and torque of the motor, it is also responsible for how the cutting solution will be set up. For the smooth movement of the robot along the cut areas, the cutting tool should cut at around the same width as the robot. As the

motor was a factor already chosen externally, the speed achieved by the blades would be controlled by the ratio chosen for the mechanical transmission in this sybsystem.

3.6.1 Cutting Disposition

First, some values related to MowIT were taken from the CAD model. These values can be seen in Table 3.14 along with a visual representation on Figure 3.14.

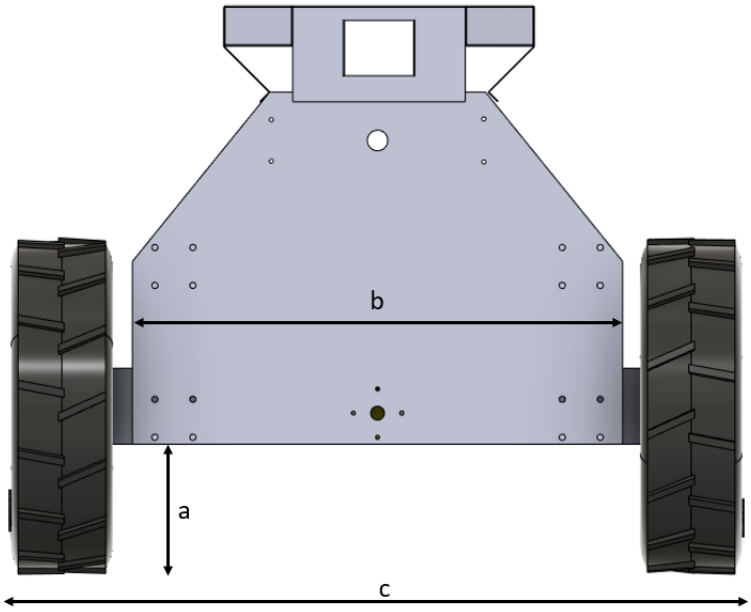

Figure 3.15: MowIT's visual dimension representation

Table 3.14: MowIT's Relevant Dimensions given by the CAD model

a	Distance to the ground (mm)	188
b	Width of the robot without wheels (mm)	710
c	Width of the robot with wheels (mm)	1040

Knowing that the cutting subsystem has a cutting diameter of 394 mm, it was understandable that a single subsystem would not be enough. A three subsystem layout was chosen, as two would not have enough cutting length without leaving an uncut area of the undergrowth. This creates an inverted triangle layout. Two subsystems will be side by side at the front of the mowing implement, while the third subsystem is mounted behind them, ensuring that the cut is even throughout the entire cutting length. In Figure 3.16 this inverted triangle layout is shown, where the circles represented are the cutting diameters of the cutting subsystem.

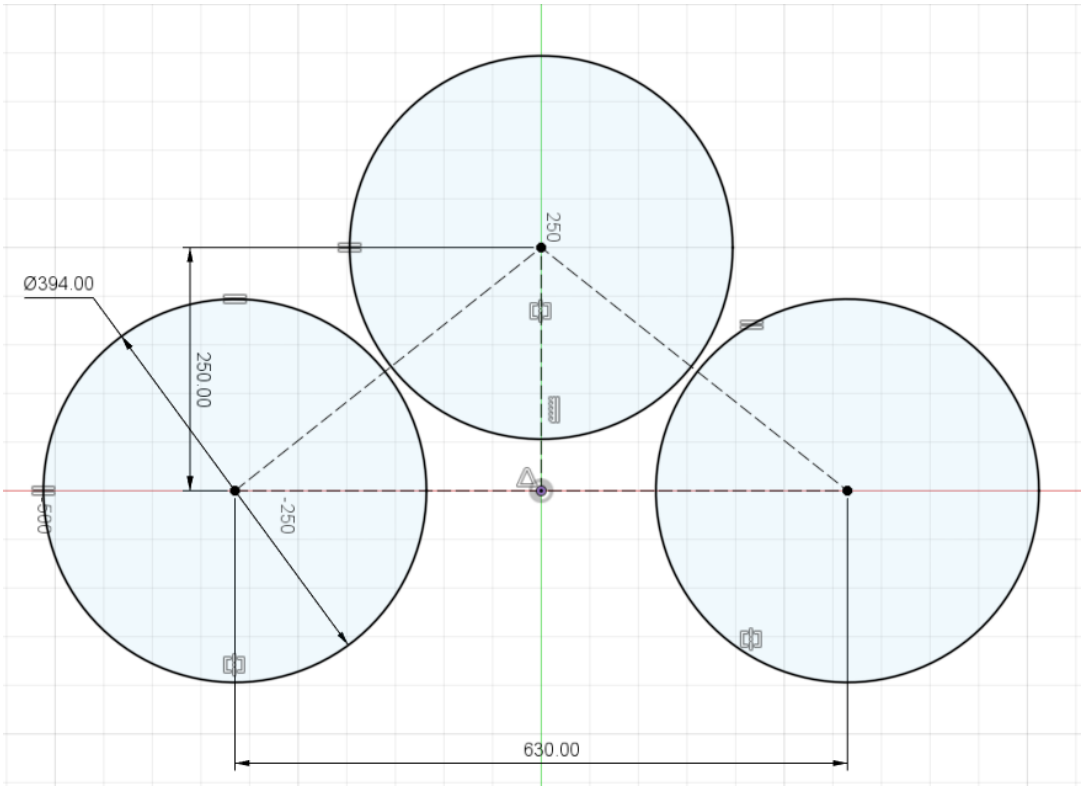

Figure 3.16: Inverted triangle setup

Table 3.15: Dimensions used in Figure 3.16

Cutting Diameter (mm)	394
Distance between front circles	630
Vertical distance between back and front circles (mm)	250

3.6.2 Transmission

To transmit the power, there were a few options observed, namely by the use of gear drives, belt drives or chain drives. Early on, gear drives were abandoned because they couldn't be employed with shafts that had a distance between the centers of the shafts and weren't suitable for high-velocity applications either, so the selection fell between belt drives and chain drives. The drive chosen was belt drive, offering many advantages that greatly matched with the needs sought after for this project. Its simplicity to use together with any load fluctuations being shock absorbed were major advantages in terms of the cutting tool's design and the jam protection and lack of regular lubrication would be advantageous when being applied to an autonomous robot. Their disadvantages could also either be mitigated or not even considered a setback in this design, as a fast wear related problem could be predicted and a replacement integrated in maintenance routines. The heavy load on the shaft would not pose a problem if the shaft was correctly dimensioned. As the tool was a mowing implement for forests, a precise and constant angular velocity was not required, as long as the angular speed would be inside certain range. The lack of compactness could pose a problem, but as said before, all the other advantages outweighed this disadvantage. In Table 3.16 a full list of advantages and disadvantages between the three types of drives is shown.

Table 3.16: Advantages and disadvantages of different drives [57]

	Advantages	**Disadvantages**
Belt Drive	Cost-effective Simple to use No need for parallel shaft Come with jam protection Load fluctuations are shock absorbed Reduce noise and vibrations	Not compact Fast wear and tear Inflict heavy load on shafts Angular velocity not constant
Chain Drive	Drive with no creep Angular velocity is constant Allows for high-speed ratio 8:10 Low maintenance costs High transmission efficiency Can work even in wet conditions Lower load on the shaft	High initial installation cost Requires regular lubrication Noisy
Gear Drive	Non-slip drives Mechanically strong Deliver high transmission efficiency Ideal for low, medium and high power transmission More compact compared to belts and chains	Cannot be used when shafts are distant between each other Not ideal for large velocities Need regular lubrication Multiple gears raise machine overall weight

3.6.3 Belt Drive

For the application of a belt drive, Optibelt was chosen by INESC TEC's lab, being a respectable brand and having been used in the past.

The power delivery was setup in a multiplication setup, which in a two pulley setup would mean that the driven pulley would have less torque available to use. However it could maintain a higher rotational speed compared to the driver pulley, while both having the same power at the shaft, theoretically. In a multi pulley setup, such as this one, the power is divided by the number of driven pulleys. Since the belt speed is the same throughout the system, if the driven pulleys

all have the same diameter, all of them will have the same rotational speed and, consequently, the same power and torque, which was split from the motor. As a multi pulley setup would be too complicated to setup by hand, Optibelt's drive calculation software *CAP 6.5*[5] was used for belt and pulley dimensioning.

For space saving measure, an overlapping layout for the belt pulleys was thought of. In this layout all the driven pulleys would be driven by the inside area of the belt, while the driver pulley would mesh with the outside of the belt, having the added benefit of acting as an idler pulley would. In Figure 3.17 a more visual representation can be seen, with numbering for each pulley. For this setup, a double sided belt would be necessary, allowing for both the use of the outside part of the belt and the inside. Using dimensions in Table 3.15, the power and rotational speed from Table 3.13 and the shafts diameter from Tables 3.7 and 3.12, a drive setup was created on the software. A service factor of 2.0 was chosen for the intermittent operation with medium to high shock up to 16 hours a day the robot could be subjected to. An original vertical distance of 110 mm between the front disks and the motor was chosen and the vertical positioning would be the middle between the front disks, aligned with the back disk.

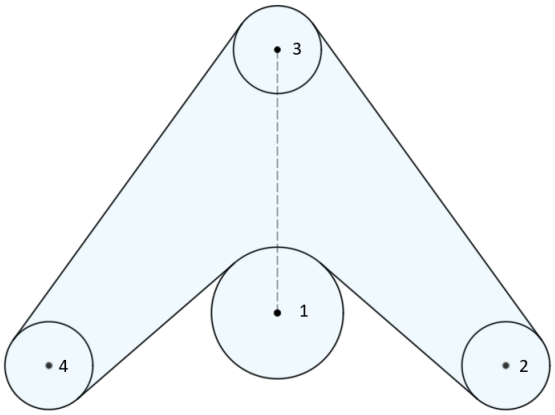

Figure 3.17: Pulley Layout
(dimensions are not to scale)

Due to design limitations, a speed of 8200 rpm on the driven shafts could not be achieved, giving a software error. The max speed achieved through the calculation was 7304 rpm. For this speed to be achieved, a timing belt had to be used, opposed to a v-belt. A timing belt carries some advantages compared to a v-belt, such as less maintenance required, higher efficiency and elimination of slippage [58]. The components determined by the software can be observed in Table 3.17.

A piece of information taken from the software informed that an offset of 7.77 mm would have to be applied to the motor positioning, in the y-axis. Other considerations from the software and relevant values for later chapters are available in Table 3.18.

[5] © Optibelt GmbH. Optibelt CAP, version 6.5, Höxter, Germany (https://www.optibelt.com/en/the-company/e-services/)

Table 3.17: Components suggested by Optibelt's software, for the motor working point

Timing Belt Profile	Optibelt OMEGA 1696 D8M-HP 20 special belt
Driver pulley	TB 40-8M-20
Driven pulley	TB 22-8M-20
Driver shaft taper bushing	Optibelt-TB taper bush 1610
Driven shafts taper bushing	Optibelt-TB taper bush 1008

Table 3.18: Relevant values taken from Optibelt's software (available in Appendix E)

Drive Ratio, i	0.55
Rotational Speed	7304 rpm
Torque, M_t, in each shaft	1.6 Nm
Power in each shaft	1.66 kW
Static belt tension	111 N
Shaft load on pulley 2 and 4	222 N
Shaft load on pulley 3	138 N

3.6.4 Pulley Assembly

To have the power from the motor deliver power to the shaft, the pulleys needed to be installed into the designated shafts. A taper lock bush system was chosen for its snug fit that would prevent the pulleys from sliding out their place and allow an easy assembly.

3.6.4.1 Assembly to the Cutting Subsystem

For the cutting subsystem, a parallel key ISO/R 773 (DIN 6885) is inserted into the keyway cut into the shaft. The TB 22-8M-20 pulley is inserted to the taper lock bush Optibelt-TB taper bush 1008 and then slid into the shaft until it is aligned with the key. Afterwards the screws are tightened into in the taper lock to secure the assembly in place. In Figures 3.18 and 3.19 the components assembled are depicted.

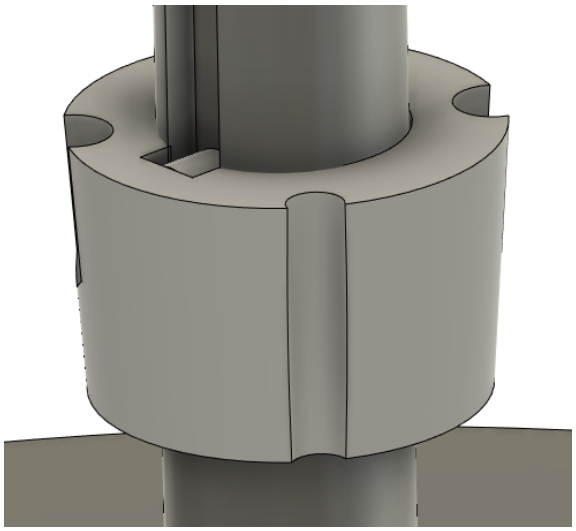

Figure 3.18: Assembly without the pulley

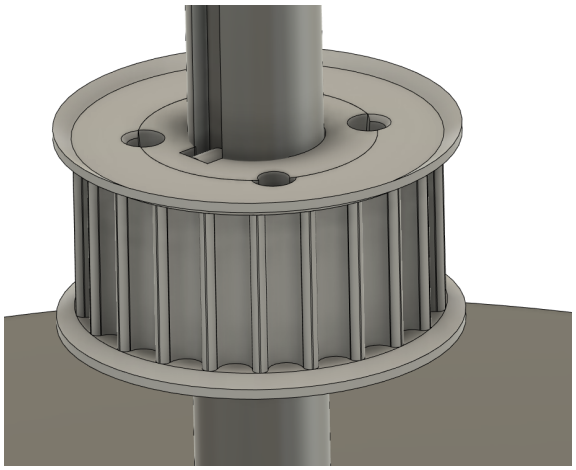

Figure 3.19: Assembly with the pulley

3.6.4.2 Assembly at the Motor

The procedure to assemble the pulley and taper lock bush into the motor is similar to the assembly mentioned previously. However, the motor had a non standardized size at the parallel keyway. To correct this, a cut was done, according with the set values in ISO/R 773 for parallel keys so that the pulley could be assembled correctly. In Figure 3.20 this detail can be observed.

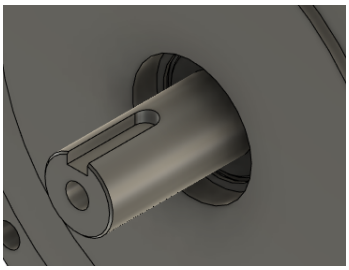

Figure 3.20: Detail of the new motor's keyway

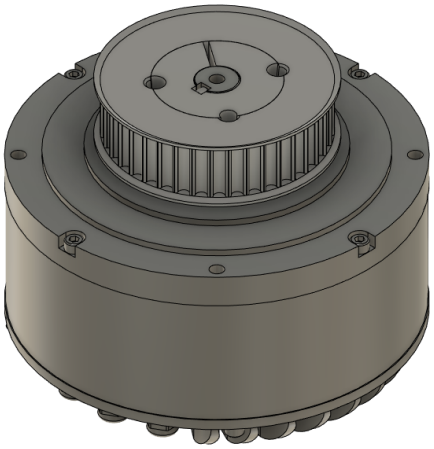

Figure 3.21: Pulley assembly in the motor

3.6.5 Power Delivery Overview

A belt drive system was chosen for its advantages and having the possibility of its disadvantages being mitigated. To avoid a big area being occupied by the belt drive system, a unorthodox pulley layout was chosen that could save space while maintaining performance. This meant the use of a double sided belt and meant that the driver pulley would be meshing with the outside area of the belt while the three driven pulleys would mesh with the inside of the belt.

Being limited by the motor used, an attempt to maximize the rotational speed of the cutting system was made in Optibelt's software, however the desired rotational speed was not achieved. Despite this, the speed achieved could already be considered a high speed. To maintain belt tension

and correct positioning of the pulleys, in the following chapters a system to adjust the driver pulley and, consequently, the motor will be devised as we;;.

3.7 Supporting Structure

In order to allow all the other subsystems to connect and interact between each other, the supporting structure subsystem needs to be designed in accordance. This subsystem is responsible for:

- connecting the cutting tool to the robot;
- holding the cutting subsystems in their geometrical place, keeping an alignment in accordance to the power delivery setup;
- holding the motor in its place but allowing adjustments to be made to the positioning for the belt drive system;
- adjusting the height of the cutting tool to allow better locomotion to the robot when not in use and make adjustments to the cutting height.

To perform these various tasks, the supporting structure is then composed by different components, all responsible for the correct functioning of the mowing implement when they are working in tandem.

3.7.1 Structural Inspiration

The design for the method of fixation of the structure to the robot was loosely based on three point trailer hitches used in tractors, like the one seen in Figures 3.22a and 3.22b. These are often used to hold agricultural equipment in place and are able to do adjustments on the angle of the tools relative to the soil.

The designed structure would then be created based upon the sketch in Figure 3.23. Some geometrical constraints were assumed, being the following:

- the connection A and B in Figure 3.23 would always maintain a relation of parallelism and have the same length;
- the connection C would have variable length to allow a variation of the tool's height to the ground.

Another design choice taken from the three point hitch design was the fact that the connection B and C in Figure 3.23 would be composed of two connections, one on each side of the supporting structure, while the connection A would be composed of only one connection. Though in the diagram it is not seen, as it is a 2D sketch representing the side view, from the front the connectors would form a triangle shape.

(a) VOWAGH 2" Receiver 3 Point Trailer Hitch Category 1 [59]

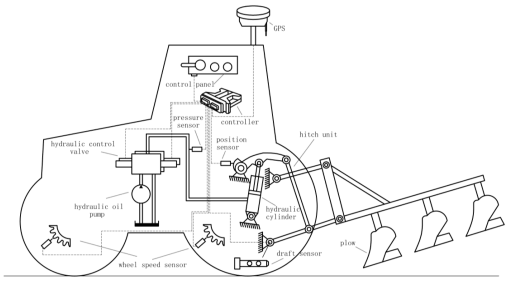

(b) The structure principle of the modern electro-hydraulic hitch system. [60]

Figure 3.22: Loose inspirations for the structural design

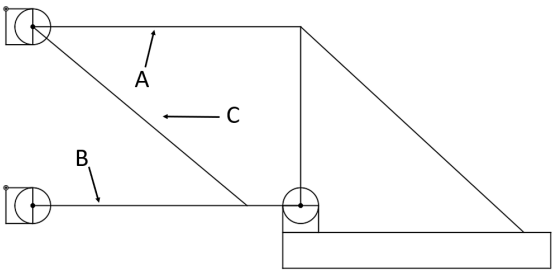

Figure 3.23: 2D sketch of an outline for the supporting structure (not to scale)

3.7.2 Materials Chosen

The material chosen for most components in this subsystem was AISI 304 in sheet metal form, a versatile stainless steel widely used in the industry for its good mechanical properties, resistance to corrosion (due to the presence of chromium in its constitution) and great machinability and welding capacities and in sheet form allows for the construction of able structures with an easier process of fabrication. The properties were taken from Granta EduPack and are as shown in Table 3.19. As such, if not mentioned, it is assumed that this was the material chosen.

Table 3.19: Material Properties of AISI 304 [53]

Material	Density (kg/m^3)	Young's Modulus (GPa)	Yield Strength (MPa)	Tensile Strength (MPa)	Poisson's Ratio	Price (€/kg)
AISI 304	7850-8060	190-203	205-310	510-620	0.265-0.275	2.34-2.67

3.7.3 Enclosure

An enclosure was designed to isolate the mechanical transmission system from the outside. As the timing belt can achieve speeds of up to 77 km/h, this additional protection can further avoid outside interference to the good operation of the tool. The enclosure will also hold the bearing units responsible for the alignment of the cutting subsystem's shafts and the supports for the connection to the robot. It is comprised by the box component and the lid component. The box component does not possess front and top faces, being covered by the lid component, which is L shaped.. This makes the enclosure parallelepiped shaped. Both components are formed by sheet metal bending and have flaps in them to allow assembly of both components into the enclosure, with the use of rivet nuts. A thickness of 2.5 mm is applied as it is a standard thickness used in the industry. The box and lid components are connected between each other by 8 bolt connections, five at the top face of the enclosure and three at the front. They are connected with hexagon head bolts ISO 4017 and spring washers DIN 127 B V2 bolted on rivet nuts which are riveted to the box component. This connection can be seen with more detail on Figure 3.24

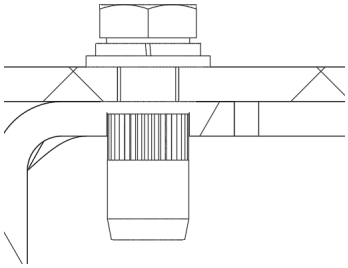

Figure 3.24: Section View of the bolting connection

The lid holds the trapezium component, mounting brackets related to the connection of the supporting structure to the robot and the support plate for the motor, which will be mentioned in the following chapters.

Both the box and lid have clearance holes in accordance to the positioning in Appendix E with the shafts' diameter found on Table 3.7. These will allow the correct positioning of the three shafts related to the cutting motion of the cutting tool and allow for the mounting of bearing units to secure and align the shafts. Around each clearance hole there are holes for the mounting of these bearing units. The lid possesses a clearance space at the top, four hexagon head bolt ISO 4014 welded with their threads facing upwards for easier mounting and alignment of the motor. Slots cut in the lid component to allow a more aligned welding of the components responsible for securing the connection to the robot on each side of the enclosure and the trapezium component. All these features can be observed in Figure 3.25 and a list of standard components for the bolt connection between the plates can be found on Table 3.20.

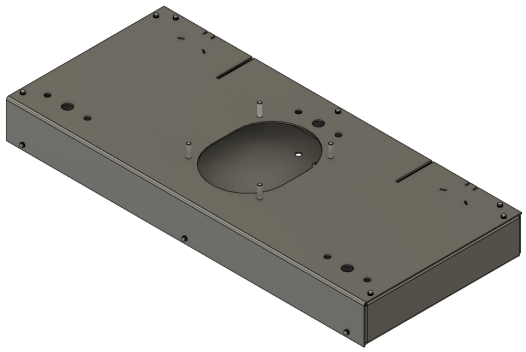

Figure 3.25: Enclosure, the box and lid bolted on each other

Table 3.20: Normalized components involved in the bolting in the enclosure

Quantity	Designation
8	Hexagon Bolt ISO 4017 M4x14-A2
8	Washer ISO 7089 4-A2
8	Spring Washer DIN 127 B V2 4-A2
8	Rivet nut with small countersunk head and M4-A2

3.7.4 Connection to Robot

For a connection of the mowing implement to the robot, some components had to be designed to maintain the geometric relations in Figure 3.23. Together they are responsible for attaching the cutting tool to the robot, but also adjust the height of the tool.

To create the connection between the enclosure and the robot, there are four types of components involved. These are the following:

- the "trapezium", welded on to the lid;
- the mounting brackets, bolted on the robot;
- the connecting appendages, welded on the lid and the trapezium;

- the union bar, connected to the mounting brackets and appendages with eye bolts.

The mounting brackets are the interface for the connection between the union bars and the robot. There are three mounting brackets bolted on the robot, two on the bottom and one on the upper side. The bottom location was chosen from pre-existing mounting holes from the tool applied to it, while the top location was chosen as the middle point between the existing mounting holes already located on the top.

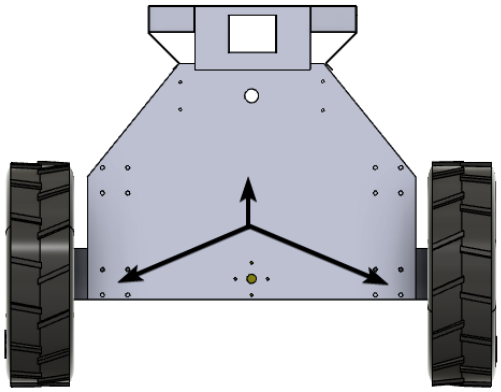

Figure 3.26: Position for the mounting brackets

They are designed using sheet metal and are comprised of a plate that is secured to the robot and the mounting flaps. The plate is squarely shaped with rounded edges and has four holes for securing the bracket to the robot via the use of bolts. The positioning of the holes were already pre-established from securing holes present in the robot. On top the bottom plate, bent sheet metal flaps are welded on to the bottom plate via butt welding. Figure 3.27 shows the mounting bracket component, Figure 3.28a shows the bottom plate with the holes for the inserts and Figure 3.28b shows the flaps with the inserts for welding, with different colored arrows for each flap. The design chosen for the flaps was chosen to allow different stresses to be applied to the brackets without risking the integrity of the weld.

Both flaps have a hole passing through to allow a DIN 1434 clevis pin to be mounted on it. This pin has a DIN 11024 spring cotter through its hole to limit the movement axially, while allowing easy assembly and removal of it. The distance between flaps is 15 mm, as an eye bolt will be inserted in it. In Figure 3.29 the mounting bracket with the clevis pin and spring cotter is shown

The mounting brackets are connected to the connecting rod. This rod formed by an AISI 304 15x1.5 mm stainless steel round tube, applied with an internal M12 thread on both of its ends and two DIN 444 B eye bolts, one on each end, that will connect the mounting brackets to the appendages. Figure 3.30 shows the tube with with both of its connectors used for the connection to the appendage in the trapezium, while table 3.21 shows the tube dimensions. The side connecting rods are cut to accommodate two elastic rings for the lifting mechanism, as seen in Figure 3.31.

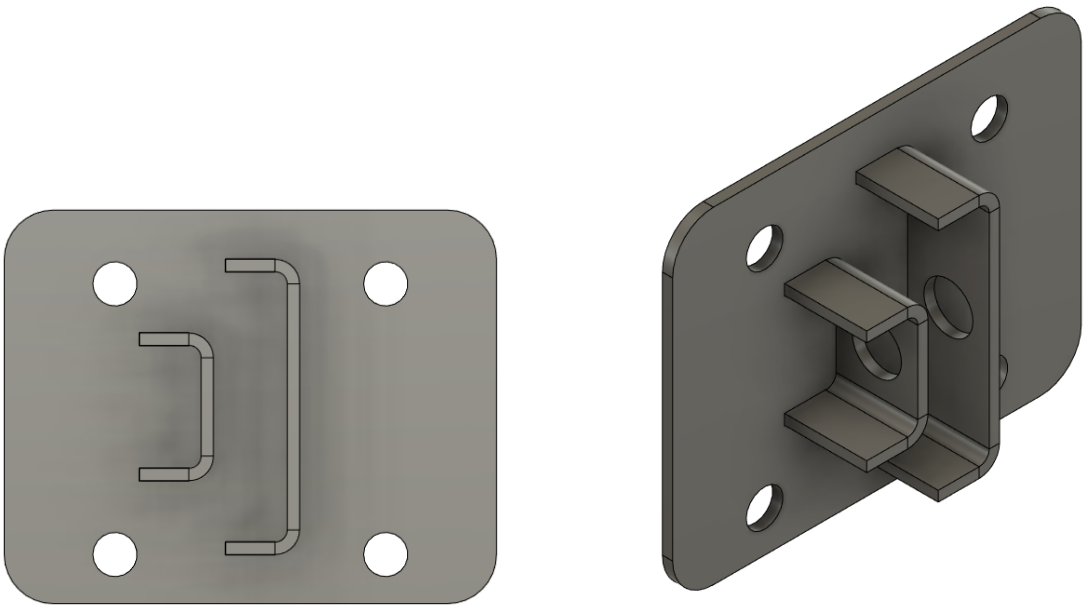

(a) Top View (b) Isometric View

Figure 3.27: Mounting Bracket component

Table 3.21: Connecting rod specifications

Outer diamter (mm)	15
Thickness (mm)	1.5
Length (mm)	286
Internal thread	M12x55

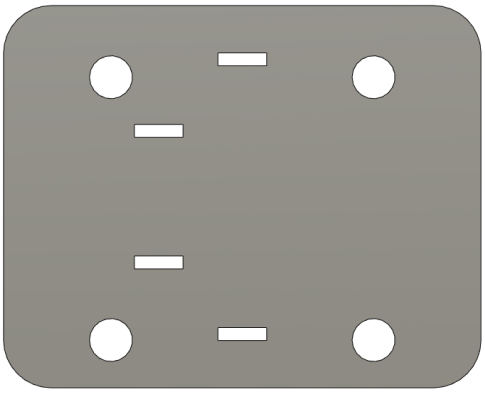

(a) Plate without the flaps

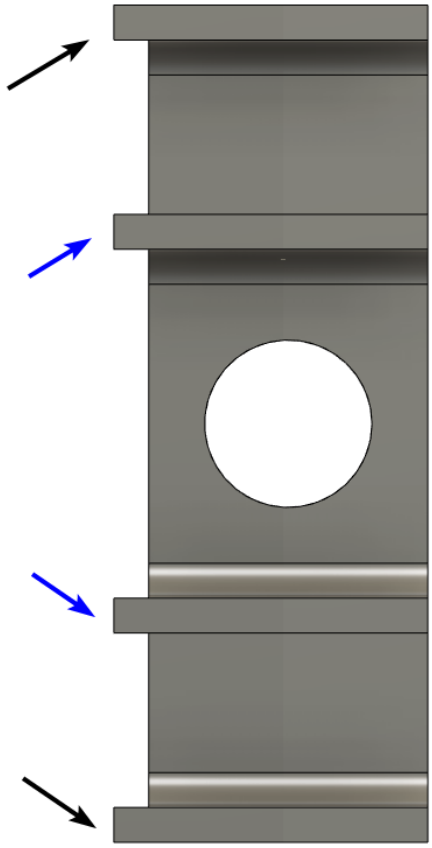

(b) Flaps with inserts for welding. The black arrows point to bigger flap and the blue arrows to the smaller flap

Figure 3.28: Weld details for the bracket

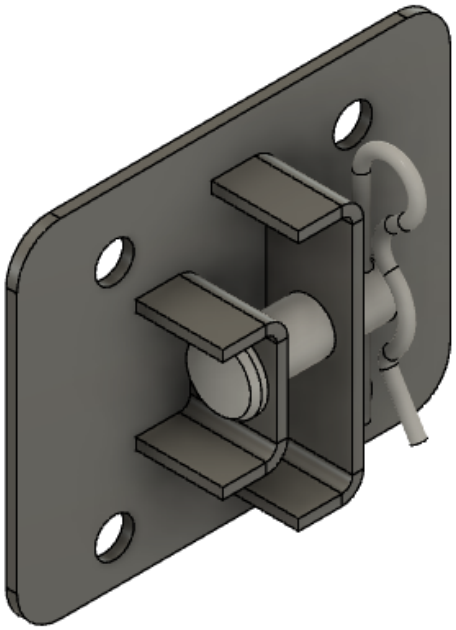

Figure 3.29: Isometric view of the mounting bracket with the clevis pin and spring cotter applied to it

Figure 3.30: Side view of the top connecting rod with the eye bolts applied

Figure 3.31: Isometric view of one side rod with the elastic ring cutouts

The appendages are sheet metal flaps that are welded to both sides of the enclosure's lid and on top of the "trapezium" to hold the clevis pin responsible for the connection of the union pipe to the enclosure. The appendages have analogue dimensions in regards to the gap between each flap and the hole in them, as the clevis pins are the same on both ends of the union assembly. The appendages are butt welded to either the lid or the "trapezium" and are bent to an angle to increase resistance to stress. As welds are more susceptible to failure by shear stress, the addition of an angle on these flaps will mitigate the shearing stress, but still maintain easy access for the mounting and removal of the clevis pin. If the angle in the bend was over 45º, the access to the pin could be affected. Both the appendages, as well as the lid and trapezium have either inserts or slots, respectively, with a 0.1 mm gap to allow butt welding to occur. In Figures 3.32a and 3.32b, the appendages are shown with the clevis pin and cotter sprint already applied and a lower view of an appendage applied to the trapezium part.

[b]

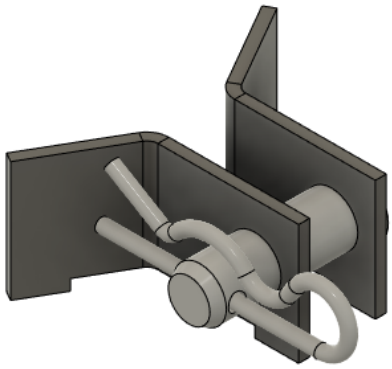

(a) Isometric view of the appendage with clevis pin and cotter spring applied

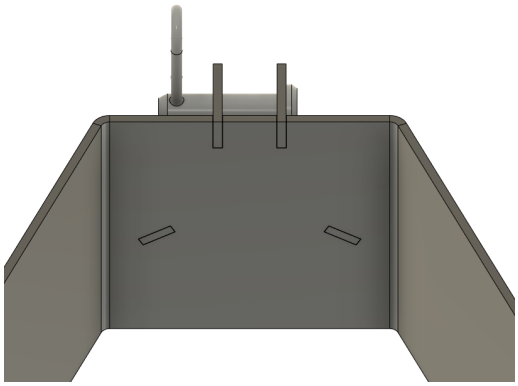

(b) Lower view of the appendage applied to the trapezium

Figure 3.32: Two views of the appendage

The trapezium is a mounting component which allows one of the appendages to be mounted in a higher height, following the diagram in Figure 3.23. As only one appendage is welded on the top, the shape of the component is a trapezium when viewed from the front, originating the nomenclature of this component. It is bent into shape and then welded said flaps to the lid component. Applying a trapezium shape can contribute to a strong geometrical shape for supporting loads, which together with the use of sheet metal can help to maintain a good rigidity in the transversal direction, while allowing for components to be mounted under it, such as the bearing units for the cutting subsystem shafts. In Figure 3.33 different perspectives of the trapezium component are shown.

In Table 3.22, the standardized components are listed as well as the total quantity for the connections.

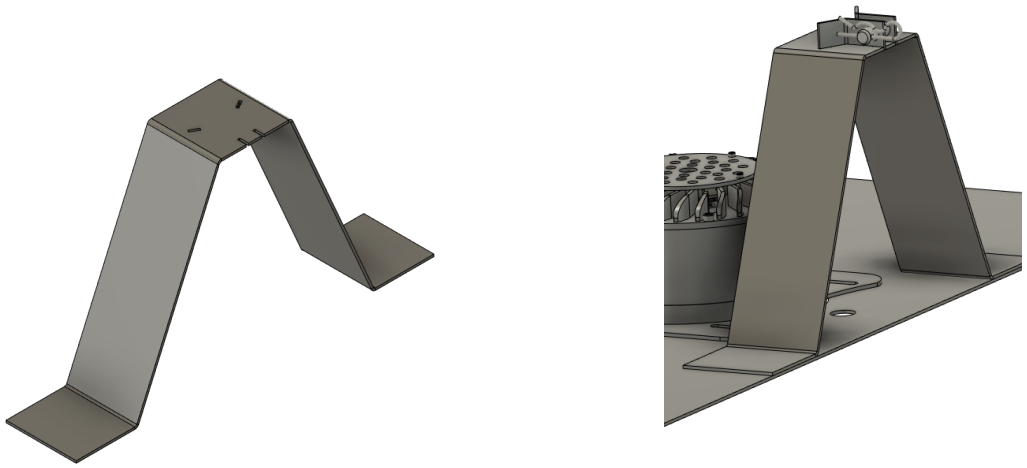

(a) Isometric view of the trapezium component

(b) Side view of the trapezium component mounted on the lid

Figure 3.33: Trapezium component in different perspectives

Table 3.22: Total number of normalized components involved in the connection

Quantity	**Designation**
6	Clevis pin with small head DIN 1434 A 12x35-A2
6	Spring cotter DIN 11024 2.5-1-A2
6	Eye bolt DIN 444 B M12x50-A2
12	Hexagon bolt ISO 4014 M8x30-A2
24	Washer ISO 7089 8-A2
12	Hexagon nut DIN 982-M8-A2

3.7.5 Lifting Mechanism

For height adjustment, electric linear actuators from Thomson Linear were chosen. The model chosen was the Electrak GX with the specifications as in Table 3.23. Mounting brackets are used to secure the actuators to the robot and maintain rotational freedom,. Mounting connectors are cut and bended sheet metal pieces welded in the same fashion as in Figure 3.28a and 3.28b, and can be seen in Figure 3.34. For the connection to the actuator, an ISO 2340 clevis pin without head is inserted to a hole and secured with two elastic rings, one on each side, as seen in3.35.

Table 3.23: Electrak GX specifications [61]

Quantity	Designation
Nominal Stroke	2 in.
Weight	4.4 kg
Dynamic load limit	1100 N
Static load limit	11 350 N
Maximum speed	54.10 mm/s
Minimum speed	32.00 mm/s

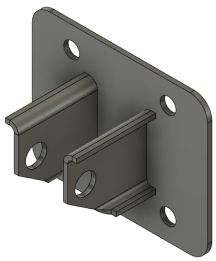

Figure 3.34: Isometric view of the mounting bracket

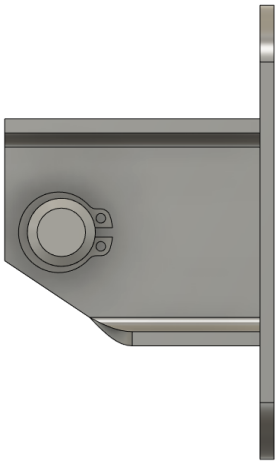

Figure 3.35: Side view with clevis pin mounted to the hole and secured by an elastic ring

To mount the actuator to the connecting rod, a securing component out of sheet metal was designed. This component is composed of four sheet metal pieces in a sandwich disposition, where the bottom piece is bent into the curvature of the rod, the middle piece is a simple sheet piece, and the top pieces are L shaped and create the bracket to secure the actuator. This is identified by numbers 1, 2 and 3, respectively, in Figure 3.36. As seen in the figure, the component is bolted into shape with two ISO 4014 hexagon head bolts and DIN 982 hexagon nuts and the connection to the actuator is done the same way as in the mounting bracket. To block the securing component from moving axially on the connecting rod, two DIN 471 elastic rings are used, as seen in Figure 3.37. Table 3.24 shows the standard components involved in the lifting mechanism.

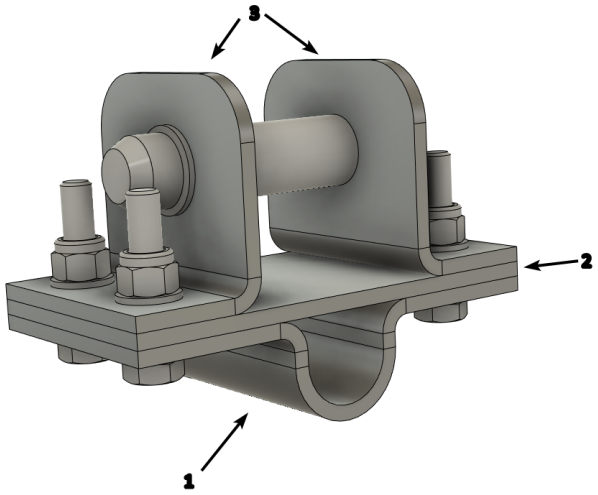

Figure 3.36: Securing component with identifying numbers

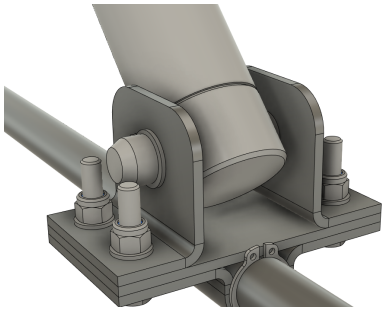

Figure 3.37: Securing component mounted on the connecting rod

In Figure 3.38 the whole lifting mechanism can be seen mounted on the connecting rod.

Table 3.24: Total number of Normalized components involved in the lifting mechanism

Quantity	Designation
4	Clevis pin without head ISO 2340 A 12x55-A2
8	Elastic ring DIN 471 V2 12x1-A2
4	Elastic ring DIN 471 V2 15x1-A2
8	Hexagon bolt ISO 4014 M8x30-A2
16	Washer ISO 7089 8-A2
8	Hexagon nut DIN 982-M8-A2
4	Hexagon bolt ISO 4014 M5x30-A2
8	Washer ISO 7089 5-A2
4	Hexagon nut DIN 982-M5-A2

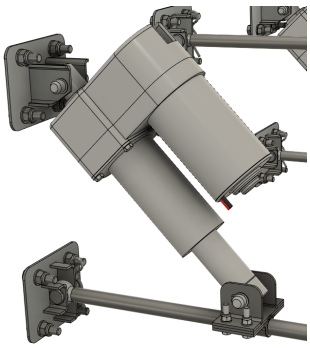

Figure 3.38: Lifting Mechanism

3.7.6 Motor Plate

A motor plate was designed for ease of use when assembling and allow adjustments to be made regarding belt tensioning. It is made out of sheet metal with a thickness of 3 mm. The thickness was chosen so that the plate would have a flush fitting in relation to the motor component containing the screw holes for fixation. The plate contains four holes aligned to the mounting holes of the motor and slots for alignment and mounting of the plate to the lid component, as seen on Figure 3.39. For the assembly of the motor plate to the lid, the welded screws on the lid are inserted into the motor plate's slots, adjusted and then four torque prevailing nuts are fastened into the screws. Torque prevailing screws were chosen to prevent any loosening from machine operation. In Table 3.25 a list of standardized components used for this connection is shown. A curved detail is removed from the plate to prevent any obstructions to the assembly of any bearing units for the cutting subsystem situated aback. To fasten the motor to the plate, four ISO 7380 screws are used. In Figure 3.40 the motor plate is shown mounted on the motor and in Figure 3.41 the motor plate is shown assembled on the the lid.

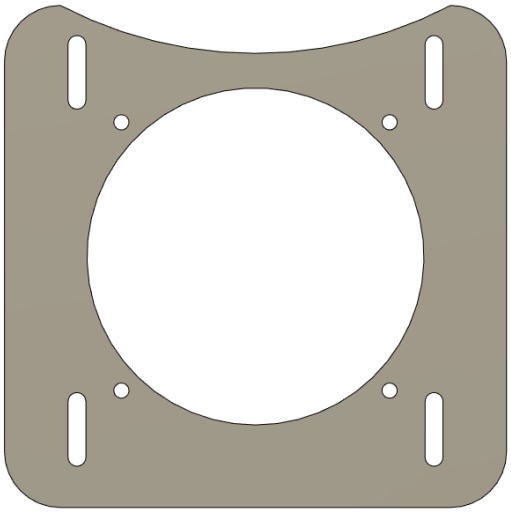

Figure 3.39: Motor plate from the top

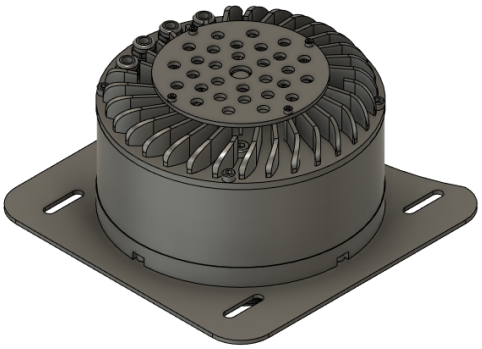

Figure 3.40: Motor mounted on the plate

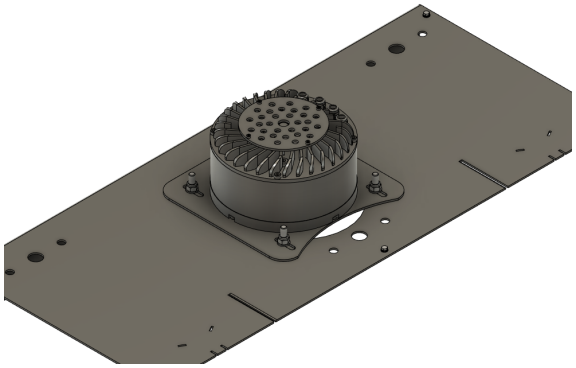

Figure 3.41: Motor and plate mounted on the lid component

Table 3.25: Normalized components for adjusting the motor position and motor fixation

Quantity	Designation
4	Hexagon bolt ISO 4014 M8x30-A2
4	Washer ISO 7089 8-A2
4	Hexagon nut DIN 982-M8-A2
4	Screw ISO 7380-1 V2 M8x10-A2

3.7.7 Bearing Units

To align the cutting subsystem shafts, axially block the shafts from moving vertically but allowing them to freely rotate along its axis, bearing units were chosen. Bearing units are mounted bearings and housings with rolling bearings which can be fastened to a machine frame and support a rotating shaft. This means that it is not necessary to machine a bearing housing in a surrounding casing. As a result, these units provide full rolling bearing performance while being inexpensive and easy to use. Bearing units from *SKF* © were chosen for their widely available status along with recognition in the industry. To select the appropriate unit for installation, *SKF* ©'s website along with PUB BU/P1 13728 EN catalogue were used [62, 63].

For the selection of the bearing unit, a few initial choices were made:

1. between roller bearing units and ball bearing units , ball bearing units had to be chosen as *SKF* did not offer roller bearing units for 20 mm shafts and this was the brand chosen;

2. between pillow block, flanged and take-up units, flanged units were chosen due to their design allowing for an easier assembly of the unit.

When choosing a bearing unit housing, there were four types of shapes considered, these being:

- square units;
- oval units;
- round or triangular units;
- three bolt bracket units.

As three bolts bracket units did not have models capable of reaching speeds of around 7300 rpm, this shape was firstly discarded. It was observed that the oval shape could achieve a lower width, compared to other shapes of units, by having higher length values for same bore diameter values. As vertical width had more limitations compared to horizontal length, as seen in Figure 3.42, an oval shape housing for the bearing unit was chosen.

As the bearing would need to rotate at speeds in the range of 7300 rpm, the next constraint chosen was the maximum speed allowed for a bore diameter of 20 mm. This reduced the choice to eleven bearing units.

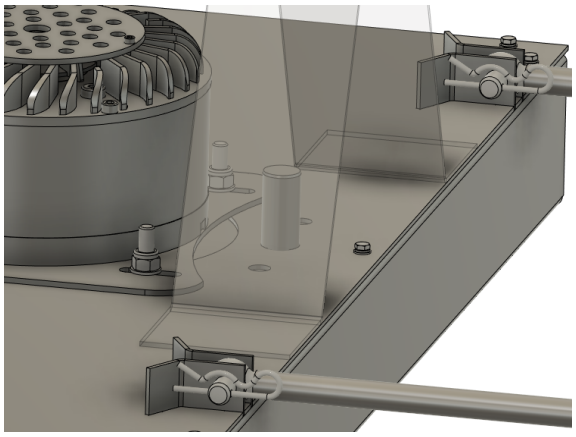

Figure 3.42: Detail of the short space between the shaft and the motor's position

SKF provides bearing units in different housing materials, such as grey cast iron, composite or pressed steel. Grey cast iron was the material chosen for the housing between grey cast iron, composite or pressed steel. The company advises the use of grey cast iron housing if the bearing unit will be under any of the following conditions:

- high levels of contamination;
- high temperatures;
- relatively heavy loads;
- high speeds.

As the bearings will be under high speeds, grey cast iron was the material chosen. The presence of a grease fitting in the housing that allows relubrication of the unit is also necessary in the case of contamination.

Another criteria chosen was the compliance with ISO standards, leaving only three options to choose from, shown in Table 3.26.

Table 3.26: The three choices remaining

Designation			**Locking Method**
Bearing Unit	**Bearing**	**Housing**	
FYTB 20 FM	YET 204	FYTB 504 M	Eccentric locking collar
FYTB 20 TF	YAR 204-2F	FYTB 504 M	Grub Screws
FYTB 20 WF	YEL 204-2F	FYTB 504 M	Eccentric locking collar

As the grub screw locking method is typically used for applications where the shaft alternates the direction of the rotation, the bearing unit chosen was the SKF FYTB 20 TF.

This model offers many advantages for the cutting tool. The grub locking mechanism allows for easy mounting and dismounting of the shaft, while allowing the high speeds desired by the system. The presence of the grease fitting can extend the lifespan of the unit. The YAR 204-2F

bearing contained in the unit possesses an extended inner ring on both sides can reduce the tilt on the shaft from the inner ring, which in turn can help the bearing to run more uniformly. The presence of the denomination 2F on it also refers to the presence of plain sheet flingers, a valuable asset on the prevention of contamination from the exterior. The bearing unit also allows the use of an end cover on it, in the form of the ECY 204.

Two SKF FYTB 20 TF were mounted on the enclosure for each shaft, one at the top of the lid, with the end cover attached to avoid accidents and one inside the box component, making it a total of six bearing units used. An assembly of the bearing units with the cutting solution can be observed in the sectioned front view in Figure 3.43. The bearings are fastened to the enclosure with the use of two ISO 4014 hexagon head screw bolted to a DIN 982 torque prevailing hexagon nut. A DIN 127 V2 B spring washer is between an ISO 7089 washer and the hexagon head screw, as per the mounting instructions by SKF. In Table 3.27 a list of standard components along with their quantity is shown.

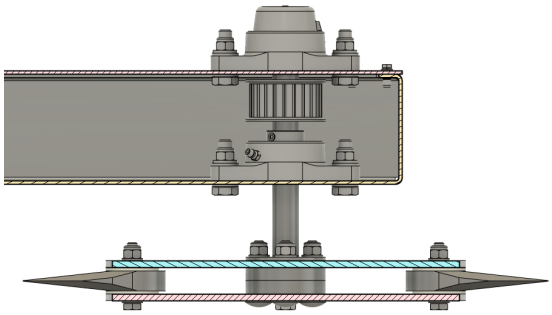

Figure 3.43: Sectioned front view of the bearing unit assembly with the cutting solution

Table 3.27: Standard components involved with the bearing units

Quantity	**Designation**
12	Hexagon bolt ISO 4014 M10x35-A2
12	Spring Washer DIN 127 B V2 10-A2
24	Washer ISO 7089 10-A2
12	Hexagon nut DIN 982-M10-A2

To achieve a proper functioning conditions, a shaft tolerance of h6 is required to achieve high rotating speeds, according to SKF. Regarding the mounting of the bearing units to the supporting surface, it is also advised for a surface of roughness of 12.5 μm or lower and a planicity of IT7 or IT8. For bearings of size 4 and a rotational speed of 7304 rpm, SKF advises relubrication every 20 000 hours for operating temperatures between 40°C and 55°C, if the shaft is vertically positioned. This relubrication period may be shortened due to the working conditions for the tool in environments with dust particles in the air.

3.7.8 Supporting Structure Overview

A supporting structure was designed to accommodate all the other subsystems while providing a mean to connect to the robot. An enclosure composed of a box and a lid made out of sheet metal was made, with cuts done to align and weld components to create a connection to the robot. The connections involve eye bolts mounted on clevis pins, allowing rotation along their axis, with no other degrees of freedom allowed. Mounting brackets were designed with sheet metal to bolt on the robot and have another rotating support on the side of the robot. To connect both of these supports, stainless steel tube with an internal thread is used. To have a height difference between the top support and bottom supports, a trapezium component was made out of bent sheet metal and welded on the enclosure. A hole is present on the lid component to allow easy assembly of the motor, which together with the use of a motor plate screwed to the motor and with slots on it, allow uniaxially adjustment of the motor. A lifting mechanism using linear actuators is used for height adjustment of the supporting structure and, consequently, of the cutting tool's height. It is comprised of a mounting bracket bolted on the robot, a linear actuator and a fixing component attached to one of the stainless steel tube with a fixing component and elastic rings. Bearing units from SKF are used to align the shafts from the cutting solution and also lock the shafts from moving vertically. In Figure 3.44, an isometric view of the whole supporting structure subsystem can be seen.

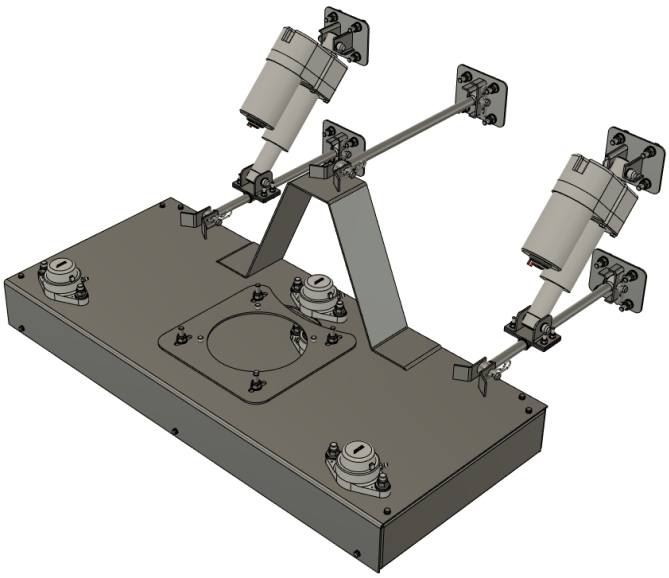

Figure 3.44: Supporting Structure final view

3.8 Design Overview

The cutting tool is then designed and assembled together in the CAD software, with all respective subsystems being mounted on the supporting structure. A render view of this system

can be seen as in Figure 3.45. The cutting subsystem is located in a triangular positioning on the enclosure, being locked from moving axially and being aligned by the bearing units. The pulleys are all inside the enclosure, protecting them from outside perturbations and their alignment is also secured by the axial locking mechanism on the bearing units, as seen in Figure 3.46.

Both the mounting brackets for the connecting rods and the mounting brackets for the linear actuators are located in their appropriate positions and have the bolt connections needed to bolt to the robot with the spacing to account for the robot's thickness. All the connections are established and the motor is mounted on the the motor plate and is allowed to make adjustments if the hexagonal nuts are unbolted. Something worth mentioning is that although not studied, due to the characteristics of the Connecting Rod component, it is possible to adjust the length of the rod by screwing or unscrewing the eye bolts, thus adjusting the angle the tool has in relation to the ground. This can in turn allow optimization of the angle of attack of the blade.

Figure 3.45: Render figure of the cutting tool

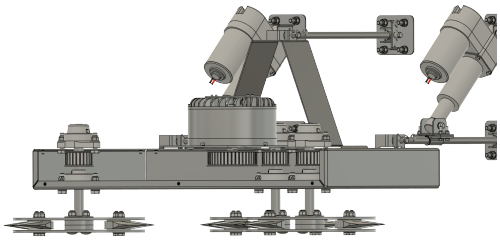

Figure 3.46: Assembly without the lid component to show interior

Chapter 4

Design Validation

To understand the proposed solution's integrity and characteristics, some validation processes were done to better comprehend the machine. Some components subjected to loads were analysed through an analytical approach to verify whether the choices previously assumed would be structurally sound. A cost analysis was executed to create a baseline on associated costs related to the construction of the tool designed in this dissertation.

4.1 Cutting Solution

4.1.1 Number of Blades

Despite the initial choice of a four-blade setup, a validation was necessary to understand if the number of blades was enough to cut through the undergrowth when the robot was moving at its desired speed. As the blades rotate through the area to be cut, it is important to ensure that at least all the blades are passing through the desired cutting area and maintain a good cut. To determine this, the notion of clip needs to explained. The forward distance covered by the cutting tool during the tool's revolution is known as clip, S. S is dependent on the rotational speed of the cutting tool and the linear speed of the robot moving forward and needs to be related to the blade's edge length. The value of S should be at most the value of a blades' edge length, which would mean that in a rotation while the robot was moving forward, the same point in that area will have all the blades pass on to it. Equation 4.1 relates the linear speed of the robot with the period of the tool's revolution and Equation 4.2 is used to determine the revolution's period, $T^{\text{cutting tool}}$, using the rotational speed of the tool, $\omega^{\text{cutting tool}}$. The value of v^{robot} is located in Table 4.1, at 1 m/s, and was given by INESC TEC's lab, $\omega^{\text{cutting tool}}$ was assumed as the max speed achieved by the belt-pulley configuration, available in Table 3.18 with a value of 7304 rpm, converted to 764.9 rad/s. A value of 8.22 seconds for $T^{\text{cutting tool}}$ and consequently 8.22 mm for S.

$$\begin{aligned} S &= v_{\text{max}}^{\text{robot}} \cdot T^{\text{cutting tool}} \\ &= 1 \cdot 8.22 \cdot 10^{-3} = 8.22 \cdot 10^{-3} \text{ m} = 8.22 \text{ mm} \end{aligned} \tag{4.1}$$

$$
\begin{aligned}
T^{\text{cutting tool}} &= \frac{2\pi}{\omega^{\text{cutting tool}}} \\
&= \frac{2\pi}{764.5} = 8.22 \cdot 10^{-3} \text{ s}
\end{aligned}
\tag{4.2}
$$

Table 4.1: MowIT's maximum linear speed

Maximum linear speed
1 m/s

The blade's edge length chosen for the comparison was the projected length, found in Table 3.4. Comparing the value of the length of 44.2 mm with S at 8.22 mm, it is possible to see that the cutting tool will do 5.38 revolutions at a point along a vertical line, meaning that with a number of four blades in the setup, a blade will pass through that point a number over 21 times. While it may seem that it is redundant the amount of times the blades passes through, if compared to the grass cutting blade on Figure 2.8b with 8 blades, where its blades would pass 34 times in that point during the forward motion, this tool can be considered between the blade in Figure 2.8a and a blade like the one on Figure 2.8b. As such, the number of blades can be said to be sufficient for cutting.

4.1.2 Rotating Blades Validation

A validation was made to make sure that the use of rotating blades would be advantageous to the effectiveness of the tool, comparing the kinetic energies of the tool with and without the rotating blades. Using the tools on the CAD software, it was determined that the moment of inertia, I_{zz} of the holding disks and the blade assembly on the z axis, the rotating axis, would amount to 6.668×10^{-2} Nm^2 and the moment of inertia of only the blades related to the center axis of the holding disks would amount to 5.852×10^{-3} Nm^2.

Using the formula present in Equation 4.3, where K is the kinetic energy in Joule, I is the moment of inertia on the rotating axis and ω is the rotational speed, the kinetic energies for rotating bodies can be obtained. 764.9

$$
K = \frac{1}{2} I \omega^2 \tag{4.3}
$$

For the whole system the kinetic energy amounts to:

$$
\begin{aligned}
K &= \frac{1}{2} \cdot 6.668 \cdot 10^{-2} \cdot 764.9^2 \\
&= 19.50 \cdot 10^3 \, J = 19.50 \text{ kJ}
\end{aligned}
$$

and the kinetic energy for the blades accounts to:

$$
\begin{aligned}
K &= \frac{1}{2} \cdot 5.852 \cdot 10^{-3} \cdot 764.9^2 0 \\
&= 1712 \, J = 1.712 \text{ kJ}
\end{aligned}
$$

In the case of an impact to the blade, in a hypothetical situation where friction between the bushing and the blade is not accounted, the blade would spin backwards and not contribute to the total kinetic energy of the cutting subsystem, meaning that the total kinetic energy of the tool would be the difference between the total system and the energy from the tools. This would amount to:

$$K = 19.50 - 1.712 = 17.79 \text{ kJ}$$

a value that would mean a loss of energy of 8.11%, meaning that a great deal of energy would be saved with this system. However, it is worth mentioning that this does not take into account losses that may occur between the compund bushings and the bolt in the blade's rotational axis.

4.1.3 Shaft Fatigue

As the shaft is a component that is subjected to cyclic loads derived from its loading aspects, a verification on component fatigue was done to ensure that the shaft would endure for a long period of time without failure. For this, the ANSI/ASME B106.1M method was applied following "*Dimensionamento à fadiga*" by Paulo M. S. Tavares de Castro [64] and the citation [65]. This method was chosen based on past knowledge regarding the use of this method.

For the ASME method, it first transforms the components of a multiaxial stress state that leads to fatigue, typically a cyclic normal stress combined with a shear stress that may or may not be cyclic, into equivalent static stresses, using a technique like Soderberg's criterion. With these values using the von Mises or the Tresca maximum shear stress criteria, a static analysis can be made and a uniaxial stress equivalent can be used to compare with the yield strength, σ_y, of the material divided by a safety coefficient [65].

The shaft possesses two bearing units apart from each other, where they are fixed connected to the shaft by the use of grub screws, and a pulley that receives power from the motor. This power is divided in three parts, one for each cutting subsystem and is transmitted to the shaft with a pulley attached to the shaft with a taper lock bushing and a parallel key. Due to the functional principle of pulleys, besides applying torque to the shaft, this torque that the pulley transmits also applies a load normal to the shaft that can in turn be responsible for a bending moment on it. While rotating, this load is applied cyclically into the loading point, creating a cyclic solicitation on the shaft. These two types of load will then in turn create shearing and normal stresses to the component.

As a preliminary step for simplification purposes regarding problem solution, a 2D static diagram was done. The shaft was considered as a horizontal beam element, the gearing units assumed as one pin support and a roller support and the force from the pulley as a vertical load facing down. Only the length of the shaft between gearing units was considered, as the load on the shaft would not apply any bending moment outside of the bearing units. The 2D problem can then be observed in Figure 4.1. The dimensions between elements shown in Table 4.2 were measured on the CAD

model by measuring the distance between bearings and distance between the pulley and the bearings. The load applied to the shaft is found in Table 3.18, for the pulleys located at the front of the cutting tool. The value was chosen as it was higher than the cutting tool located further behind and for this dimensioning the worst-case scenario was devised.

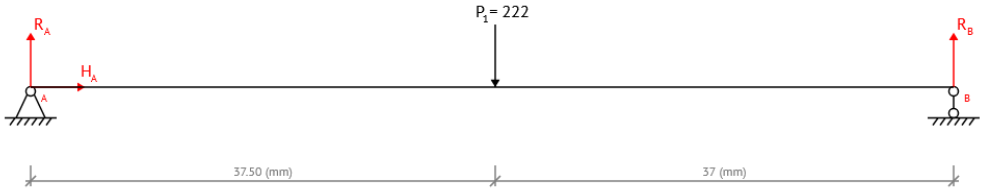

Figure 4.1: 2D problem of the shaft

Table 4.2: Beam Dimensions

Variable	Value
Total beam length	74.5 mm
Distance between pin support and applied load	37.5 mm
Distance between applied applied load a roller support	37 mm
Load applied	222 N

As expected, results showed that the point where the highest bending moment was located would be in the position where the pulley was mounted on the shaft. In Table 4.3 the reactions on the supports are as shown. In Table 4.4 the maximum and minimum values for bending moment on the beam are represented, as well as visual representations of where these values are located.

Table 4.3: Reaction forces at the supports

Support at	Reaction Force
Pin support	110.3 N
Roller support	111.7 N

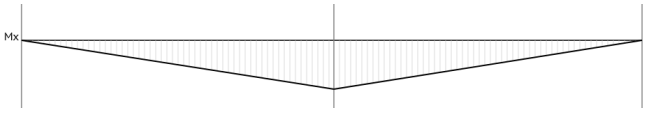

Figure 4.2: Bending moment diagram

Table 4.4: Maximum and minimum values for bending moment and shear forces

	Max	Min
Bending Moment	4.135 Nm	0 Nm

Typically, if the component is subjected to static tensions, the value of the tension σ only needs to be compared to the yield strength of the material from which the component is made out of. However, when the tensions to which the component are subjected to are cyclic, a different strength value needs to be calculated and that would theoretically make the component last indefinitely.

The type of cyclic load case can vary depending on the amplitude of stresses, σ_a that the component is subjected to and the average values of stress, σ_{avg}. In a pure bending situation, the maximum stress value, σ_{max}, and the minimum stress value, σ_{min} are symmetric, meaning that the amplitude of stress will be the same as the the maximum value and the average stress value will be null, like in Figure 4.3 and Equations 4.4 and 4.5.

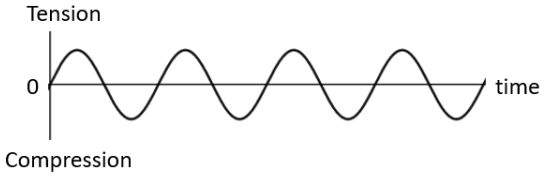

Figure 4.3: Stress values throughout time in a pure bending situation

$$\sigma_{\text{avg}} = \frac{\sigma_{\text{max}} + \sigma_{\text{min}}}{2} = 0 \tag{4.4}$$

$$\sigma_a = \frac{\sigma_{\text{max}} - \sigma_{\text{min}}}{2} = \sigma_{\text{max}} \tag{4.5}$$

Adapted from the ASME method, to calculate the shaft diameter, Equation 4.6 can be used, where SF is the safety factor, d is the shaft diameter in metres, M_f is the bending moment in newton metres, M_t is the torque in newton metres, σ^c_{f0} is the corrected endurance limit in megapascal and σ_y is the yield strength in megapascal.

$$d^3 = \frac{32 \cdot \text{SF}}{\pi \sigma_y} \sqrt{(\frac{\sigma_y M_f}{\sigma^c_{f0}})^2 + \frac{3}{4} M_t^2} \tag{4.6}$$

The endurance limit, σ_{f0}, of a material is a value of strength that if it is not reached during cyclic loads applied to a test specimen, it could be subjected to a cycle load for an infinite time, on steel alloys for pure bending loads. As the test specimen is under almost perfect conditions, without stress concentration, this value needs to be corrected with correction factors. This corrected endurance limit, σ^c_{f0}, can be determined by:

$$\sigma^c_{f0} = k_a k_b k_c k_d k_e k_f k_g \sigma_{f0}, \tag{4.7}$$

where :

- k_a is the surface factor;
- k_b is the size factor;

- k_c is the reliability factor;
- k_d is the temperature factor;
- k_e is the duty cycle factor;
- k_f is the fatigue stress concentration factor;
- k_g is the miscellaneous factor;
- σ_{f0} is the endurance limit of a test specimen.

The material under study is C45 steel and its properties are as shown in Table 3.3. For steel shaft designs, the endurance limit can also be estimated by using the ultimate tensile strength of the material, σ_{UTS} as follows:

$$\sigma_{f0} = \begin{cases} 0.504\sigma_{\text{UTS}} & \text{, if } \sigma_{\text{UTS}} \leq 1400 \text{ MPa} \\ 700 \text{ MPa} & \text{, if } \sigma_{\text{UTS}} > 1400 \text{ MPa} \end{cases} \tag{4.8}$$

As the ultimate tensile strength of C45 steel is 565 MPa, σ_{f0} is determined to be 285 MPa.

To determine the surface factor, Table 4.5 was used together with Equation 4.9, as the surface would have to be machined after the welding procedure. The value of this factor came at 0.841. For size factor, Equation 4.10 was used, giving a value of 0.896. For k_c, a 90% nominal reliability for the shaft was used, giving it a value of 0.897. As temperature and duty cycle factors were not considered, both of these values were assumed as 1. k_g was also assumed as 1 as no other factors were considered for this.

$$\begin{aligned} k_a &= a \cdot \sigma_{\text{UTS}}^{b} \\ &= 4.51 \cdot 565^{-0.265} = 0.841 \end{aligned} \tag{4.9}$$

Table 4.5: Values of a and b for machined shafts [64]

Type	***a* / MPa**	***b***
Machined	4.51	-0.265

$$\begin{aligned} k_b &= \left(\frac{d}{7.62}\right)^{-0.1133} \\ &= \left(\frac{20}{7.62}\right)^{-0.1133} = 0.896 \end{aligned} \tag{4.10}$$

The stress concentration factor, k_f, derives from K_f, the practical coefficient of stress concentration. This factor can be calculated with Equation 4.12, where K_t is the theoretical coefficient of stress concentration and q is the notch sensitivity. As the critical section of the shaft is located

at the pulley location, the keyway is also present in that section, so k_t will be derived from this. According to Pilkey and Peterson, by using Equation 4.11 for a relation of torque and bending moment:

$$\frac{M_t}{M_b} = \frac{1.6}{4.135} = 0.39 \tag{4.11}$$

a relation of 0.39 is achieved, corresponding to a value of K_t of 3 [66]. According to Tavares de Castro, notch sensitivity for annealed steel is 0.55 at a K_t of 3 [64]. This leads to a K_f value of 2.1, as in Equation 4.12.

$$\begin{aligned} K_f &= 1 + q(K_t - 1) \\ &= 1 + 0.55(3-1) = 2.1 \end{aligned} \tag{4.12}$$

To obtain k_f from K_f, Equation 4.13 is followed, obtaining a value of 0.476

$$\begin{aligned} k_f &= \frac{1}{K_f} \\ &= \frac{1}{2.1} = 0.476 \end{aligned} \tag{4.13}$$

With all the factors and the endurance limit obtained, following Equation 4.7 gives out a value of 91.7 MPa for σ^c_{f0}. By rearranging Equation 4.6 into and inputting all the values in accordance to SF:

$$\begin{aligned} \text{SF} &= \frac{d^3 \pi \sigma_y}{32\sqrt{(\frac{\sigma_y M_f}{\sigma^c_{f0}})^2 + \frac{3}{4}M_t^2}} \\ &= \frac{0.02^3 \cdot \pi \cdot 310}{32\sqrt{(\frac{310 \cdot 4.135}{91.7})^2 + \frac{3}{4}1.6^2}} = 3.4 \end{aligned} \tag{4.14}$$

a value of 3.4 for the Safety Factor is obtained.

While this validation is an approximation and might vary in relation to real life performance, it gives an idea that the diameter of the shaft together with the material chosen are able to withstand the loads subjected to them for an indefinite amount of time. While a smaller diameter could be chosen for shaft, the 20 millimeters of shaft also allow expanded the choice of bearing units to be chosen, something needed due to the high rotational speeds at which they perform. As such, it is concluded that the shaft diameter is in conformity with an acceptable safety factor.

4.2 Supporting Structure

4.2.1 Bearing Unit

A validation analysis was done one the bearing units according to SKF's catalogue [63]. Firstly, the calculation data for the bearing unit was taken from Appendix G to be used on the calculus. According to SKF, since the bearing units are mounted on a shaft with a belt connection, the dynamic bearing load, P needs to be determined. To determine the dynamic bearing load when using toothed belts, the effective belt pull needs to be multiplied by a factor to make an estimate. For toothed belts, SKF recommends a factor between 1.1 and 1.3 to be applied to the effective belt load. SKF also advises for the larger value on short distances between shafts, heavy loads or high belt tension, however, this value was assumed due to the complexity of the belt disposition.

Table 4.6: Calculation data for SKF FYTB 20 TF bearing unit [62]

	Symbol	Value (kN)
Basic dynamic load rating	C	12.7
Basic static load rating	C_0	6.55
Fatigue load limit	P_u	0.28

It is recommended when calculating load components for bearings in shafts to assume the shaft as a static beam resting on moment free supports. As this was done previously in Chapter 4.1.3 for calculating the bending moment, this simplification was already done, as seen in Figure 4.4, and reaction force values on the bearings, considered supports in the simplification, were already available in Table 4.3. As such, the dynamic load, P, was calculated with the factor of 1.3 and the force at the bearing with the higher reaction force, R, with a value of 111.7 N , using the following equation:

$$\begin{aligned} P &= R \cdot 1.3 \\ &= 111.7 \cdot 1.3 = 145.2 \text{ N} \end{aligned} \tag{4.15}$$

The basic rating life at 90% reliability for ball bearings, L_{10}, is calculated with Equation 4.16, where C is the basic dynamic load rating of the bearing, found in Table 4.6 and P was calculated in the previous equation and comes at a value of 669131 millions of rotations.

$$\begin{aligned} L_{10} &= \left(\frac{C}{P}\right)^3 \\ &= \left(\frac{12700}{145.2}\right)^3 = 669\ 131 \text{ [millions of revolutions]} \end{aligned} \tag{4.16}$$

With the use of Equation 4.17, where L_{10h} is the basic rating life at 90%, n is the rotational speed in Table 3.18 and L_{10} is the life rating calculated in Equation 4.16, a value of approximately 1.537 million hours was determined.

$$\begin{aligned} L_{10\text{h}} &= \frac{1\,000\,000}{60n} L_{10} \\ &= \frac{1\,000\,000}{60 \cdot 7304} \cdot 669\,131 = 1\,526\,860 \text{ h} \\ &\approx 1.537 \times 10^6 \text{ h} \end{aligned} \tag{4.17}$$

This value validates the bearing units chosen for this application. It can be argued that the large amount of hours might mean that the bearing unit are over dimentioned, if not for the fact that for this range of speeds and shaft diameter SKF did not offer any alternatives of less capable bearings. The fact that the cast iron model permits lubrication is important as the working conditions can be considered contaminated due to the dust involved in forest operation and the possibility to install an end cover also simplifies the installation process of the cutting tool.

4.2.2 Weight Validation

To hold the weight of the whole system, the connecting rods need to be structurally sound and resist the weight of the structure without bending, which could provoke a failure in the proper functioning of the cutting tool. Besides this, it is also important to understand whether the linear actuator's load capacity is enough for the lifting motion. Firstly an early analysis of the structure concluded that there would be two situations where the weight had an influence These being the grouping of the linear actuator and and the bottom connecting rods, which would be responsible for bearing the weight of the structure and the grouping between the bottom connecting rods to the top connecting rod, which were responsible for the alignment of the structure to the ground. These two groupings can be seen in Figure 4.4a and Figure 4.4b, respectively.

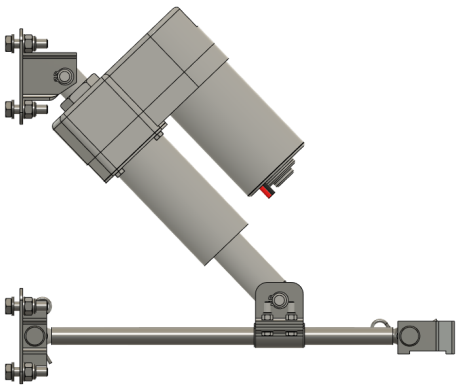

(a) Grouping between the bottom connecting rods and the linear actuator, in a 2D view

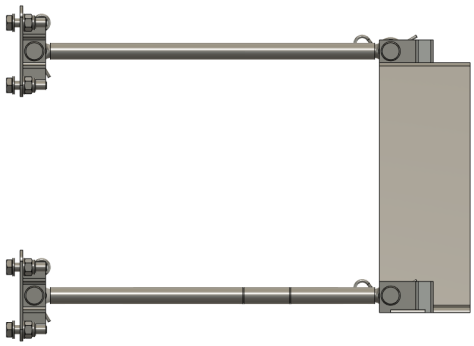

(b) Grouping between the bottom and top connecting rods, in a 2D view

Figure 4.4: The two considered groupings

If both groups were to be considered connected in a static analysis, it would create a hyperstatic problem. As such, since the bottom connecting rods may bear the weight of the system, a logical

approach was to separate the two groups, and analyze the rod which would be under higher values of stress.

The first step was to analyse the system and determine the weight affected. For this, the whole system except for the connecting rods, mounting brackets and the linear actuators, together with their sub parts, was considered. The mass of the considered system came at 50.89 kg, which translates to 499.2 N for its weight, using Equation 4.18 and admitting that the acceleration due to gravity g is 9.81 m/s^2. In Table 4.7 a scrutiny of the components weight can be observed. The weight of the bearing units and the motor came from their spec sheets available in Appendix G and Table 3.12, respectively.

$$\begin{aligned} W &= m \cdot g \\ &= 50.89 \cdot 9.81 = 499.2 \text{ N} \end{aligned} \tag{4.18}$$

Table 4.7: Mass of the considered system

	Mass (kg/object)	Quantity	Total mass (kg)
Motor + Pulley Assembly	8.73	1	8.73
Cutting Solution	7.43	3	22.29
Box	8.56	1	8.46
Lid + Fasteners	6.41	1	6.41
Trapezium + Top Appendage	1.23	1	1.23
Side Appendages	0.17	2	0.34
Motor Plate	0.7	1	0.7
Bearing Unit	0.45	6	2.7
Bearing Unit Cover	0.01	3	0.03
		Total mass (kg)	50.89

The second step was to, considering the symmetric geometry of the system, split it in two halves. This means that only half of the weight would be used in the analysis and allow for a 2D simplification of the problem. For simplification purposes the linear actuator was considered a beam, representing the behaviour of the linear actuator when it is not changing the height of the cutting tool. The clevis pin/eye bolt connection, along with the clevis pin/actuator connection were simplified into pin supports, allowing for rotation in the normal axis but no translation. The point of connection between the linear actuator and the connecting rod was simplified into a pin support on the beam. However it's worth noting that in the designed connection, the force is actually distributed throughout a certain length. In Figure 4.5 this simplified 2D problem is drawn and in Table 4.8 relevant dimensions between elements are as shown. The dimensions for the horizontal beam's length (Beam 1-2 in the figure) and the angled beam's length (Beam 3 in the figure) were measured in the CAD model as the distances between the centers of the clevis pins. However the distance between point 1 and point 4 in the drawing was measured by the distance between the clevis pin on the mounting bracket and a midplane of the securing component mounted on the connecting rod.

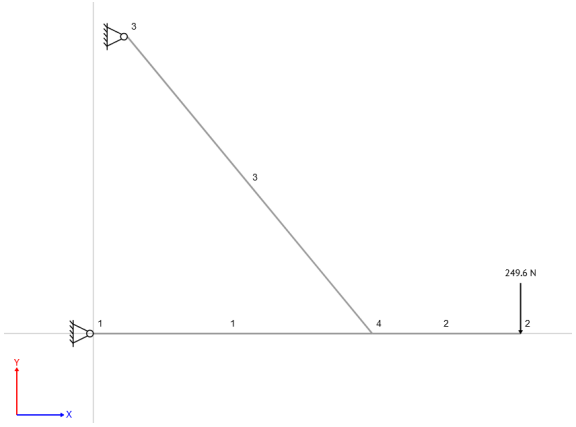

Figure 4.5: 2D sketch of the simplified problem

Table 4.8: Relevant Dimensions for Figure 4.5

Distance between point 1 and 2 (mm)	312
Distance between point 1 and 4 (mm)	205
Horizontal distance between point 1 and 3 (mm)	25
Vertical distance between point 1 and 3 (mm)	218

With the drawing from Figure 4.5, appropriate dimensions from Table 4.8 and the force applied to the beam determined by using half of the weight that was calculated in Equation 4.18, the static problem could be solved. The support pins would each have a reaction force, that could be decomposed into two forces, one for each axis direction, y and z. For determination of the forces, the two beams are decomposed into two separated beams, Beam 1-2 and Beam 3-4. Each beam will have a force applied at the point where the support pin connection was previously attached, with symmetrical values values between each beam. In Figure 4.6 the horizontal beam 1-2 can be seen, while in Figure 4.7 the angled beam 3-4 can be seen, in simplified forms.

Figure 4.6: Beam 1-2 represented

Solving Beam 1-2 using the parameters calculated before and the sum of moment at point 4:

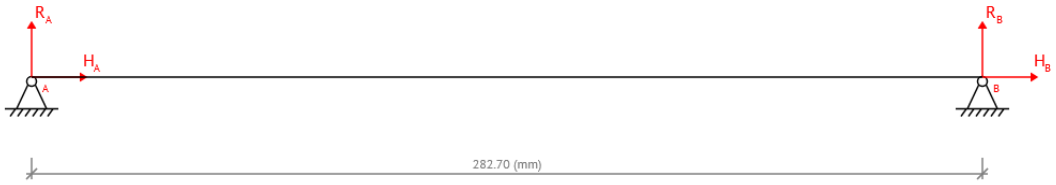

Figure 4.7: Beam 3-4 represented

$$\begin{aligned} &\Sigma M_3 = 0 \\ \Leftrightarrow &-\overline{L1-4}\cdot R_1^y = \overline{L4-2}\cdot(-F_w) \\ \Leftrightarrow &-205\cdot R_1^y = 107\cdot(-249.6) \\ \Leftrightarrow &R_1^y = -130.3\ \text{N} \end{aligned} \tag{4.19}$$

and the sum of forces in the y direction:

$$\begin{aligned} &\Sigma F_y = 0 \\ \Leftrightarrow &R_1^y + F_4^y - F_w = 0 \\ \Leftrightarrow &F_4^y = 379.9\ \text{N} \end{aligned} \tag{4.20}$$

where, ΣM_3 is the sum of moments at point 3, $\overline{L1-4}$ is the distance between point 1 and 4, $\overline{L4-2}$ is the distance between point 4 and 2, R_1^y is the reaction force in the y axis at point 1 and F_4^y is the force at point 4. The distances are as shown in Table 4.8.

Knowing F_4^y, it is possible now to determine R_3^y, the reaction force in the y direction, following Equation 4.20:

$$\begin{aligned} &R_3^y - F_4^y = 0 \\ \Leftrightarrow &R_3^y = 379.9\ \text{N} \end{aligned}$$

To determine the reaction force in the x direction for point 3, R_3^x, a sum of moments in point 4 is done

$$\begin{aligned} &\Sigma M_3 = 0 \\ \Leftrightarrow &\begin{bmatrix} -80 \\ 218 \end{bmatrix} \times \begin{bmatrix} R_3^x \\ 379.9 \end{bmatrix} = 0 \\ \Leftrightarrow &-218 \cdot R_3^x = 80 \cdot 379.9 \\ \Leftrightarrow &R_3^x = -139.4 \text{ N} \end{aligned} \tag{4.21}$$

Knowing R_3^x, it is possible to also determine the reaction in 1 in the x direction, using the sum of forces in the x direction for the whole problem.

$$\begin{aligned} &\Sigma F_x = 0 \\ \Leftrightarrow &R_1^x + R_3^x = 0 \\ \Leftrightarrow &R_1^x = 139.4 \text{ N} \end{aligned} \tag{4.22}$$

With this equation all the reaction forces are determined in the static problem presented and are as shown in Table 4.9.

Table 4.9: Forces in the static problem

Forces	***x* direction**	***y* direction**
Forces in Point 2 (N)	0	-249.6
Reaction in Point 1 (N)	139.4	-130.3
Reaction in Point 3 (N)	-139.4	379.9

Knowing all the reactions and forces applied to the model, it is now possible to determine the maximum bending moment and where it is located. Using the Beam 1-2 from Figure 4.6, the bending diagram from Figure 4.8 is formed, where the maximum bending moment achieved, M_b, is 26.71 Nm and where the connection with Beam 3-4 would be.

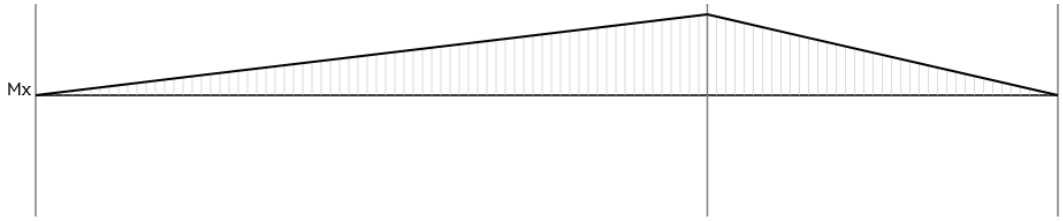

Figure 4.8: Bending diagram for Beam 1-2

After this analysis, it is now possible to turn back to the non simplified model. Knowing the maximum bending moment, as well as where it is located, it is now possible to ascertain whether combination of tube dimensions and material are enough to withstand the weight of the system.

By knowing the formula for bending stress,σ, the moment of inertia for a hollow tube, I and for the inner radius of a hollow tube, r_i:

$$r_e = d_e/2 \tag{4.23}$$

$$\sigma = \frac{M_b \cdot 10^3 \cdot r_e}{I} \tag{4.24}$$

$$I = \frac{\pi}{4}(r_e^4 - r_i^4) \tag{4.25}$$

$$r_i = r_e - e \tag{4.26}$$

where r_e is the external radius of the tube, which is half of the outer diameter of the tube and r_i is the internal radius of the tube and e is the thickness and the values for the outer diameter and the thickness of the tube are as shown in Table 3.21.

This gives values of:

$$\sigma = \frac{26.71 \cdot 10^3 \cdot 7.5}{1467} = 136.6 \text{ MPa}$$
$$I = \frac{\pi}{4}(7.5^4 - 6^4) = 1467 \text{ mm}^4$$
$$r_e = 15/2 = 7.5 \text{ mm}$$
$$r_i = 7.5 - 1.5 = 6 \text{ mm}$$

The bending stress value is then 136.6 MPa. To determine if this bending stress is under reasonable values, Equation 4.27 was used. The value for the yield strength of AISI 304 steel is located in 3.19. As the value has a range between 205 and 310 MPa, both extremes were considered to deliver a range of safety factors.

$$\begin{aligned} \sigma &= \frac{\sigma_y}{\text{SF}} \\ \Leftrightarrow \text{SF} &= \frac{205}{136.3} = 1.5 \end{aligned} \tag{4.27}$$

OR

$$\text{SF} = \frac{310}{136.3} = 2.27$$

A safety factor between 1.5 and 2.27 was achieved with these dimensions. Even in its lower range, this proves that the most critical part of the supporting structure is able to withstand the weight of the system, while providing extra leeway. If deemed necessary, a temper treatment could be considered to increase the yield strength of the material.

Another validation that can be done with the reaction calculations done previously in this section is the validation of the linear actuators. As seen in Table 3.23 they have a dynamic load limit of 1100 N and a static load limit of 11 350 N.

When determining the forces for Beam 3-4, if isolated, the beam had a force of 139.4 N in the x direction and -379.9 N in the y direction. By calculating the magnitude of the force with:

$$\begin{aligned} F &= \sqrt{F_x^2 + F_y^2} \\ &= \sqrt{139.4^2 + (-379.9)^2} = 404.7 \text{ N} \end{aligned} \tag{4.28}$$

and obtaining a value of 404.7 N for the magnitude of the force, it is possible to verify that the linear actuators can withstand together the weight of the machine, both in static situations, as well as dynamic, comparing with the values from Appendix F.

4.3 Cost of Production

An analysis on associated costs was made regarding the cutting tool. As access to prices in Fabory's website was only possible for businesses accounts, Norelem's website [1] was used as an alternative to procure the prices of the vast majority of normalized components. As some components were not found on Norelem's website, alterantives were searched. When no other vendor with prices available to the public was found, adaptations were made. For branded components, like the motor, linear actuators, pulley system and bearing unit, the cost was taken either from the official website or from an alternative vendor.

The analysis was done by taking into account all the normalized or branded components which the mowing implement is made out of and its quantities and correlate them to their price per unit. The total price of these parts come at 1915.80€. All the components considered, together with their quantities and price per unit are scrutinized in Table I.1 located in Appendix I. Any sources of price per unit not available in Norelem's website or any adaptation considered are shown in the Observation column. From this amount, there are some points worth noting. Firstly, the price of the linear actuator units comes at 1130.45€, amounting to nearly 60% of the total price of components. It is worth mentioning that much lower prices can be achieved by using equipment from other brands, namely some Chinese manufacturers who offer similar equipment. Despite this, the choice to use a recognized brand such as Thomson Linear, ensures the good functioning of the equipment and a baseline for researching into cheaper alternatives. Secondly, as the prices applied were available to the public, there may be some deviation related to the prices that some vendors might practice to business and research groups, lowering the value of the normalized values.

It is then concluded that the value of 1915.80€ produces a reference value for the cost of acquiring standard and branded components, that from which it is possible to further reduce with the use of specific normalized component sellers and alternative actuator manufacturers.

[1] https://norelem.es/pt

4.4 Specification Discussion

To understand whether the design choices would be enough to create a cutting solution, a comparison was made. As the tool was based on a design for a cutting head for a brush cutter, a brushcutter model was used as a benchmark.

For this comparison, Husqvarna 535iFR shown in Chapter 2.4.1 and used as the point of reference for the tool's maximum rotational speed did not provide enough information on its specifications to hold a comparison. Despite this, the brand claimed on its website that its power would be equivalent to a brush cutter powered by fuel and with a displacement of 35 cubic centimeters. The closest model found by the same brand was the Husqvarna 336FR, with 34.6 cubic centimeters of displacement. In Table the specifications of this model are shown, together with the equivalent specifications to the cutting solution.

Table 4.10: Torque and speed comparison between Husqvarna 336FR [67] and the cutting subsystem.

	Husqvarna 336FR	**Cutting Subsystem**
Torque (Nm)	1.8	1.6
Speed at designated torque (rpm)	6600	7304

It is possible to observe that while the Husqvarna brush cutter possesses a slightly higher torque compared to the cutting subsystem, the designed system actually achieves a higher speed. Determining the power in the movement, it is observed that both possess similar power outputs, at 1.24 for the brush cutter and 1.22 for the designed solution. Possessing an equivalent power outputs, together with a higher rotational speed could be proven to hold benefits despite its lower torque, thus helping with efficiency, both in power consumption and in cutting performance [68].

Another point worth mentioning is that while calculations were done in relation to the working point determined in Chapter 3.5.2, if a higher torque is needed, a different working point in the motor could be chosen, where a higher torque could be achieved at the expense of the maximum rotational speed and a higher energy consumption.

Chapter 5

Conclusion e Future Works

In this chapter of the dissertation, conclusions regarding the development of the mechanical project are made, together with suggestions for future works, with the purpose of further developing this solution and areas which can be improved upon or tackled.

5.1 Conclusion

While there has been some research and development regarding the area of robotics for forest utilization firing the recent years, its benefits have not been as widely seen as agricultural applications.

Most of the preventive silviculture operations still use human operated machines, such as chainsaws and brush cutters, to prune and maintain forest undergrowth. These solutions carry risks to the operator in the form of work related injuries, both in the form of injuries related to the steep locations where the the job is done combined with the type of tools used, or from chronic injuries derived from working principles of the machines being used. When possible, heavier machinery, like agricultural vehicles adapted with forestry tools are used. However, their higher proportions deem it unusable in tighter forests and may even destroy ecosystems.

There are already some different solutions regarding remotely operated machines, where the machine controller does not need to be handling or riding the machine, posing a much lower risk of injuries, while having good field productivity.

To create a mechanical project, firstly a list of requirements was generated and a conceptual idea was made, decomposing the whole solution into a set of smaller subsystems that would work together after assembly and ensure correct functioning of the tool. The subsystems devised were the cutting solution, the motor drive subsystem, the power delivery subsystem and the supporting structure.

Through research for the cutting solution, this lack of solutions was observed, as well as the low variety of cutting solutions applied to both the existing robots and to remotely operated machines. As an alternative, research regarding brush cutters proved helpful in inspiring a conceptual design. The design was based on a dropped patent developed at INEGI and revolved around a

brush cutter head where free rotating blades were attached to rotating disk heads. Similar designs were found both in the form of Chinese branded products and in the form of a branded product reviewed by the United States' Department of Agriculture. The blades were designed with some already available solutions as inspiration and a material selection process was done to ensure the proper material for them. For other components, designing was done as well, except when the use of normalized components was involved. To allow the rotation of the blades, a bushing and two washers for each blade were designed, and a material selection process was made using Ashby charts on a computer software. POM polymer based with PTFE filling was the material chosen for its low friction coefficient, together with other desirable mechanical properties allied to a not excessive price point.

For the motor drive subsystem, the motor was limited to two alternatives and one of them was chosen. A working point was chosen to allow calculation for baseline values regarding power, torque and motor speed. For the power delivery system, a belt drive was chosen for its many advantages outweighing the disadvantages. A setup was chosen using three cutting solutions to ensure a cutting length matching the width of the robot where it would be applied. To save space on the size of the solution, a setup using a double sided belt was done with 3 shafts working on the inside of the belt and the motor pulley meshing on the outside. The speed chosen as a baseline from an electric commercial brush cutter was not matched, however a high speed was nonetheless achieved.

The supporting structure was responsible for aligning all the other subsystems mentioned previously, connect the solution to the robot and hold everything together. An enclosure was done to assemble all the other components within, mounting brackets, appendages and connecting rods were designed to connect the enclosure to the robot while maintaining parallelism to the ground and a lifting mechanism comprised of a linear actuator was mounted to allow height regulation.

After proper assembly of the components in the CAD software, a technical drawing was made of this mechanism. Design validation in the form of structural validation to ensure that the critical components can perform correctly without failure and in the form of a cost analysis to better understand the costs involved in the assembly of such a prototype.

It is concluded that while no numerical simulations or experiment testing was done regarding the cutting performance or the electrical efficiency, a comparative analysis using a similar setup on a brush cutter leads into a positive outcome on the solution. However, further analysis should be done to ascertain proper working conditions.

5.2 Future Works

As this is a field of study with much to be developed, it is natural that future works were to be devised regarding this dissertation.

While a mechanical design was achieved of this machine, further research through the use of numerical analysis could be done on certain components. However, due to the complexity of the

systems involved and the working conditions present in the field, experimental testing through the form of prototyping would be highly beneficial for an assessment of performance.

Further development on the geometry and material design of the blades. Through the use of numerical analysis would be a fundamental contribution to further innovate this solution, as this is a field of study where a lot can be experimented and requires extensive research and development.

While it is possible to adjust the angle of attack of the cutting mechanism by regulating the length of the connecting rods, this requires human intervention. A solution for cutting angle adjustments could improve upon cutting efficiency, together with an assessment of cutting performance versus a cutting angle variation.

Regarding the rotational speed of the cutting tool, as it achieves really high speeds, attachments to the tool related to security could be designed, with proper material selection and designing to avoid any accidents, in the event of something like a blade failure.

As information regarding prices for materials and manufacturing processes are not readily available for academic uses, it would be interesting to expand the cost analysis to the manufacturing aspect of the components, together with a comparison of cost between using the vendor chosen for the CAD designs, in this case Fabory and the vendor used for finding the prices, in this case Norelem.

References

[1] PEFC Portugal. A floresta portuguesa, 2023. In Portuguese. Available at https://www.pefc.pt/o-que-fazemos/porque-e-importante-cuidar-da-floresta/a-floresta-portuguesa, last accessed in 12th of March 2023.

[2] José Uva. 6.º Inventário Florestal Nacional. Technical Report 6, Instituto da Conservação da Natureza e das Floresta, 2015. In Portuguese. Available at https://www.pordata.pt/portugal/area+ardida+e+incendios+rurais+em+portugal+continental-1192-9576, last accessed in 30th of June 2023.

[3] João L. Lourenço, Luís C. Bento, António P. Coimbra, and Aníbal T. De Almeida. Comparative Evaluation of Mobile Platforms for Non-Structured Environments and Performance Requirements Identification for Forest Clearing Applications. *Forests*, 13(11):1889, November 2022. Publisher: Multidisciplinary Digital Publishing Institute.

[4] Surviving-Wildfire. Wildfire and wildlife habitat, December 2019. Available at https://surviving-wildfire.extension.org/wildfire-and-wildlife-habitat/, last accessed in 1st of May 2023.

[5] Montado de Sobro e Cortiça. O sobreiro. In Portuguese. Available at https://montadodesobroecortica.pt/o-montado/o-sobreiro/, last accessed in 1st of May 2023.

[6] Agência Lusa. Incêndio em pedrógão grande, há um ano, matou 66 pessoas, feriu 253 e atingiu 261 habitações, June 2018. In Portuguese. Available at https://observador.pt/2018/06/14/incendio-em-pedrogao-grande-ha-um-ano-matou-66-pessoas-feriu-253-e-atingiu- last accessed in 1st of July 2023.

[7] Fundação Francisco Manuel dos Santos. Área ardida e incêndios rurais em portugal continental, December 2022. In Portuguese. Available at https://www.pordata.pt/portugal/area+ardida+e+incendios+rurais+em+portugal+continental-1192-9576, last accessed in 10th of March 2023.

[8] Floresta - Portugal Chama. In Portuguese. Available at https://portugalchama.pt/comportamentos-de-risco/floresta/, last accessed in 1st of July 2023.

[9] Environment and Climate Action Ministry. Decreto-lei n.º 82/2021. *Diário da República*, October 13 2021. Portugal. In Portuguese.

[10] Documentação comunicacional. In Portuguese. Available at https://portugalchama.pt/comunicacao/, last accessed in 1st of July 2023.

[11] Oxford University Press. robot noun. Available at https://www.oxfordlearnersdictionaries.com/definition/american_english/robot, last accessed in 1st of July 2023.

[12] Luiz F. P. Oliveira, António P. Moreira, and Manuel F. Silva. Advances in forest robotics: A state-of-the-art survey. *Robotics*, 10(2), 2021.

[13] Diogo Vieira. Conceção de equipamento radio-comandado para limpeza de terrenos. Master's thesis, Faculty of Engineering at University of Porto, 2016. In Portuguese.

[14] F. Corella Justavino, R. Jimenez Ramirez, N. Meza Perez, and S. A. Borz. The Use of OWAS in Forest Operations Postural Assessment: Advantages and Limitations. *Bulletin of the Transilvania University of Brasov. Series II: Forestry • Wood Industry • Agricultural Food Engineering*, pages 7–16, December 2015.

[15] Mehmet Altuntaş and Ali Çelik. Analysis of Brush Cutter-Related Accidents: Describing an Extraordinary Kind of Agricultural Injury. *The Journal of Emergency Medicine*, 62(1):9–15, January 2022.

[16] Safety bulletin 5: The safe use of brushcutters. https://www.justice.tas.gov.au/__data/assets/pdf_file/0004/76900/Brush_cutters.pdf, last accessed in 10th of March 2023, Workplace Standards Tasmania.

[17] Robots Science. Robot vs machine: Difference between a robot and a machine?, October 2020. Available at https://www.robotsscience.com/resource/difference-between-a-robot-and-a-machine/, last accessed in 25th of July 2023.

[18] Ashwani K. What is the difference between a robot and a machine?, May 2023. Available at https://www.devopsschool.com/blog/what-is-the-difference-between-a-robot-and-a-machine/, last accessed in 12th of July 2023.

[19] Maquilendro. Robôs. Available at https://maquiloendro.pt/collections/floresta-robos, last accessed in 14th of April 2023.

[20] Almovi. Limpeza de Mato. Available at https://www.almovi.pt/pt/florestal/limpeza-de-mato, last accessed in 14th of April 2023.

[21] Daniel Moleiro. Equipamento de limpeza florestal. Master's thesis, Faculty of Engineering at University of Porto, 2020. In Portuguese.

[22] McConnel. Remote Control Technology. Available at https://www.mcconnel.com/remote-control-technology/, last accessed in 14th of April 2023.

[23] Green Climber. Models. Available at https://www.greenclimber.com.au/models/, last accessed in 14th of April 2023.

[24] Green Climber. LV300 PRO. Available at https://www.greenclimberna.com/green-climber-lv300-pro, last accessed in 14th of April 2023.

[25] Energreen. Remote Controlled Tool Carriers Machines for Slopes. Available at https://en.energreen.it/green-maintenance-machines-energreen/robo-remote-controlled-tool-carriers/, last accessed in 14th of April 2023.

[26] Rajesh Singh, Anita Gehlot, Shaik V. Akram, Amit K. Thakur, Dharam Buddhi, and Prabin K. Das. Forest 4.0: Digitalization of forest using the Internet of Things (IoT). *Journal of King Saud University - Computer and Information Sciences*, 34(8, Part B):5587–5601, September 2022.

[27] Milrem Robotics. Multiscope Forester Planter. Available at https://milremrobotics.com/product/robotic-forester-planter/, last accessed in 2nd of July 2023.

[28] Milrem Robotics. Multiscope Forester Brushcutter. Available at https://milremrobotics.com/product/robotic-forester-brushcutter/, last accessed in 2nd of July 2023.

[29] Milrem Robotics. Multiscope Rescue with Hydra. Available at https://milremrobotics.com/product/multiscope-rescue-hydra/, last accessed in 2nd of July 2023.

[30] Joel Cowen. Clearing saw vs brush cutter | what's the difference. Available at https://theyardandgarden.com/clearing-saw-vs-brush-cutter/, last accessed in 17th of May 2023.

[31] Ed Malaker. Brush cutter vs clearing saw: What's the difference?, April 2023. Available at https://housegrail.com/brush-cutter-vs-clearing-saw/, last accessed in 17th of May 2023.

[32] Stihl. Fs 561 c-em. Available at https://www.stihlusa.com/products/trimmers-and-brushcutters/brushcutters-and-clearing-saws/fs561cem/, last accessed in 2st of June 2023.

[33] Husqvarna. 535ifr. Available at https://www.husqvarna.com/ca-en/brushcutters/535ifr/, last accessed in 2st of June 2023.

[34] Echo Tools. Cls-520es. Available at https://www.echotools.com/en_us/products/trimmers-brushcutters/clearing-saw/cls-520es, last accessed in 2st of June 2023.

[35] Stihl. Selecting the cutting attachment. Available at https://www.stihl.com/selecting-the-cutting-attachment.aspx, last accessed in 30th of May 2023.

[36] Stihl. Brushcut brush knife - 3 blades. Available at https://www.stihl.co.uk/en/ap/brush-knife-3-blades-13666, last accessed in 30th of May 2023.

[37] Forester. Forester carbide tipped chainsaw tooth brush cutter blade - 9" diameter. Available at https://forestershop.com/forester-9-in-carbide-chainsaw-tooth-blade.html, last accessed in 30th of May 2023.

[38] António A. Fernandes. *Desenvolvimento de Novos Produtos e Serviços*. Lidel - Edições Técnicas. Lda, 1st edition, 2017. In Portuguese.

[39] Michael F. Ashby. *Materials Selection in Mechanical Design*. Elsevier Ltd., 3rd edition, 2005.

[40] ANSYS, Inc. Material property charts. https://www.grantadesign.com/education/students/charts/.

[41] Marco P. C. de Sá Portocarrero, João F. M. G. Da Silva, and António T. Marques. Universal Cutting Device for Portable Trimmers. US20080307763A1, December 18 2008. US Patent App. 11/665,150.

[42] Andy Trent. Brush-Clearing Head Evaluation. Technical report, United States Department of Agriculture Forest Service, December 2003. Technology Development Program.

[43] Tenyu Tools. Grass cutting blade. Available at https://www.tenyutool.com/grass-cutting-blade/, last accessed in 5th of June 2023.

[44] Weerg. Steel C45. Available at https://www.weerg.com/cnc-machining-materials/steel/c45, last accessed in 30th of June 2023.

[45] AZO Materials. Aisi 1045 medium carbon steel, July 2012. Available at https://www.azom.com/article.aspx?ArticleID=6130, last accessed in 9th of April 2023.

[46] Stihl. Grasscut 230-4 grass-cutting blade. Available at https://www.stihl.co.uk/en/ap/grass-cutting-blade-4-blades-9516, last accessed in 30th of May 2023.

[47] Jozef Krilek, Ján Melicherčík, Tomáš Kuvik, Ján Kováč, Arkadiusz Gendek, Monika Aniszewska, and Jan Mareček. Analysis of Cutting Forces in Cross-Sawing of Wood: A Study of Sintered Carbide and High-Speed Steel Blades. *Forests*, 14(7), 2023.

[48] Lucas F. M. da Silva, Fernando J. Lino., and António T. Marques. Aços de ferramentas. In *Materiais de Construção*, chapter 2.6, pages 93–97. Publindústria, Edições Técnicas, 2013. In Portuguese.

[49] W.M. Garrison. Steels: Classifications. In K.H. J. Buschow, Robert W. Cahn, Merton C. Flemings, Bernhard Ilschner, Edward J. Kramer, Subhash Mahajan, and Patrick Veyssière, editors, *Encyclopedia of Materials: Science and Technology*. Elsevier, Oxford, 2001.

[50] Donald B. Richardson, Tadeusz Z. Blanzymski, Edward N. Gregory, Allan R. Hutchinson, and Leslie M. Wyatt. 16 - Manufacturing methods. In Edward H. Smith, editor, *Mechanical Engineer's Reference Book (Twelfth Edition)*, pages 16–1–16–112. Butterworth-Heinemann, 12th edition, 1994.

[51] Z. Zak Fang, Mark C. Koopman, and Hongtao Wang. 1.04 - Cemented Tungsten Carbide Hardmetal-An Introduction. In Vinod K. Sarin, editor, *Comprehensive Hard Materials*. Elsevier, Oxford, 2014.

[52] Ramesh Singh. 7 - Cast iron and cast steel. In Ramesh Singh, editor, *Applied Welding Engineering (Third Edition)*, pages 61–76. Butterworth-Heinemann, 3rd edition, 2020.

[53] ANSYS, Inc. Ansys® GRANTA Edupack 2023 R1 software, version 23.1.1. Cambridge, UK. https://www.ansys.com/products/materials.

[54] J. W. M. Mens and A. W. J. de Gee. Friction and wear behaviour of 18 polymers in contact with steel in environments of air and water. *Wear*, 149(1):255–268, September 1991.

[55] Roger Rothon and Christopher DeArmitt. Chapter 8 - Fillers (Including Fiber Reinforcements). In Marianne Gilbert, editor, *Brydson's Plastics Materials (Eighth Edition)*, pages 169–204. Butterworth-Heinemann, 8th edition, 2017.

[56] Golden Motor. Axial Flux BLDC Motors. Available at https://www.goldenmotor.com/, last accessed in 10th of March 2023.

[57] MROSupply. Belt, Chain, and Gear Drives: Which Is Better For You? Available at https://www.mrosupply.com/blog/belt-chain-and-gear-drives-which-is-better-for-you/, last accessed in 15th of March 2023.

[58] Megadyne Group. KSynchronous Belts vs. V-Belts, February 2020. Available at https://megadynegroup.com/pt/blog/synchronous-belts-vs-v-belts, last accessed in 15th of August 2023.

[59] VOWAGH store. VOWAGH 2" Receiver 3 Point Trailer Hitch Category 1 Tractor Tow Drawbar Adapter Compatible with BX Kubota John Deere LM25H WLM Tractor NorTrac Kioti Yanmar, Black. Available at https://www.amazon.com/VOWAGH-Receiver-Trailer-Category-Tractor/dp/B083WB4TVV?th=1, last accessed in 1st of August 2023.

[60] Xiaoxu Sun, Zhixiong Lu, Yue Song, Zhun Cheng, Chunxia Jiang, Jin Qian, and Yang Lu. Development Status and Research Progress of a Tractor Electro-Hydraulic Hitch System. *Agriculture*, 12(10):1547, October 2022.

[61] Thomson Linear. Actuator, electrak gx. Available at https://www.thomsonlinear.com/en/product/D48N05A5-02M0NN-AMM#!, last accessed in 30th of August 2023.

[62] SKF ©. Mounted bearings and housings, June 2013. Available at https://www.skf.com/group/products/mounted-bearings, last accessed in 4th of September 2023.

[63] SKF ©. Y-bearings and y-bearing units, June 2013. Available at https://cdn.skfmediahub.skf.com/api/public/0901d196802a2b8f/pdf_preview_medium/0901d196802a2b8f_pdf_preview_medium.pdf#cid-129182, last accessed in 4th of September 2023.

[64] Paulo M. S. T. de Castro. Dimensionamento à fadiga. Draft from 26th of October 2017.

[65] Sérgio M. O. Tavares and Paulo M. S. T. de Castro. A comparison of methodologies for fatigue analysis of shafts: DIN 743 vs. approaches based on Soderberg criterion. *Ciência & Tecnologia dos Materiais*, 29(1):e76–e81, January 2017. Publisher: Elsevier.

[66] Walter D. Pilkey and Rudolph E. Peterson. *Peterson's stress concentration factors*. Wiley, New York, 2nd edition, 1997.

[67] Husqvarna. 336fr. Available at https://www.husqvarna.com/ca-en/brushcutters/336fr/, last accessed in 1st of September 2023.

[68] Solomon Musa, Desa Ahmad, Khalina Abdan, and Jamarie Othman. Effect of cutting speed on cutting torque and cutting power of varying kenaf-stem diameters at different moisture contents. 38:549–561, 11 2015.

Appendix A

US20080307763A1 Patent

US 20080307763A1

(19) **United States**

(12) **Patent Application Publication**

Correia De Sa Portocarrero et al.

(10) **Pub. No.: US 2008/0307763 A1**

(43) **Pub. Date: Dec. 18, 2008**

(54) **UNIVERSAL CUTTING DEVICE FOR PORTABLE TRIMMERS**

(75) Inventors: **Marco Paolo Correia De Sa Portocarrero**, Caminha (PT); **Joao Francisco Machado Gomes Da Silva**, Gondomar (PT); **Antonio Torres Marques**, Matosinhos (PT)

Correspondence Address:
SUGHRUE MION, PLLC
2100 PENNSYLVANIA AVENUE, N.W., SUITE 800
WASHINGTON, DC 20037 (US)

(73) Assignee: **INEGI-INSTITUTO DE ENGENHARIA MECANICA E GESTAO INDUSTRIAL**, Leca do Balio (PT)

(21) Appl. No.: **11/665,150**

(22) PCT Filed: **Oct. 18, 2005**

(86) PCT No.: **PCT/IB2005/053416**

§ 371 (c)(1),
(2), (4) Date: **Jan. 17, 2008**

(30) **Foreign Application Priority Data**

Oct. 19, 2004 (PT) 103203

Publication Classification

(51) **Int. Cl.**
A01D 34/73 (2006.01)

(52) **U.S. Cl.** **56/255**

(57) **ABSTRACT**

The object of the invention is a cutting device to be used with portable trimmers, made by a rigid disc (**1**) where several centrifugal cutting blades (**2**) are conveniently fixed. This device can be used with any existing portable trimmers. Also, this device can efficiently cut virtually any kind of vegetation, from small grass to small trees. It was designed to keep cutting with efficiency even after several hard impacts against extremely hard objects, such as stones.

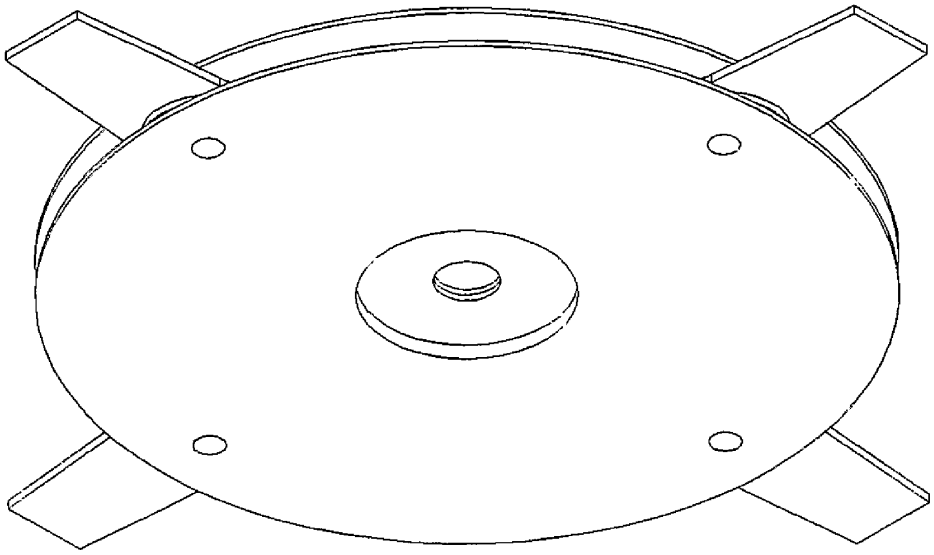

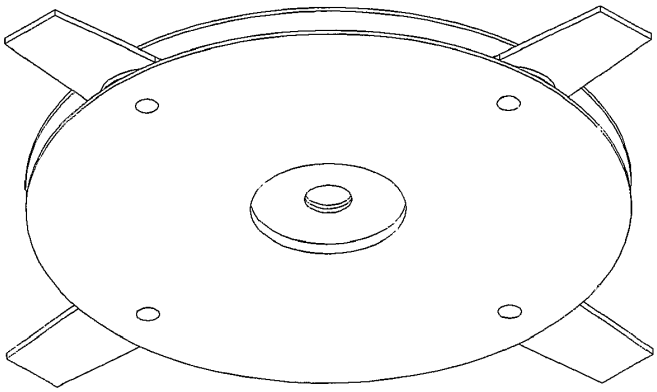

Fig. 1

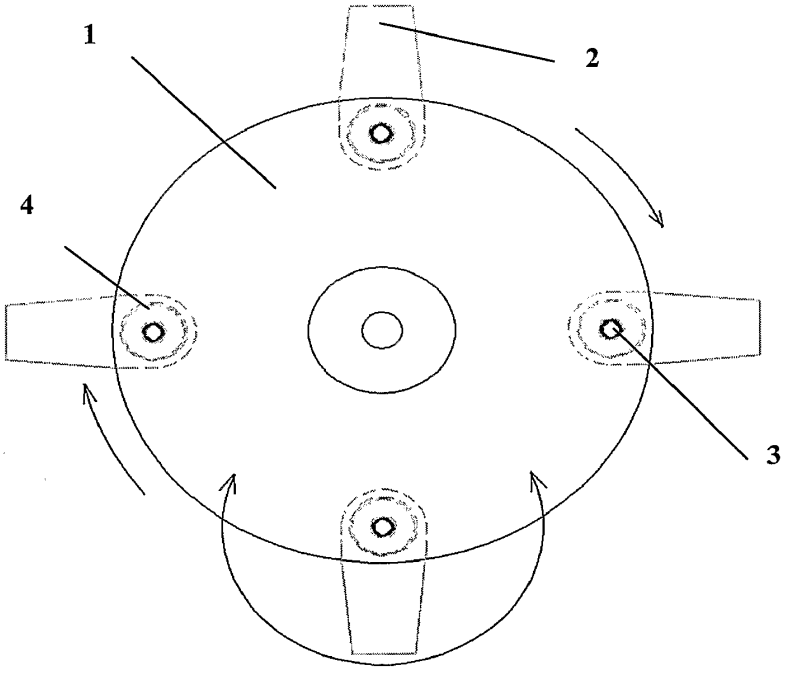

Fig. 2

UNIVERSAL CUTTING DEVICE FOR PORTABLE TRIMMERS

FIELD OF INVENTION

[0001] Universal cutting device for portable clearing equipments.

STATE OF THE ART

[0002] Portable trimmers are devices with a thermal combustion engine that transmits rotational motion trough an axis which can have different lengths, to a device, allowing the cut of different kinds of vegetation.

[0003] Today, there are several kinds of said cutting devices, distinguished, among other features, by:

1. accessories for grass cutting:
   - **[0004]** 1. several models of twine heads working with several lines, generally of polymeric material (polyamide);
   - **[0005]** 2. knife heel head coupled to the trimmer, only trough one side, and works by using the centrifugal force on the mentioned plastic blades which are fixed with bearings or metallic bushes.
2. accessories for heavy grass, although not ligneous:
   - **[0006]** 1. here are several variants of rigid disks with three or more teeth made with different heights for the different vegetation to cut;
   - **[0007]** 2. disks allowing the substitution of blades rigidly fixed therein;
   - **[0008]** 3. rigid blade, folded on both ends, specially designed for the grinding of non ligneous vegetation;
3. accessories for cutting small trees:
   - **[0009]** 1. circular blades with different teeth configurations that can include diamond materials
   - **[0010]** 2. chains similar to the ones used in power chainsaws, placed on a rigid device.

DETAILED DESCRIPTION OF THE INVENTION

[0011] The object of the invention is a cutting device for portable trimmers and that can be coupled to any portable trimmer model commercially available. It allows cleaning (by cutting) efficiently any kind of vegetation, from grass to small trees.

[0012] This device was designed and conceived to keep cutting efficiently even after continuous impacts against hard objects (e.g., stones, iron) generally present in the fields that are invaded with vegetation in general. In the existing accessories for trimmers the said impact against hard objects deeply limits its usable life time constraining an early substitution.

[0013] On the other hand, all existing accessories have a specific use, related with the kind of vegetation that they should cut; there are tools for vegetation like grass, others for more fibrous vegetation, others for cutting thin ligneous vegetation and finally, others that allow cutting small trees. The developed device allows, due to its characteristics, the substitution with advantages of all existing accessories by this one that cuts efficiently from small grass to small trees and therefore having productivity profits. The innovative device is made of several metallic blades conveniently fixed to a rigid support and that vary automatically their cutting angle according to the found cutting force. In limit situations (which can arise from the impact against a stone) they can make a complete rotation around their own axis and be able to cut again. The cutting angle results from the balance between the cutting force and the centrifugal one.

[0014] The developed device (see FIG. **1**) is made of a main platform (**1**) with axial symmetry, allowing its use with both sides coupled to the existing trimmers. The cutting blades (in number of two or more) (2) can be fixed to this main system through double bushes—one being made from a friction resistant material (3) fixes the two parts of the main fixing system and a second one (4), made of a material with less friction resistance than the blades or the bushes 3. Thus, any accidental ejection of the blades is excluded.

1. Cutting device to be used with portable trimmers characterized in that it is made up by more than one metallic blades that are fixed to a rigid system with a generic circular shape and for which the cutting angle varies automatically according to the found cutting force, being such defined as a result of the balance between the centrifugal and cutting forces.

2. Cutting device for portable trimmers according to claim **1**, characterized in that it is composed by a main axially symmetric fixing system (1) allowing the work with both of it's sides coupled to the commercially available trimmers, where two or more metallic blades are fixed (2) through, at least, two bushes. One (3), made of a friction resistant material should be fixed to the fixing system and the other (4), made of a less friction resistant material than the blade or the bushes referenced (3) and to be manufactured with the appropriated drawing clearances, allowing for a safe and mild work, based on the balance between the centrifugal force and the force required to cut the vegetation.

3. Cutting device for trimmers according to the previous claims characterized in that it can be attached to the trimmer, undistinguishly, from whichever of both sides, allowing an equilibrated blade detrition and therefore extending it's wear-out life.

* * * * *

Appendix B

AISI 1045 Medium Carbon Steel

AISI 1045 Medium Carbon Steel

Jul 5 2012

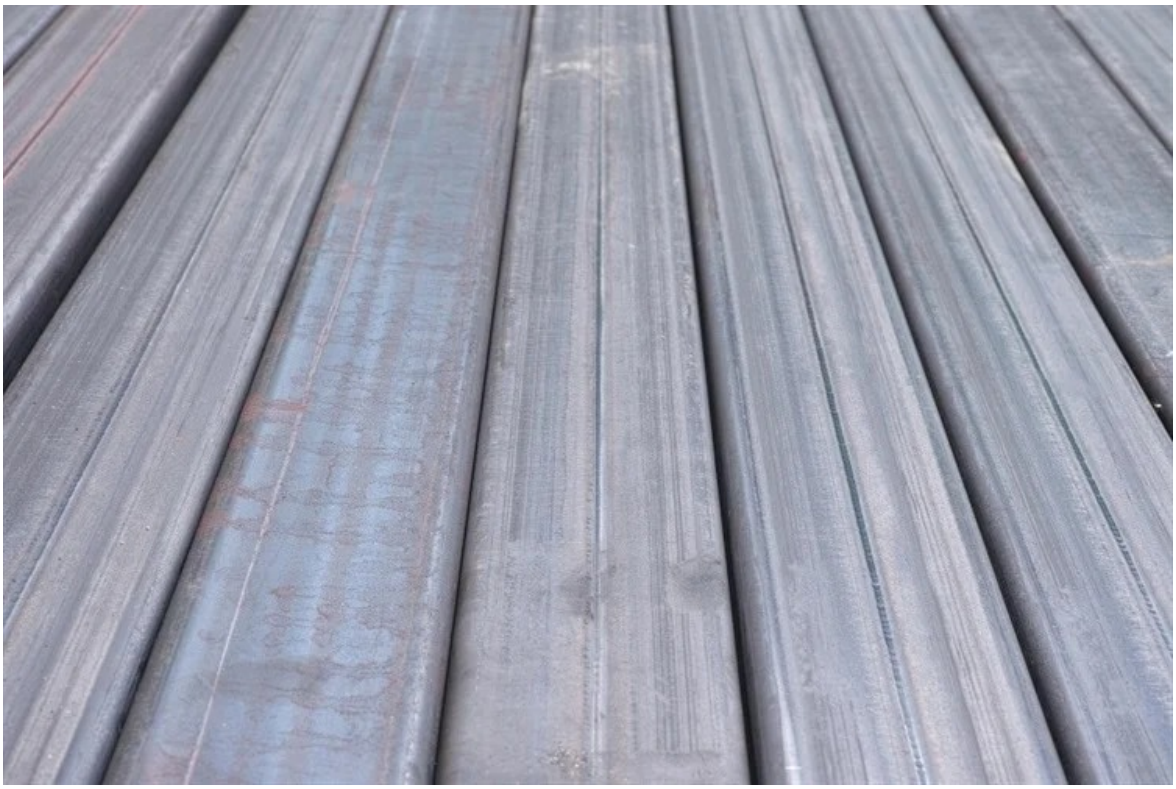

Image Credits: kwanchai/shutterstock.com

AISI 1045 steel is a medium tensile steel supplied in a black hot-rolled or normalized condition. It has a tensile strength of 570 - 700 MPa and Brinell hardness ranging between 170 and 210.

AISI 1045 steel is characterized by good weldability, good machinability, and high strength and impact properties in either the normalized or hot-rolled condition.

AISI 1045 steel has a low through-hardening capability with only sections of around 60 mm in size being recommended as suitable for tempering and through-hardening. However, it can be efficiently flame- or induction-hardened in the normalized or hot rolled condition to obtain surface hardnesses in the range of Rc 54 - Rc 60 based on factors such as section size, type of set up, quenching medium used etc.

AISI 1045 steel lacks suitable alloying elements and hence does not respond to the nitriding process.

Chemical Composition

Element	Content
Carbon, C	0.420 - 0.50 %
Iron, Fe	98.51 - 98.98 %
Manganese, Mn	0.60 - 0.90 %
Phosphorous, P	≤ 0.040 %
Sulfur, S	≤ 0.050 %

Physical Properties

Physical Properties	Metric	Imperial
Density	7.87 g/cc	0.284 lb/in^3

Mechanical Properties

Mechanical Properties	Metric	Imperial
Hardness, Brinell	163	163
Hardness, Knoop (Converted from Brinell hardness)	184	184
Hardness, Rockwell B (Converted from Brinell hardness)	84	84
Hardness, Vickers (Converted from Brinell hardness)	170	170
Tensile Strength, Ultimate	565 MPa	81900 psi
Tensile Strength, Yield	310 MPa	45000 psi
Elongation at Break (in 50 mm)	16.0 %	16.0 %
Reduction of Area	40.0 %	40.0 %
Modulus of Elasticity (Typical for steel)	200 GPa	29000 ksi
Bulk Modulus (Typical for steel)	140 GPa	20300 ksi
Poissons Ratio (Typical For Steel)	0.290	0.290
Shear Modulus (Typical for steel)	80 GPa	11600 ksi

Machining

AISI 1045 steel has good machinability in a normalized or hot-rolled condition. Based on the recommendations given by the machine manufacturers, operations like tapping, milling, broaching, drilling, turning and sawing can be carried out on AISI 1045 steel using suitable feeds, tool type, and speeds.

Welding

AISI 1045 steel is readily welded when the correct procedure is followed, but welding AISI 1045 steel in through-hardened, tempered and flame- or induction-hardened conditions is

not recommended. Low hydrogen electrodes are preferred for welding AISI 1045 steel.

The workpiece is:

- Pre-heated at 200°C–300°C (392°F - 572°F);
- maintained at the same temperature during welding;
- cooled slowly using sand or ashes; and
- stress relieved at 550°C - 660°C (1022°F - 1220°F).

Heat Treatment

AISI 1045 is subjected to forging, annealing, normalizing, stress-relieving, hardening and tempering processes – each of which is explained in more detail below:

- **Forging** - Heat to 850°C - 1250°C (1562°F - 2282°F). Hold until the temperature is uniform. Cool in a furnace.
- **Annealing** - Heat to 800°C - 850°C (1472°F - 1562°F). Hold until the temperature is uniform. Cool in a furnace.
- **Normalizing** - Heat to 870°C - 920°C (1598°F-1688°F). Hold until the temperature is uniform. Soak for 10 - 15 minutes. Cool in still air.
- **Stress-Relieving** - Heat to 550°C - 660°C (1022°F - 1220°F). Hold until the temperature is uniform. Soak for 1 hour per 25mm of section. Cool in still air.
- **Hardening** - Heat to 820°C - 850°C (1508°F - 1562°F). Hold until the temperature is uniform. Soak for 10 - 15 minutes per 25mm of section. Quench in water or brine.
- **Tempering** - Re-heat to 400°C - 650°C (752°F - 1202°F) as required. Hold until the temperature is uniform. Soak for 1 hour per 25mm of section. Cool in still air.

Applications

AISI 1045 is widely used for all industrial applications requiring more wear-resistance and strength. Typical applications of AISI 1045 are as follows:

Gears	Pins	Rams
Shafts	Rolls	Sockets
Axles	Spindles	Worms
Bolts	Ratchets	Light gears
Studs	Crankshafts	Guide rods
Connecting rods	Torsion bars	Hydraulic clamps

This article was updated on 7th August, 2019.

Appendix C

Granta EduPack Material Selection Charts

C.1 Bushing and Washers' Material Selection

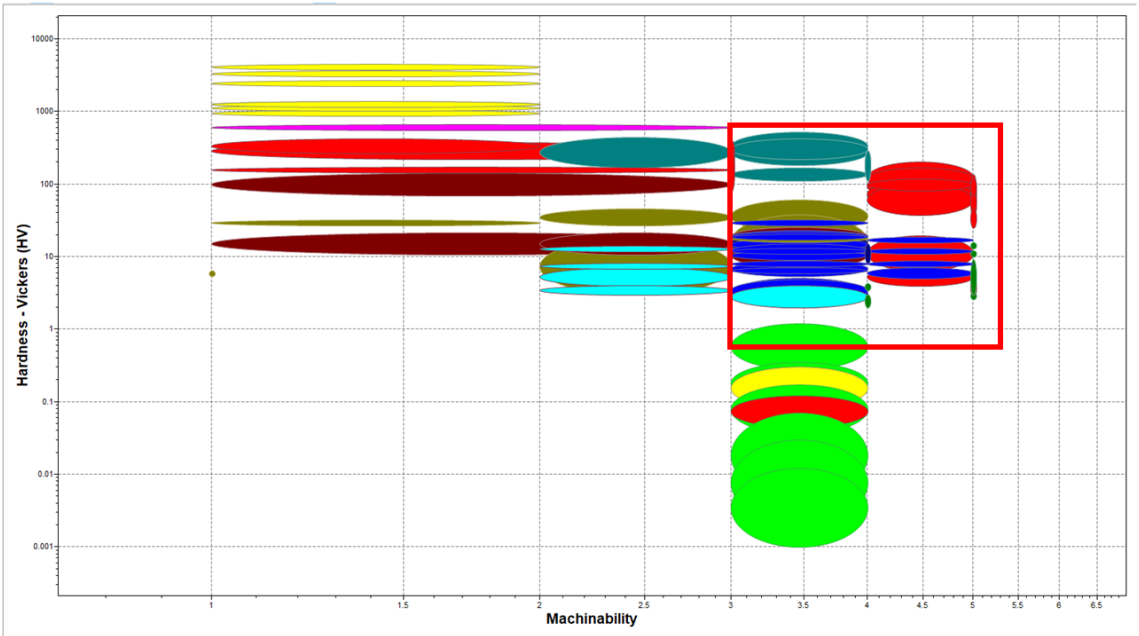

Figure C.1: Hardness - Vickers vs Machinability Ashby Chart, created using ANSYS EduPack 2023

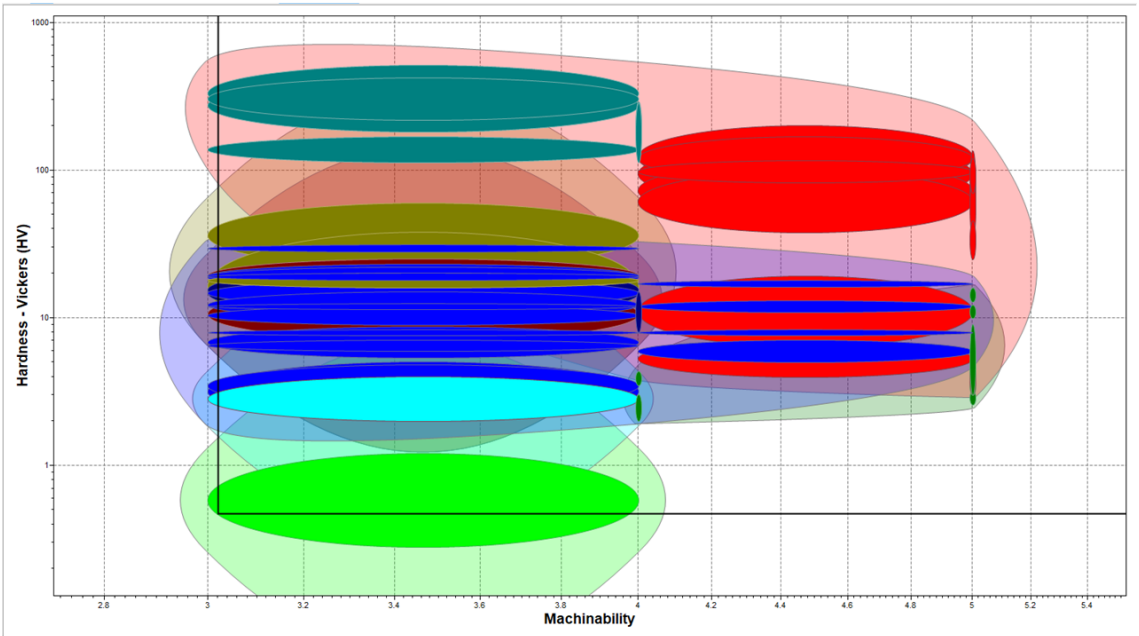

Figure C.2: Detailed View of the Hardness - Vickers vs Machinability Ashby Chart, created using ANSYS EduPack 2023

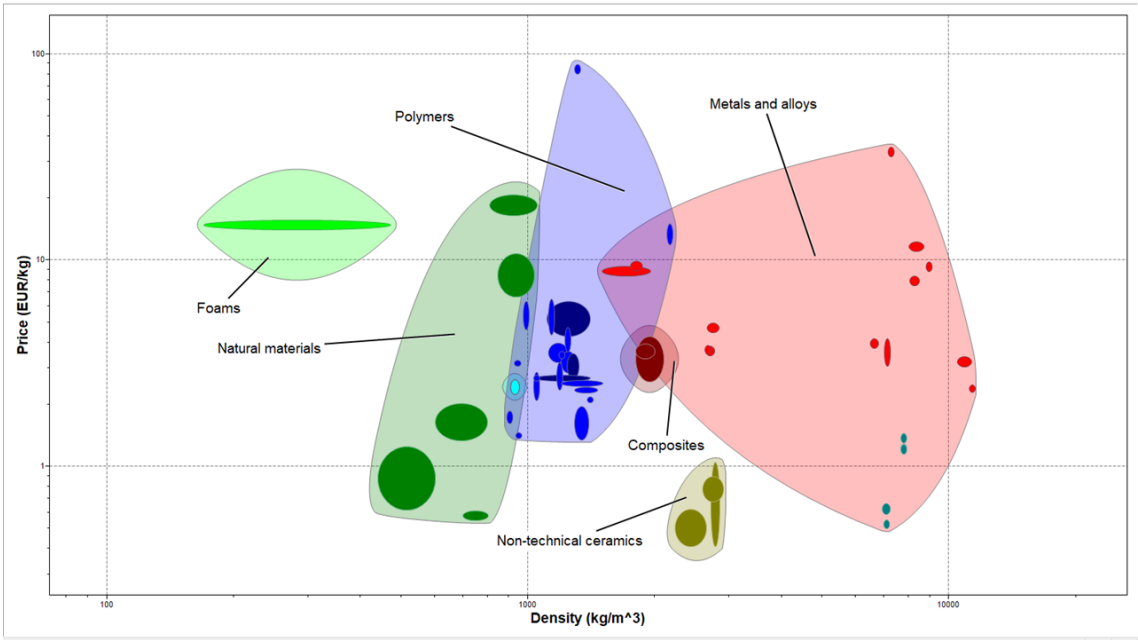

Figure C.3: Density vs Price Ashby Chart, created using ANSYS EduPack 2023

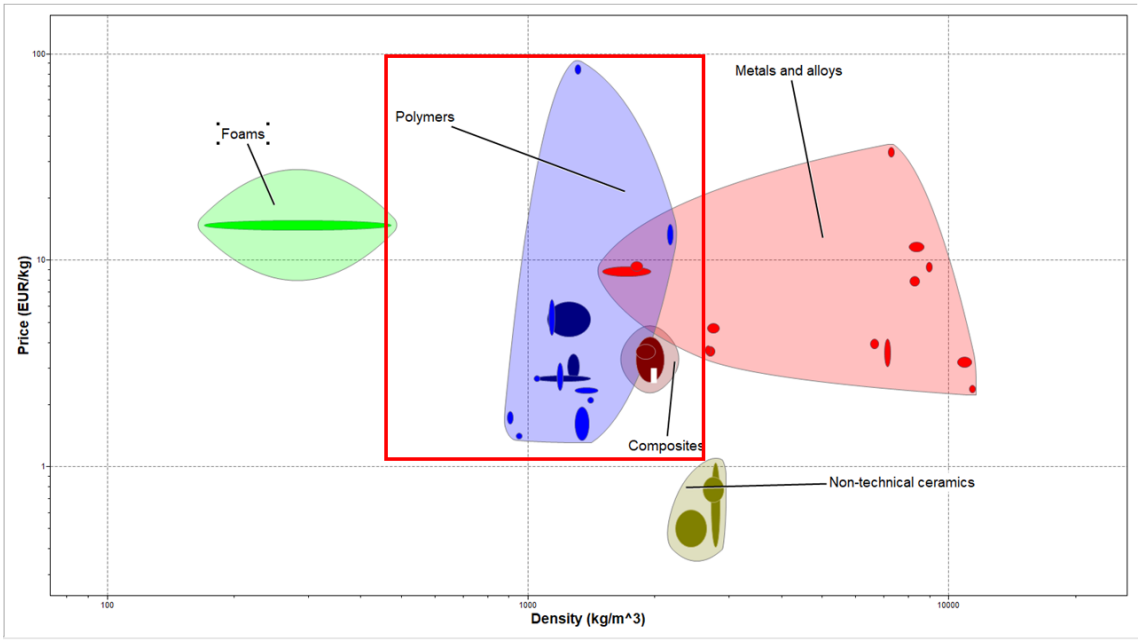

Figure C.4: Density vs Price Ashby Chart without low lubricating oil durability, created using ANSYS EduPack 2023

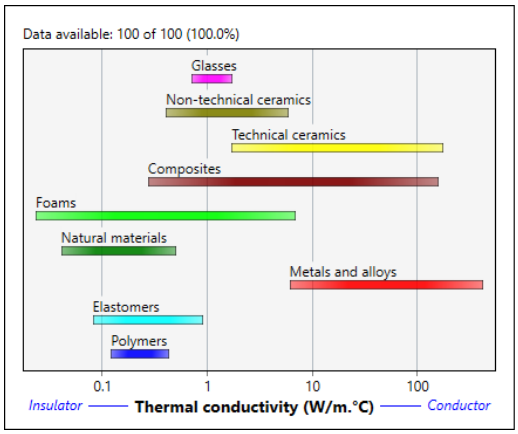

(a) Thermal Conductivity range on different material families

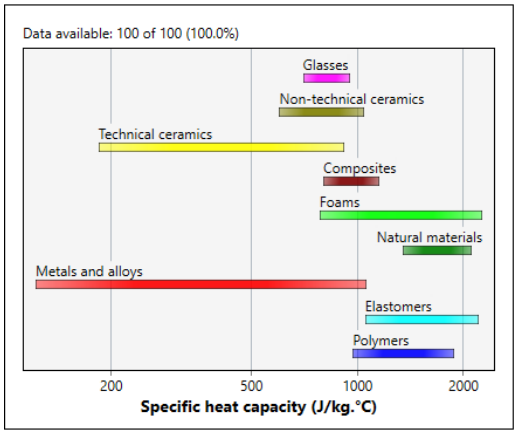

(b) Specific heat capacity range on different material families

Figure C.5: Range of property values on different material families [53]

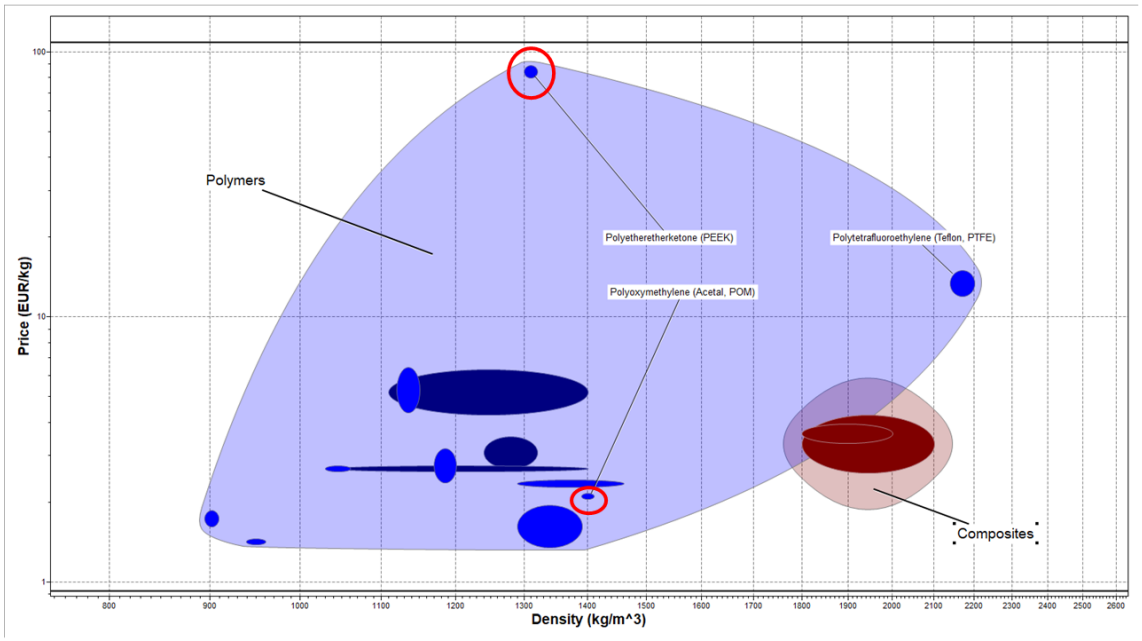

Figure C.6: Density vs Price Ashby Chart with polymer thermal conductivity values as filter, created using ANSYS EduPack 2023

Appendix D

HPM3000B - High Power BLDC Motor

D.1 HPM3000 (3KW) Motor Performance Curve (48V)

Golden Motor电机测试报告

电机型号(Type)：	3KW	额定电压(Voltage)：	48(V)
单位名称(Company)：	GOLDEN MOTOR	额定电流(Current Rated)：	85(A)
测试人(Tester)：	1	额定功率(Power Rated)：	3000(W)
测试日期(Test Date):2014-12-31		额定转速(Speed Rated)：	4000(r/m)

电机负载特性曲线

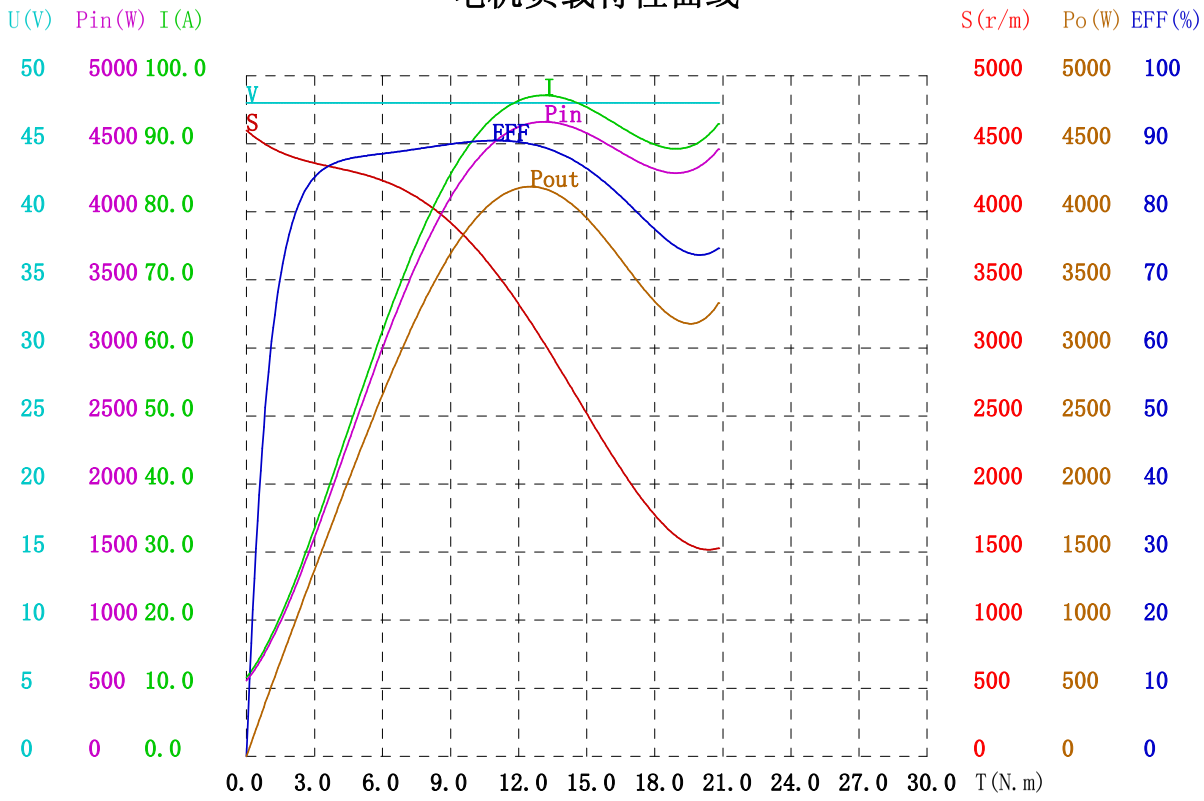

起始点(Start):0.7(N.m)
- 转速 = 4489 (r/m)
- 电流 = 14.87 (A)

最大转矩点(Max_Torque):
- 转矩 = 20.80 (N.m)
- 转速 = 1529 (r/m)
- 电流 = 92.93 (A)
- 输出功率 = 3329.3 (W)
- 效率 = 74.64 (%)

最大输出功率点(Max_Pout):4184.6 (W)
- 转矩 = 12.52 (N.m)
- 转速 = 3191 (r/m)
- 电流 = 96.89 (A)
- 效率 = 89.97 (%)

最高效率点(Max_Pout):90.47 (%)
- 转矩 = 11.06 (N.m)
- 转速 = 3539 (r/m)
- 电流 = 94.38 (A)
- 输出功率 = 4098.4 (W)

D.2 HPM3000 (3KW) Motor Performance Data (48V)

Golden Motor电机测试数据报表

电机型号	3KW			额定电压		48(V)	
单位名称	GOLDEN MOTOR			额定电流		85(A)	
测试人	1			额定功率		3000(W)	
测试日期	2014-12-31			额定转速		4000(r/m)	
No.	U(V)	I(A)	Pin(W)	T(N.m)	N(r/m)	Pout(W)	η(%)
001	48.0	14.87	715.3	0.7	4489	371.0	51.9
002	48.0	15.30	735.7	0.9	4487	433.0	58.9
003	48.0	16.07	773.0	0.9	4484	432.0	55.9
004	48.0	16.82	809.2	1.0	4480	494.0	61.0
005	48.0	18.10	870.5	1.1	4472	554.0	63.6
006	48.0	19.91	957.6	1.4	4461	676.0	70.6
007	48.0	22.67	1090	1.7	4445	796.0	73.0
008	48.0	26.16	1258	2.1	4421	975.0	77.5
009	48.0	30.02	1443	2.5	4396	1152	79.8
010	48.0	34.17	1643	3.0	4366	1384	84.2
011	48.0	38.39	1845	3.5	4339	1615	87.5
012	48.0	43.64	2097	4.0	4308	1841	87.8
013	48.0	49.07	2358	4.6	4267	2061	87.4
014	48.0	54.37	2613	5.2	4234	2338	89.5
015	48.0	59.81	2874	5.9	4200	2610	90.8
016	48.0	65.69	3157	6.5	4159	2866	90.8
017	48.0	71.96	3458	7.3	4119	3180	92.0
018	48.0	78.72	3783	8.0	4073	3425	90.5
019	48.0	87.20	4186	8.9	4017	3773	90.1
020	48.0	94.31	4527	10.0	3914	4098	90.5
021	48.0	94.55	4538	10.9	3578	4084	90.0
022	48.0	94.83	4551	12.2	3170	4050	90.0
023	48.0	94.60	4540	14.0	2632	3859	85.1
024	48.0	93.03	4465	16.8	2167	3812	85.4
025	48.0	92.81	4455	20.8	1508	3284	73.7

Appendix E

Timing Belt

E.1 Optibelt CAP 6.5 calculation

Optibelt-CAP Drive Calculation

Sender

Tel. No.	:		Tel. No.	:	
Fax No.	:		Fax No.	:	
E-Mail	:		E-Mail	:	
Internet	:		Internet	:	

Length-Calculation

Calc.-No.	:	C000000002	Date	:	30.08.2023	SN	:
Project	:	0001	Drawing No.	:	0001	Drive	: 0001

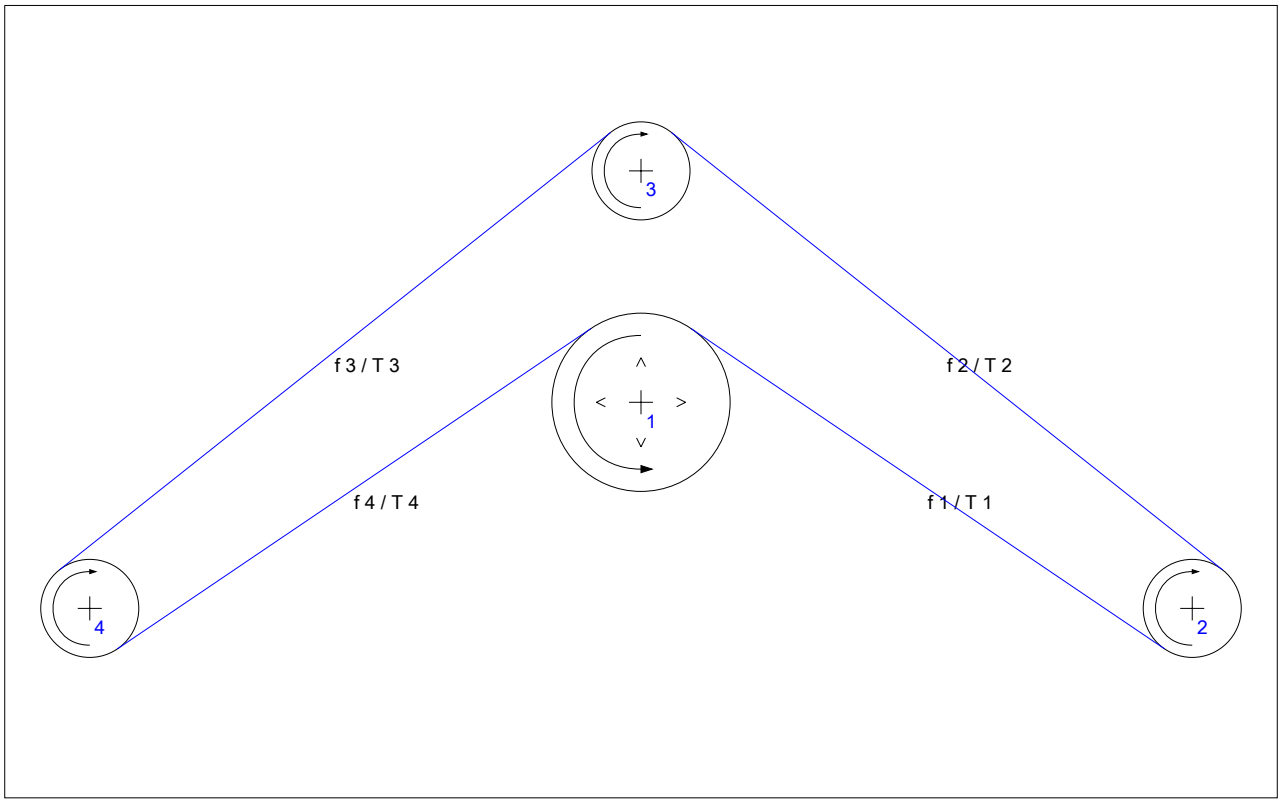

timing belt profile Optibelt OMEGA 1728 D8M-HP 20 special belt

Standard pitch length	Lw	:	1728	mm
Number of teeth	zr	:	216	
Pitch	t	:	8	mm
Width	b	:	20	mm
Belt speed	v	:	21.42	m/s
Actual service factor	c2	:	5.37	
Transmitted power	PÜ	:	20.24	kW

Our 'General Conditions of Sale' are applicable.

Sender

Length-Calculation

Calc.-No.	: C000000002	Date	: 30.08.2023	SN	:
Project	: 0001	Drawing No.	: 0001	Drive	: 0001

pulley 1 TB 40-8M-20 Optibelt-TB taper bush 1610 (Bore-diameter 20 mm)

Diameter	dw_1	:	101.86	mm
Number of teeth	z	:	40	
Teeth in mesh	ze	:	8	
Speed	n_1	:	4017	1/min
Actual drive ratio	i	:	---	
power	P_{an}	:	3.77	kW
Torque	Nm	:	9.0	Nm
static belt tension new	T_1	:	111	N
Shaft load new	Sa	:	125	N
Frequence new	f_1	:	44.08	Hz
static belt tension used	T_1	:	97	N
Shaft load used	Sa	:	108	N
Frequence used	f_1	:	41.11	Hz
Span length	L	:	326.90	mm
x-coordinate	x	:	0.00	mm
y-coordinate	y	:	7.77	mm
X-input coordinate	xs	:	0.00	mm
Y-input coordinate	ys	:	0.00	mm
X-deviation from theoretical	Dxs	:	0.00	mm
Y-deviation from theoretical	Dys	:	7.77	mm

pulley 2 TB 22-8M-20 Optibelt-TB taper bush 1008 (Bore-diameter 20 mm)

Diameter	dw_2	:	56.02	mm
Number of teeth	z	:	22	
Teeth in mesh	ze	:	11	
Speed	n_2	:	7304	1/min
Actual drive ratio	i	:	0.55	
power	P_{ab}	:	1.26	kW
Torque	Nm	:	1.6	Nm
static belt tension new	T_2	:	111	N
Shaft load new	Sa	:	222	N
Frequence new	f_2	:	35.83	Hz
static belt tension used	T_2	:	97	N
Shaft load used	Sa	:	193	N
Frequence used	f_2	:	33.41	Hz
Span length	L	:	402.15	mm
x-coordinate	x	:	315.00	mm
y-coordinate	y	:	-110.00	mm

Our 'General Conditions of Sale' are applicable.

Length-Calculation

Calc.-No.	: C000000002	Date	: 30.08.2023	SN	:
Project	: 0001	Drawing No.	: 0001	Drive	: 0001

pulley 3 TB 22-8M-20 Optibelt-TB taper bush 1008 (Bore-diameter 20 mm)

Diameter	dw_3 :	56.02	mm
Number of teeth	z :	22	
Teeth in mesh	ze :	5	
Speed	n_3 :	7304	1/min
Actual drive ratio	i :	0.55	
power	P_{ab} :	1.26	kW
Torque	Nm :	1.6	Nm
static belt tension new	T_3 :	111	N
Shaft load new	Sa :	138	N
Frequence new	f_3 :	35.83	Hz
static belt tension used	T_3 :	97	N
Shaft load used	Sa :	120	N
Frequence used	f_3 :	33.41	Hz
Span length	L :	402.15	mm
x-coordinate	x :	0.00	mm
y-coordinate	y :	140.00	mm

pulley 4 TB 22-8M-20 Optibelt-TB taper bush 1008 (Bore-diameter 20 mm)

Diameter	dw_4 :	56.02	mm
Number of teeth	z :	22	
Teeth in mesh	ze :	11	
Speed	n_4 :	7304	1/min
Actual drive ratio	i :	0.55	
power	P_{ab} :	1.26	kW
Torque	Nm :	1.6	Nm
static belt tension new	T_4 :	111	N
Shaft load new	Sa :	222	N
Frequence new	f_4 :	44.08	Hz
static belt tension used	T_4 :	97	N
Shaft load used	Sa :	193	N
Frequence used	f_4 :	41.11	Hz
Span length	L :	326.90	mm
x-coordinate	x :	-315.00	mm
y-coordinate	y :	-110.00	mm

Our 'General Conditions of Sale' are applicable.

E.2 Optibelt OMEGA HP Technical Sheet

Profil *Profile* 8M		
t [mm]	h_s [mm]	W [mm]
8,00	7,65 ±0,25	1,14

Prinzip-Skizze
Principle sketch

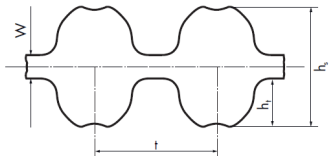

Aufbau *Construction*
- Zahnseitiges Gewebe: Polyamid verstärkt
- Elastomer: CR-Mischung mit Aramidfasern
- Zugstrang: Glascord
- Härte: 89 ±5 Shore A

- *Fabric on teeth: Polyamide reinforced*
- *Elastomer: CR compound with aramid fibres*
- *Tension cord: Glass cord*
- *Hardness: 89 ±5 Shore A*

Eigenschaften *Characteristics*
- Antistatisch nach ISO 9563: ja
- Scheibenprofile: HTD und RPP nach ISO 13050
- Temperaturbeständigkeit: -30° C bis +100° C
- Metergewicht: 0,067 kg/m für 10 mm Breite

- *Antistatic to ISO 9563: yes*
- *Pulley profile: HTD and RPP to ISO 13050*
- *Temperature resistance: -30° C to +100° C*
- *Weight per meter: 0,067 kg/m for 10 mm width*

Riemenbreite *Belt width* [mm]	Standardriemenbreite *Standard belt width* [mm]	Zulässige Toleranz der Zahnriemenbreite *Permissible tolerance of belt width* [mm] ISO 13050		
		Wirklänge bis *Pitch length up to* 838,2 mm	Wirklänge *Pitch length* 838,3 mm -1676,4 mm	Wirklänge über *Pitch length over* 1676,4 mm
3,0 - 11,0		+0,4 / -0,8	+0,4 / -0,8	-
11,1 - 38,1	20, 30	+0,8 / -0,8	+0,8 / -1,2	+0,8 / -1,2
38,2 - 50,8	50	+0,8 / -1,2	+1,2 / -1,2	+1,2 / -1,6
50,9 - 63,5		+1,2 / -1,2	+1,2 / -1,6	+1,6 / -1,6
63,6 - 76,2		+1,2 / -1,6	+1,6 / -1,6	+1,6 / -2,0
76,3 - 101,6	85	+1,6 / -1,6	+1,6 / -2,0	+2,0 / -2,0
101,7 - 177,8		+2,4 / -2,4	+2,4 / -2,8	+2,4 / -3,2
177,9 – 469,9		-	-	+4,8 / -6,4
Wickelbreiten *Sleeve widths*		300 mm ±10 mm		

Längentoleranzen *Length tolerance* [mm] ISO 13050										
Wirklänge *Pitch length* [mm]	≤ 250	> 250 ≤ 500	> 500 ≤ 750	> 750 ≤ 1000	> 1000 ≤ 1250	> 1250 ≤ 1500	> 1500 ≤ 1750	> 1750 ≤ 2000	> 2000 ≤ 2250	> 2250
Längentoleranz auf Achsabstand *Length tolerance on centre distance*	±0,20	±0,23	±0,27	±0,30	±0,33	±0,36	±0,39	±0,42	±0,45	±0,49 ±0,03*

Längen-Messbedingungen nach ISO 13050
Length measurement according to ISO 13050

* Für größere Länge sind in Schritten von 250 mm jeweils weitere 0,03 mm zu addieren
** For longer lengths an additional 0.03 mm should be added for every 250 mm increase*

Kennzeichnungsbeispiel *Marking example*

= Made in Germany **optibelt *OMEGA HP* 1200 D8M 20** 123 1 2

Werkscode *Plant code* | Länge, Profil, optionale Breite *Length, profile, optional width* | Lfd. Nummer *Count code* | Datumscode *Date code*

Mindestzähnezahl der Scheibe: z_{min} = 22
Wirkdurchmesser: d_w = 56,02 mm
Mindestdurchmesser der Außenrolle: d_{min} = 56,02 mm

Minimum no. of teeth pulley: z_{min} = 22
Pitch diameter: d_w = 56,02 mm
Minimum diameter of backside idler: d_{min} = 56,02 mm

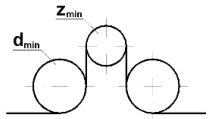

Techn. Datenblatt *Techn. datasheet*
optibelt OMEGA HP Code 77ZA
Doppelt verzahnt *double toothed*
In Anlehnung *According to* ISO13050

Profil *Profile* **8M**

Zust.	Änderungen	Datum	Name
4			
3			
2			
1			
0	Erstellt	18.10.2018	FBe

Wir beraten Sie gerne über die Produkteigenschaften und -anpassungen bei besonderen Anforderungen. Bitte beachten Sie auch die Hinweise in den Optibelt Dokumentationen. Irrtümer und technische Änderungen vorbehalten. www.optibelt.com, © Arntz Optibelt Gruppe
We would be pleased to offer advice about technical characteristics and drive design as well as special requirements. Further information can be found in Optibelt documentation. Subject to technical modification and change, errors and omissions excepted. www.optibelt.com, © Arntz Optibelt Group

Appendix F

Thomson Linear Electrak GX Actuator

Specification Sheet Online:
https://www.thomsonlinear.com/en/product/D48N05A5-02M0NN-AMM

Thomson Customer Support:
https://www.thomsonlinear.com/en/support/global-customer-service-call

THOMSON
Linear Motion. Optimized.™
A REGAL REXNORD BRAND

D48N05A5-02M0NN-AMM

Actuator, Electrak GX, 48 Vdc, Dynamic Load: 1100 N, acme, 54 mm/s , Max Stroke Length: 2 inch, Control: None

Lead Time: 73 Days

$607.66 each+

- Robust and Reliable
- Acme and Ball Screw Models
- Static Load up to 18kN/4000lbf
- Dynamic Load up to 9kN/2000lbf
- Overload Clutch for Mid and End of Stroke Protection
- Motor With Thermal Switch
- Maintenance Free

+The price shown here is the North American List Price for general reference only. Please Contact Thomson for actual net price and current delivery schedule which will vary with geographic region, quantity ordered and distribution channel. Estimated costs for shipping, packaging and import taxes/duty are not included in this list price. Please contact Thomson Customer Support for more information.

Dimensions

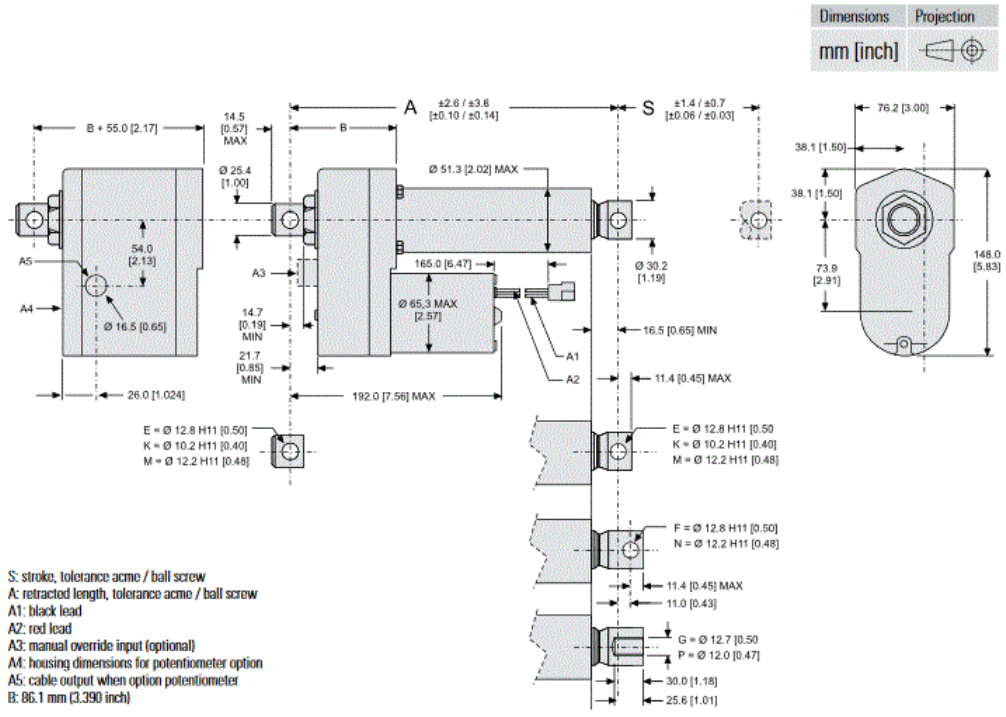

Dimension	Value
A	211.3 mm (8.319 in)
S	50.8 mm (2.000 in)

Specifications

Specifications	Value
Anti-Rotation	No
Brake	Yes with ball screw, self-locking lead screw
Certifications	CE
Special Connector	AMP term 42098-2, house 180908-5
End Play, Max	1.016 mm / 0.040 in
IP Rating, Dynamic	N/A
IP Rating, Static	IP66, IP69K
Manual Override	No
Material	Painted Zinc Alloy, Stainless Steel
Nominal Stroke	50.80 mm / 2.00 in
Protection, End of Stroke	Overload Clutch
Protection, Mid Stroke	Overload Clutch
Screw Type	Acme
Temperature Max	65 °C / 149 °F
Temperature Min	-26 °C / -15 °F
Temperature Monitoring	No
Voltage	48 Vdc
Voltage Tolerance	40-56 VDC
Maximum Current Draw	8.3 amp
Weight	4.400 kg / 9.700 lbs
Control	None
Feedback	None
Serialized	No
Smart Actuation	No
Contains Liquids	No
Returnable	No

Performance

Performance	Value
Duty Cycle	25%
Load, Dynamic	1,100 N / 247 lbf

Performance	Value
Load, Static	11,350 N / 2,552 lbf
Restraining Torque	11.30 N / 2.54 lbf
Salt Spray Resistance	N/A
Max Speed	54.10 mm/s / 2.13 in/s
Min Speed	32.00 mm/s / 1.26 in/s

Appendix G

SKF Y-bearing Unit

G.1 SKF FYTB 20 TF specification

FYTB 20 TF

Oval flanged ball bearing unit with set screw locking, cast iron housing, ISO

These oval flanged ball bearing units are compliant with ISO standards. They consist of an insert bearing, with an extended inner ring and set screw locking, and are suitable for applications where the direction of rotation is constant or alternating. The bearing is mounted in a cast iron housing, which can be bolted to a machine wall or frame. Ball bearing units can accommodate moderate initial misalignment, but normally do not permit axial displacement.

- Resist high levels of contamination
- Designed for high temperatures and speeds
- Accommodate relatively heavy loads
- Cost-effective

Overview

Dimensions

Shaft diameter	20 mm
Housing overall width	29.5 mm
Width, total	37.3 mm
Centre distance between bolt holes	90 mm
Bearing width, total	31 mm

Performance

Basic dynamic load rating	12.7 kN
Basic static load rating	6.55 kN
Limiting speed	8 500 r/min
Note	Limiting speed with shaft tolerance h6

Properties

Housing type	Flanged
Flanged housing type	Oval
Number of bolt holes for fasteners	2
Fastening bolt hole type	Plain
Retaining feature, inner ring	Set screws
Bore type	Cylindrical
Rubber seating ring	Without
Material, housing	Cast iron
Material, bearing	Bearing steel
Coating	Without
Sealing, bearing	Seal and flinger on both sides

Sealing type	Contact, standard
Sealing, unit	Optional end cover
Lubricant	Grease
Relubrication hole	With
Grease fitting	With

Technical Specification

Compliance with standard	ISO
Purpose specific	For material handling applications
Material, housing	Cast iron
Sealing, bearing	Seal and flinger on both sides
Sealing type, bearing	Contact, standard
Sealing, unit	Optional end cover
Coating	Without

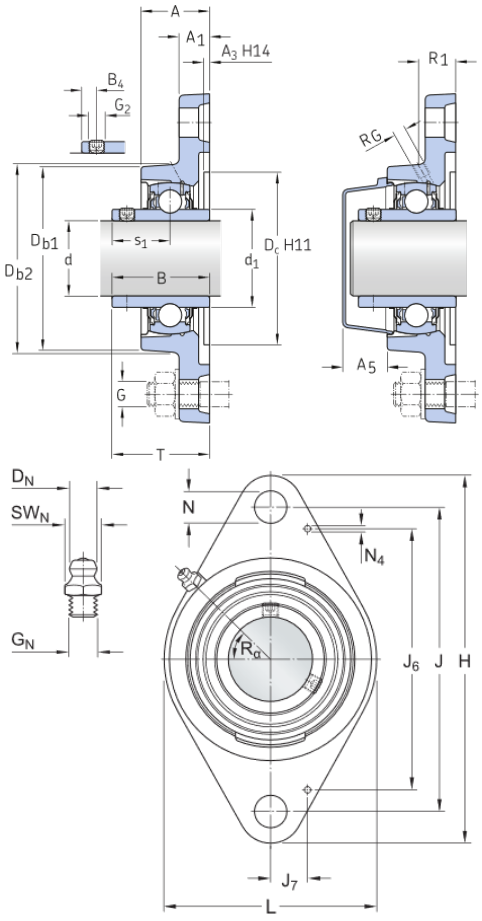

Dimensions

d	20 mm	Bore diameter
d_1	≈ 28.2 mm	Outer diameter of inner ring
A	29.5 mm	Overall width
A_1	11 mm	Flange width
A_3	3.2 mm	Depth of centring recess
A_5	20.5 mm	Width including end cover
B	31 mm	Width of inner ring
B_1	31 mm	Overall bearing width
B_4	4.5 mm	Distance from locking device side face to thread centre
D_{b1}	58 mm	Top external diameter
D_{b2}	60.5 mm	Base external diameter
D_c	50.8 mm	Diameter of housing centering recess
H	112 mm	Overall height
J	90 mm	Distance between attachment bolts
L	60.5 mm	Overall length

N	11.5 mm	Diameter of attachment bolt hole
s_1	18.3 mm	Distance from locking device side face to raceway centre
T	37.3 mm	Overall unit width

Threaded hole

R_G	1/4-28 UNF	Housing thread for grease fitting
R_1	20 mm	Axial position of the housing thread
R_o	45 °	Angular position of the housing thread

Grease fitting

D_f	6.5 mm	Diameter of head sphere of grease fitting
S_W	7 mm	Hexagonal key size for the grease fitting
G_f	1/4-28 SAE-LT	Thread of grease fitting

Dowel pins

J_6	74 mm	Distance of dowel pins
J_7	11.5 mm	Axial offset of dowel pins
N_4	2 mm	Recommended diameter for dowel pins

Calculation data

Basic dynamic load rating	C	12.7 kN
Basic static load rating	C_0	6.55 kN
Fatigue load limit	P_u	0.28 kN
Limiting speed		8 500 r/min
		Limiting speed with shaft tolerance h6

Mass

Mass bearing unit		0.45 kg

Mounting information

Set screw	G_2	M6x0.75
Hexagonal key size for set screw		3 mm
Recommended tightening torque for set screw		4 N·m
Recommended diameter for attachment bolts, mm	G	10 mm
Recommended diameter for attachment bolts, inch	G	0.375 in

Terms and conditions

By accessing and using this website / app owned and published by AB SKF (publ.) (556007-3495 · Gothenburg) ("SKF"), you agree to the following terms and conditions:

Warranty Disclaimer and Limitation of Liability

Although every care has been taken to assure the accuracy of the information on this website / app, SKF provides this information "AS IS" and DISCLAIMS ALL WARRANTIES, EXPRESS OR IMPLIED, INCLUDING, BUT NOT LIMITED TO, IMPLIED WARRANTIES OF MERCHANTABILITY AND FITNESS FOR A PARTICULAR PURPOSE. You acknowledge that your use of this website / app is at your sole risk, that you assume full responsibility for all costs associated with use of this website / app, and that SKF shall not be liable for any direct, incidental, consequential, or indirect damages of any kind arising out of your access to, or use of the information or software made available on this website / app. Any warranties and representations in this website / app for SKF products or services that you purchase or use will be subject to the agreed upon terms and conditions in the contract for such product or service. Further, for non-SKF websites / apps that are referenced in our website / app or where a hyperlink appears, SKF makes no warranties concerning the accuracy or reliability of the information in these websites / apps and assumes no responsibility for material created or published by third parties contained therein. In addition, SKF does not warrant that this website / app or these other linked websites / apps are free from viruses or other harmful elements.

Third Party Services

When viewing YouTube content via the SKF website(s) (i.e. using YouTube API Services), you agree to be bound by the YouTube Terms of Service.

Copyright

Copyright in this website / app copyright of the information and software made available on this website / app rest with SKF or its licensors. All rights are reserved. All licensed material will reference the licensor that has granted SKF the right to use the material. The information and software made available on this website / app may not be reproduced, duplicated, copied, transferred, distributed, stored, modified, downloaded or otherwise exploited for any commercial use without the prior written approval of SKF. However, it may be reproduced, stored and downloaded for use by individuals without prior written approval of SKF. Under no circumstances may this information or software be supplied to third parties.
This website /app includes certain images used under license from Shutterstock, Inc.

Trademarks and Patents

All trademarks, brand names, and corporate logos displayed on the website / app are the property of SKF or its licensors, and may not be used in any way without prior written approval by SKF. All licensed trademarks published on this website / app reference the licensor that has granted SKF the right to use the trademark. Access to this website / app does not grant to the user any license under any patents owned by or licensed to SKF.

Changes

SKF reserves the right to make changes or additions to this website / app at any time.

G.2 SKF ECY 204 specification

ECY 204

End cover for bearing units

End covers protect the exposed shaft end and help to avoid accidents. They have good resistance to most chemicals and can withstand operating temperatures up to 100 °C (210 °F). They are easy to install and are cost effective. Most ball bearing units can accommodate specifically designed end covers.

- Easy to install
- Good chemical resistance
- Cost effective

Overview

Dimensions

Outside diameter	49 mm
Width	23 mm

Properties

Accessory type	End cover
Material	Polypropylene (PP)

Technical Specification

Material	Polypropylene (PP)

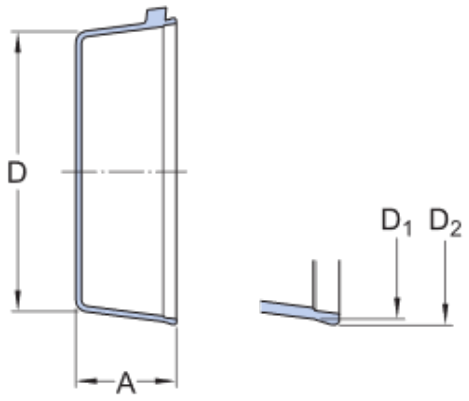

Dimensions

A	23 mm	Overall width
D	44.1 mm	Outside diameter at closed end
D_1	49 mm	Outside diameter at open end
D_2	50.5 mm	Anchorage diameter

Mass

Mass end cover	10 g

Terms and conditions

By accessing and using this website / app owned and published by AB SKF (publ.) (556007-3495 · Gothenburg) ("SKF"), you agree to the following terms and conditions:

Warranty Disclaimer and Limitation of Liability

Although every care has been taken to assure the accuracy of the information on this website / app, SKF provides this information "AS IS" and DISCLAIMS ALL WARRANTIES, EXPRESS OR IMPLIED, INCLUDING, BUT NOT LIMITED TO, IMPLIED WARRANTIES OF MERCHANTABILITY AND FITNESS FOR A PARTICULAR PURPOSE. You acknowledge that your use of this website / app is at your sole risk, that you assume full responsibility for all costs associated with use of this website / app, and that SKF shall not be liable for any direct, incidental, consequential, or indirect damages of any kind arising out of your access to, or use of the information or software made available on this website / app. Any warranties and representations in this website / app for SKF products or services that you purchase or use will be subject to the agreed upon terms and conditions in the contract for such product or service. Further, for non-SKF websites / apps that are referenced in our website / app or where a hyperlink appears, SKF makes no warranties concerning the accuracy or reliability of the information in these websites / apps and assumes no responsibility for material created or published by third parties contained therein. In addition, SKF does not warrant that this website / app or these other linked websites / apps are free from viruses or other harmful elements.

Third Party Services

When viewing YouTube content via the SKF website(s) (i.e. using YouTube API Services), you agree to be bound by the YouTube Terms of Service.

Copyright

Copyright in this website / app copyright of the information and software made available on this website / app rest with SKF or its licensors. All rights are reserved. All licensed material will reference the licensor that has granted SKF the right to use the material. The information and software made available on this website / app may not be reproduced, duplicated, copied, transferred, distributed, stored, modified, downloaded or otherwise exploited for any commercial use without the prior written approval of SKF. However, it may be reproduced, stored and downloaded for use by individuals without prior written approval of SKF. Under no circumstances may this information or software be supplied to third parties.
This website /app includes certain images used under license from Shutterstock, Inc.

Trademarks and Patents

All trademarks, brand names, and corporate logos displayed on the website / app are the property of SKF or its licensors, and may not be used in any way without prior written approval by SKF. All licensed trademarks published on this website / app reference the licensor that has granted SKF the right to use the trademark. Access to this website / app does not grant to the user any license under any patents owned by or licensed to SKF.

Changes

SKF reserves the right to make changes or additions to this website / app at any time.

Appendix H

Mechanical Drawing of the tool

H.1 Cutting Tool

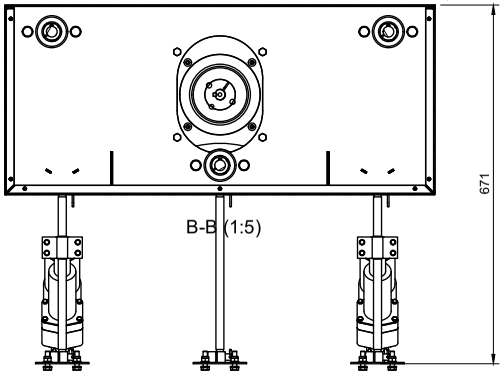

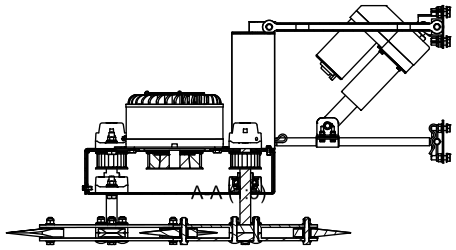

124

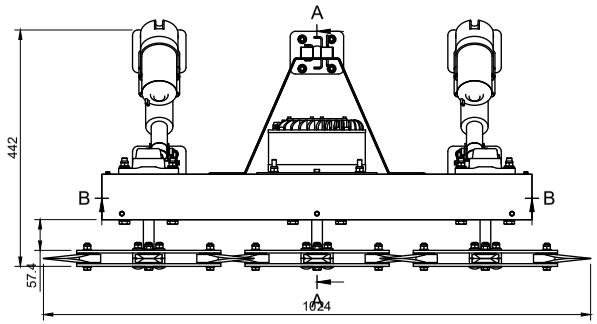

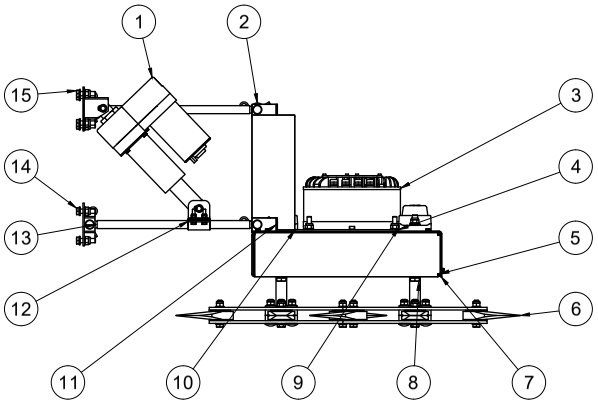

3.3	1	Parallel key	DIN 6885-1 A 6x6x22-A2
3.2	1	Taper lock bushing	1610-20
3.1	1	Pulley	TB 40 8M 20-1610
3	1	Golden Motor BCDC motor	HPM3000B
Item	Qty	Part Number	Description
Parts List			
15	2	Actuator mounting bracket	AISI 304 sheet metal
14	3	Mounting Bracket	AISI 304 sheet metal
13	2	Side Connecting Tube	AISI 304 15x1.5x286
12	2	Fixation Device	AISI 304 sheet metal
11	2	Appendage	AISI 304 sheet metal
10	1	Trapezium	AISI 304 sheet metal
9	3	SKF bearing unit and cover	FYTB 20 TF+ECY 204
8	3	SKF bearing unit	FYTB 20 TF
7	1	Lid	AISI 304 sheet metal
6	3	Cutting Subsystem	
5	1	Box	AISI 304
4	1	Motor Support	AISI 304 sheet metal
3	1	Golden Motor BCDC motor	HPM3000B
2	1	Top Connecting Tube	AISI 304 15x1.5x286
1	2	Thomson Linear Electrak GX	D48N05A5-02M0NN-AMM
Item	Qty	Part Number	Description
Parts List			

Dept.	Technical reference	Created by	Material
DeMec		Ricardo Carvalho 11/09/2023	----
		Document type	Scale
			1:5
		Title	Paper Size
		Cutting Tool	A1
		Qty.	Date of issue / Sheet
			1/16

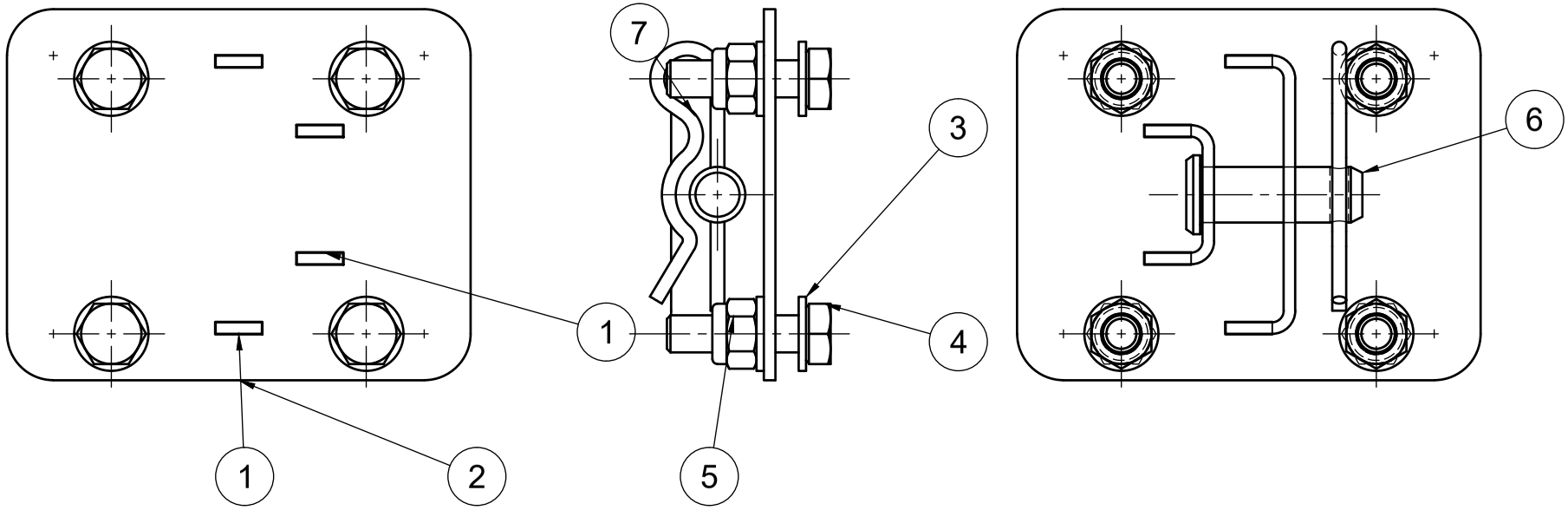

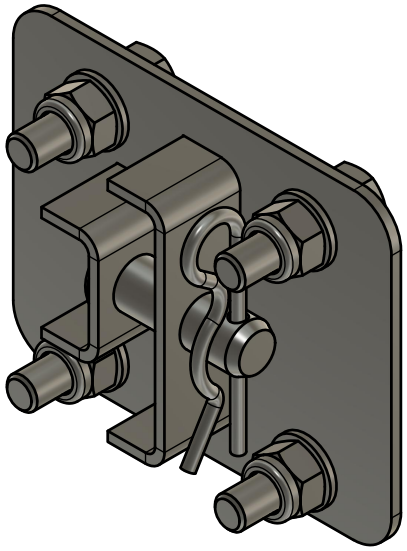

Isometric View

Item	Qty	Part Number	Description
7	1	Spring cotter	DIN 11024 2.5-A2
6	1	Clevis pin with small head	DIN 1434 A 12x35-A2
5	4	Hexagon nut	DIN 982 M8-A2
4	4	Hexagon head bolt	ISO 4014 (DIN 931) M8x30-A2
3	8	Washer	ISO 7089 8-A2
2	1	Plate	AISI 304 sheet metal
1	1	Flaps	AISI 304

Parts List

Dept.: DeMec	Technical reference:	Created by: Ricardo Carvalho 11/09/2023	Material: ----
		Document type:	Scale: 1:1
		Title: Cutting Tool Mounting Bracket	Paper Size: A3
			Qty. / Date of issue / Sheet: 2/16

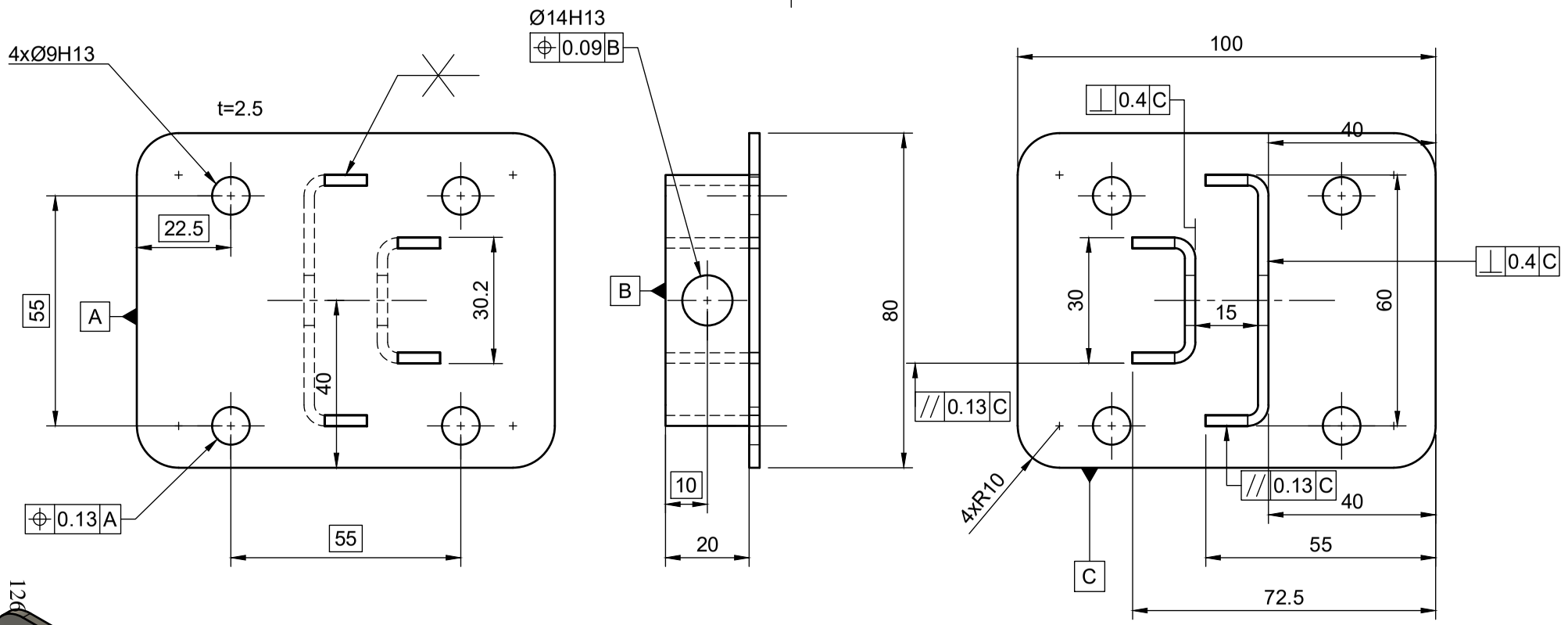

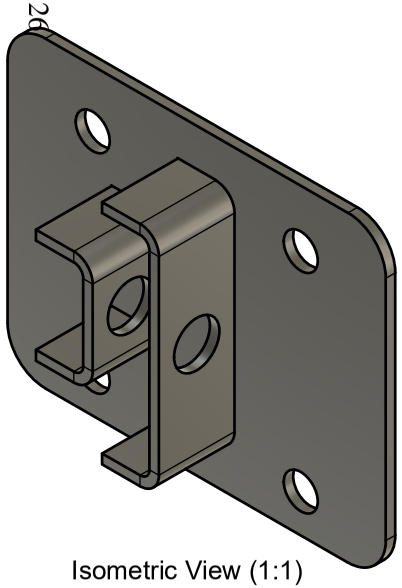

Isometric View (1:1)

ISO 2378-mK
ISO 8015
ISO 13920-BF

Dept.	Technical reference	Created by	Material
DeMec	ISO 2378-mK	Ricardo Carvalho 11/09/2023	AISI 304 sheet metal
		Document type	Scale 1:1
		Title: Cutting Tool Mounting Bracket	Paper Size A3
			Qty. / Date of issue / Sheet 3/16

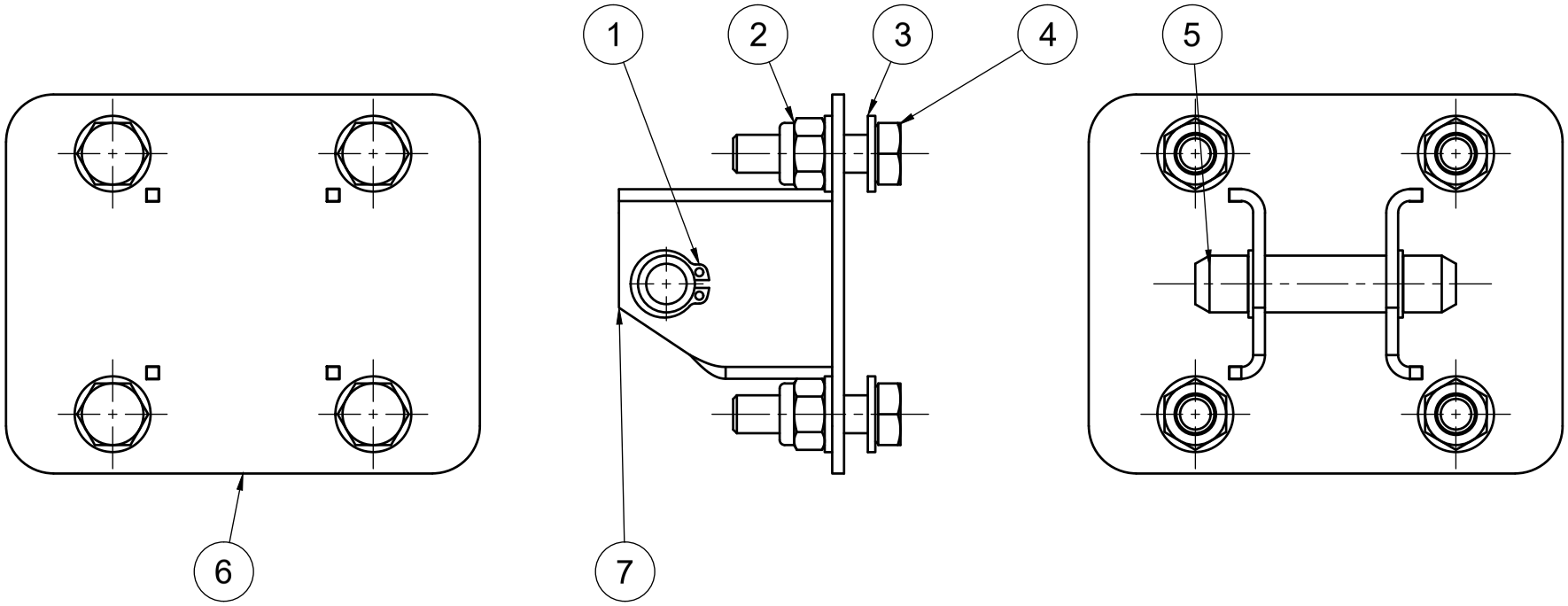

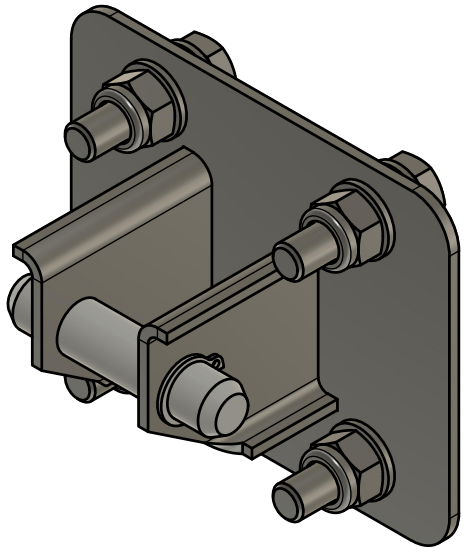

Isometric View (1:2)

Item	Qty	Part Number	Description
7	1	Mounting Bracket support	AISI 304 sheet metal
6	1	Mounting Bracket Plate	AISI 304
5	1	Clevis pin without head A	ISO 2340 12x55-A2
4	4	Hexagon head bolt	ISO 4014 (DIN 931) M8x30-A2
3	8	Washer	ISO 7089 8-A2
2	4	Hexagon nut	DIN 982 M8-A2
1	2	Elastic Ring	DIN 471 V2 12x1-A2

Parts List

Dept. DeMec	Technical reference	Created by Ricardo Carvalho 11/09/2023	Material
		Document type	Scale 1:2
		Title: Cutting Tool Linear Actuator Mounting Bracket	Paper Size A3
			Qty. / Date of issue / Sheet 4/16

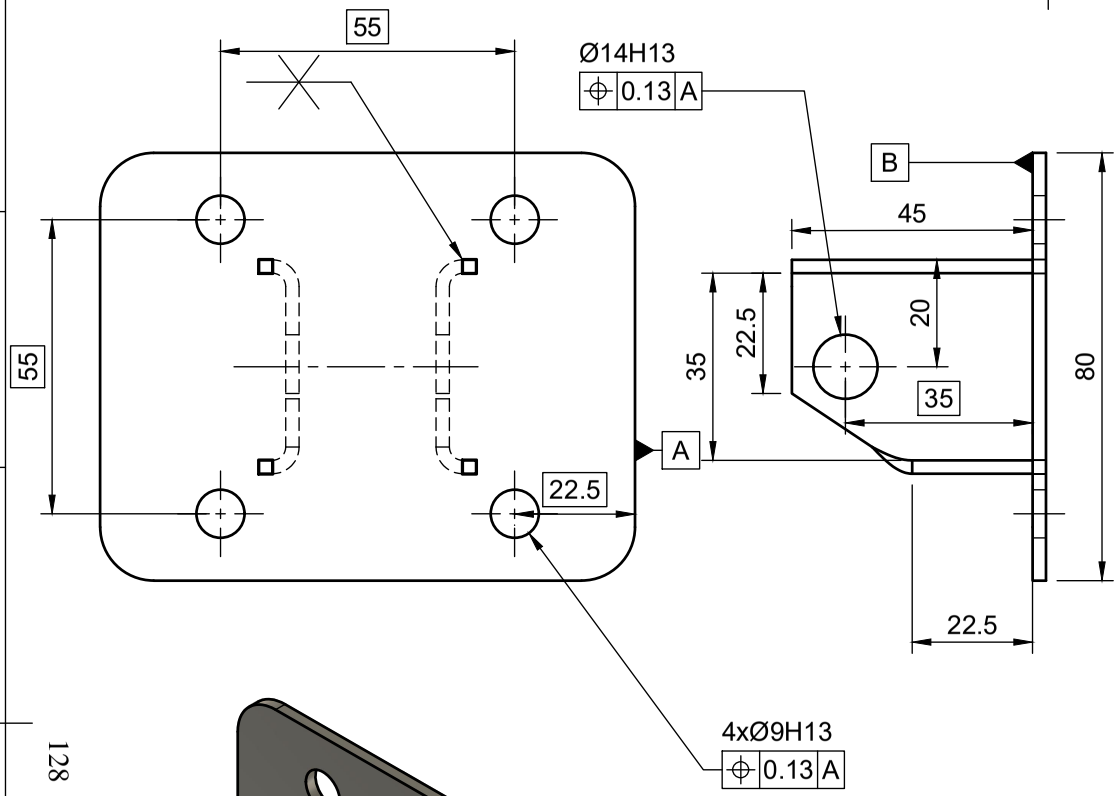

128

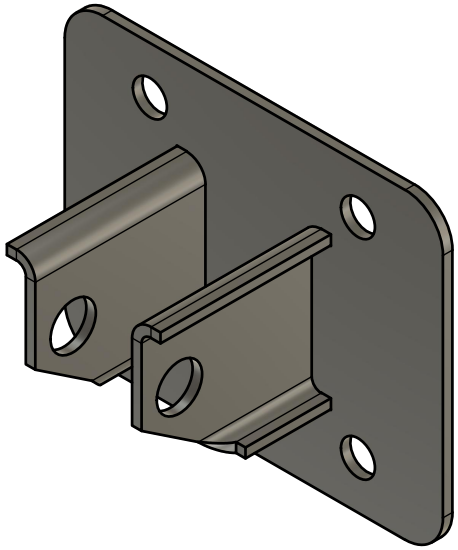

Isometric View

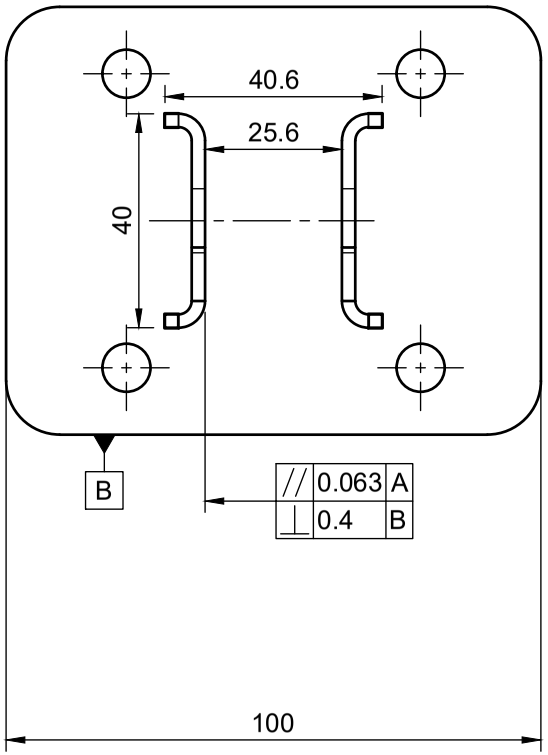

ISO 2378-mK
ISO 8015
ISO 13920-BF

Dept. DeMec	Technical reference	Created by Ricardo Carvalho 11/09/2023	Material AISI 304 sheet metal
		Document type	Scale 1:1
		Title Cutting Tool Linear Actuator Mounting Bracket	Paper Size A3
			Qty. / Date of issue / Sheet 5/16

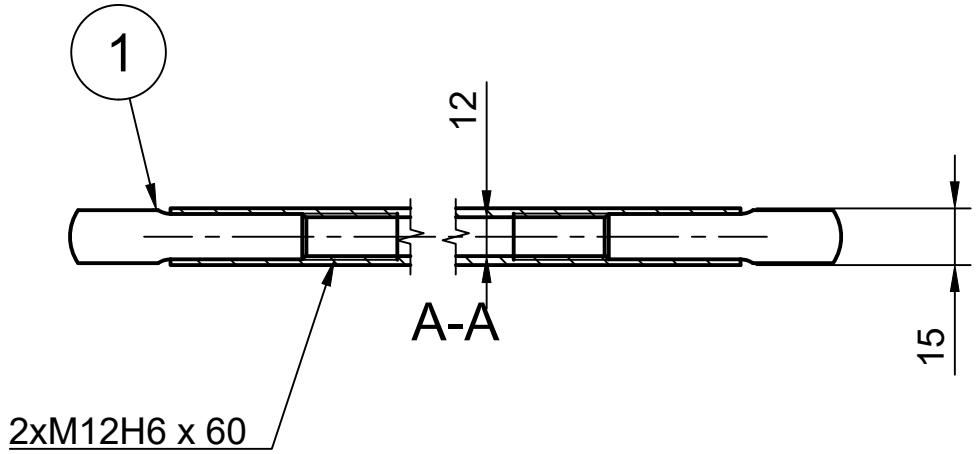

Top Connecting Rod

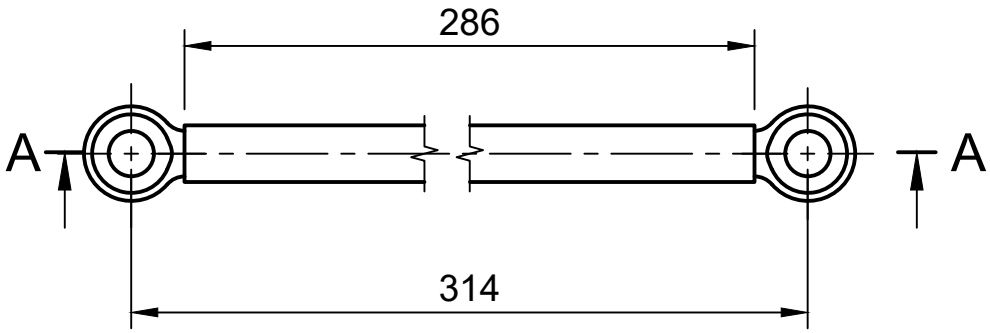

ISO 2378-mK
ISO 8015

Item	Qty	Part Number	Description
1	2	Eye Bolt	DIN 444 B & DIN 444 LB B M12x50-A2
2	1	Hollow Tube	AISI 304 15x1.5x286

Parts List

Dept. DeMec	Technical reference	Created by Ricardo Carvalho 11/09/2023	Material
		Document type	Scale 1:4
		Title Cutting Tool Top Connecting Rod	Paper Size A4
			Qty. / Date of issue / Sheet 6/16

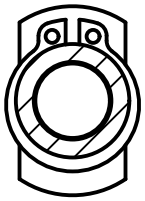

A-A (2:1)

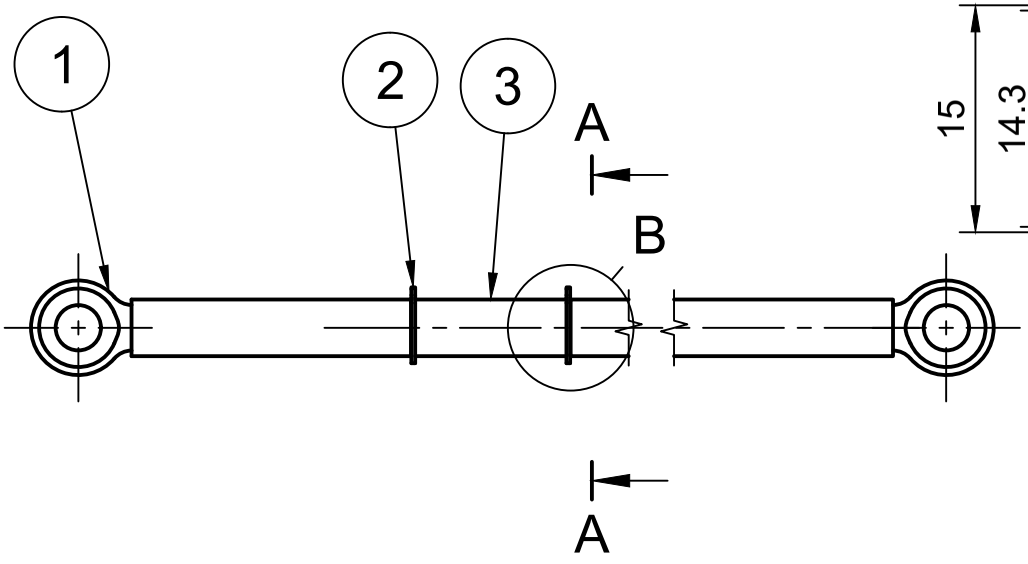

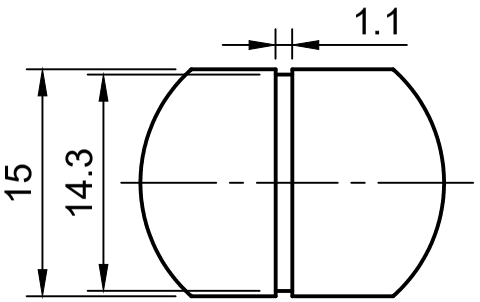

B (2:1)

Item	Qty	Part Number	Description
4	1	Eye Bolt	DIN 444 B & DIN 444 LB B M12x50-A2
3	1	Hollow Tube	AISI 304 15x1.5x286
2	2	Elastic Ring	DIN 471 V2 15x1-A2
1	1	Eye Bolt	DIN 444 B & DIN 444 LB B M12x50-A2

Parts List

Same dimensions as Top Connecting Rod

Dept. DeMec	Technical reference	Created by Ricardo Carvalho 11/09/2023	Material
		Document type	Scale 1:2
		Title: Cutting Tool Side Connecting Rod	Paper Size A4
			Qty. / Date of issue / Sheet 7/16

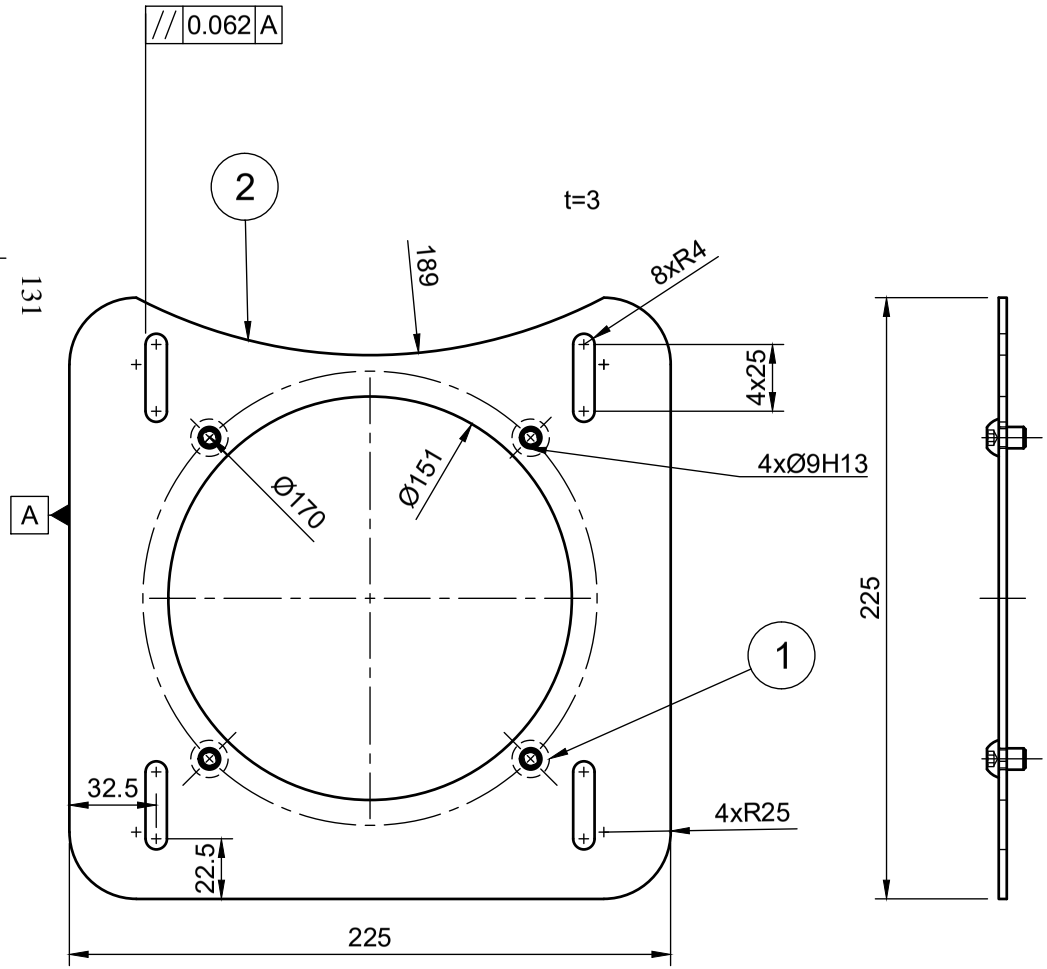

ISO 2378-mK
ISO 8015

Item	Qty	Part Number	Description
2	1	Motor Support	AISI 304 sheet metal
1	4	Screw	ISO 7380-1 M8x10-A2

Parts List

Dept. DeMec	Technical reference ISO 2378-mK	Created by Ricardo Carvalho 11/09/2023	Material AISI 304 sheet metal
		Document type	Scale 1:2
		Title: Cutting Tool Motor Support	Paper Size A3
			Qty. / Date of issue / Sheet 8/16

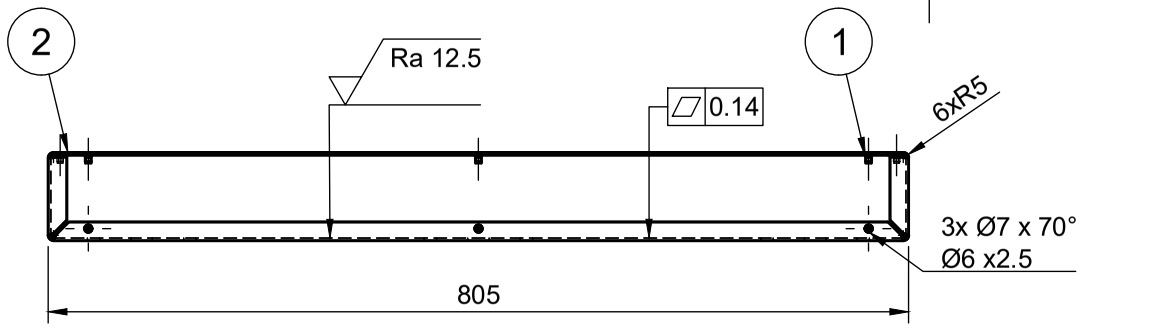

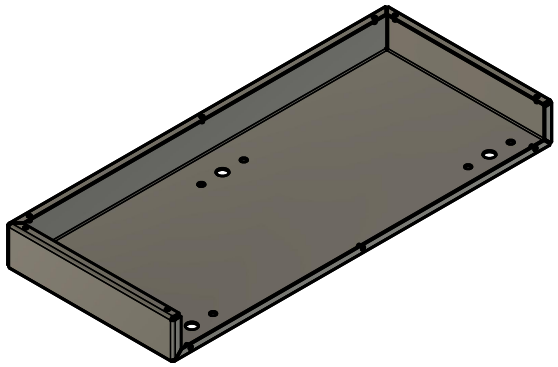

Isometric View (1:8)

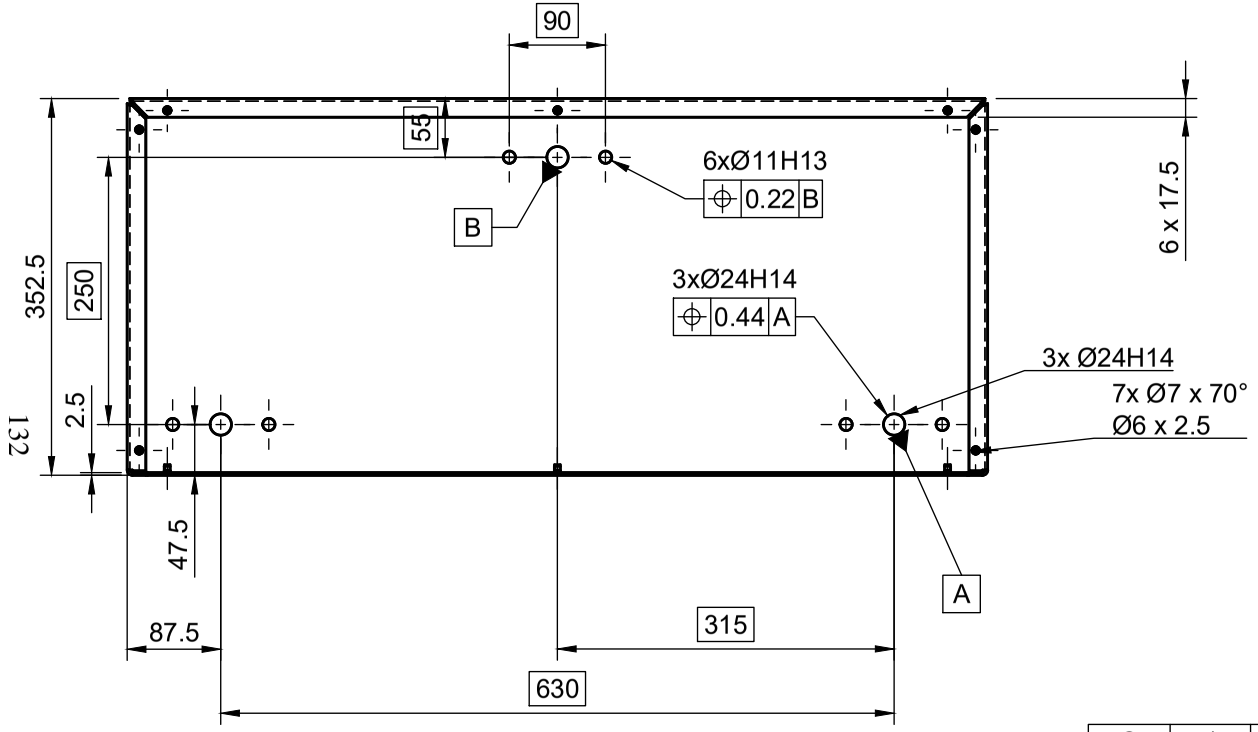

ISO 2378-mK
ISO 8015

Item	Qty	Part Number	Description
2	1	Box	AISI 304
1	10	Rivet Nut	M4

Parts List

Dept. DeMec	Technical reference	Created by Ricardo Carvalho 11/09/2023	Material AISI 304 sheet metal
		Document type	Scale 1:5
		Title Cutting Tool Box	Paper Size A3
			Qty. / Date of issue / Sheet 9/16

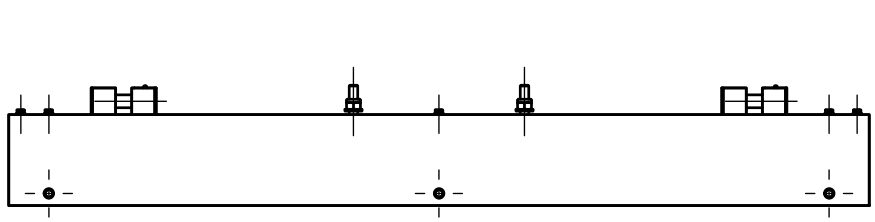

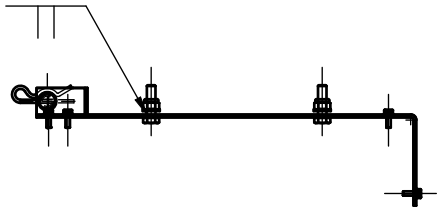

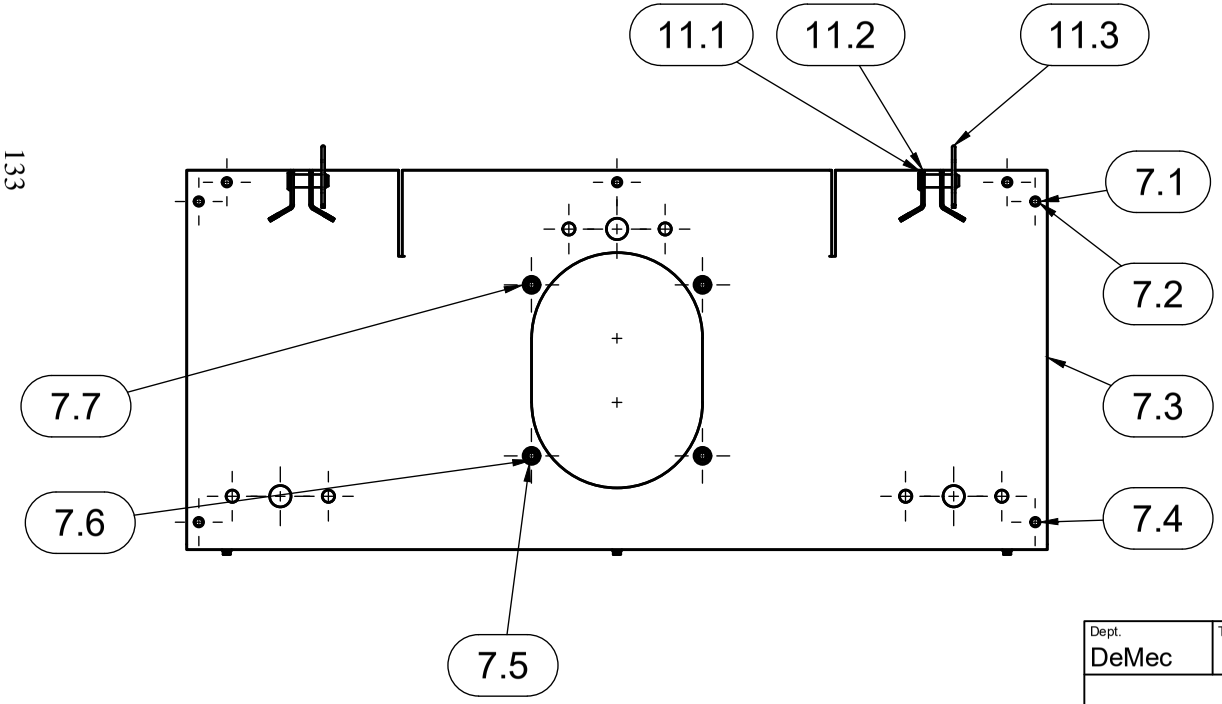

133

Item	Qty	Part Number	Description
11.3	1	Spring cotter	DIN 11024 2.5-A2
11.2	1	Side Appendage	AISI 304 sheet metal
11.1	1	Clevis pin with small head	DIN 1434 A 12x35-A2
11	2	Appendage	AISI 304 sheet metal
7.7	4	Washer	ISO 7089 8-A2
7.6	4	Hexagon head bolt	ISO 4014 (DIN 931) M8x30-A2
7.5	4	Hexagon nut	DIN 982 M8-A2
7.4	10	Spring Washer	DIN 127 V2 B 4-A2
7.3	1	Lid	AISI 304
7.2	10	Hexagon bolt	ISO4017 (DIN933) M4x14-A2
7.1	10	Washer	ISO 7089 4-A2
7	1	Lid	AISI 304 sheet metal

Parts List

Dept. DeMec	Technical reference	Created by Ricardo Carvalho 11/09/2023	Material AISI 304 sheet metal
		Document type	Scale 1:5
		Title: Cutting Tool Lid and Side Appendages	Paper Size A3
			Qty. / Date of issue / Sheet 10/16

t=2.5

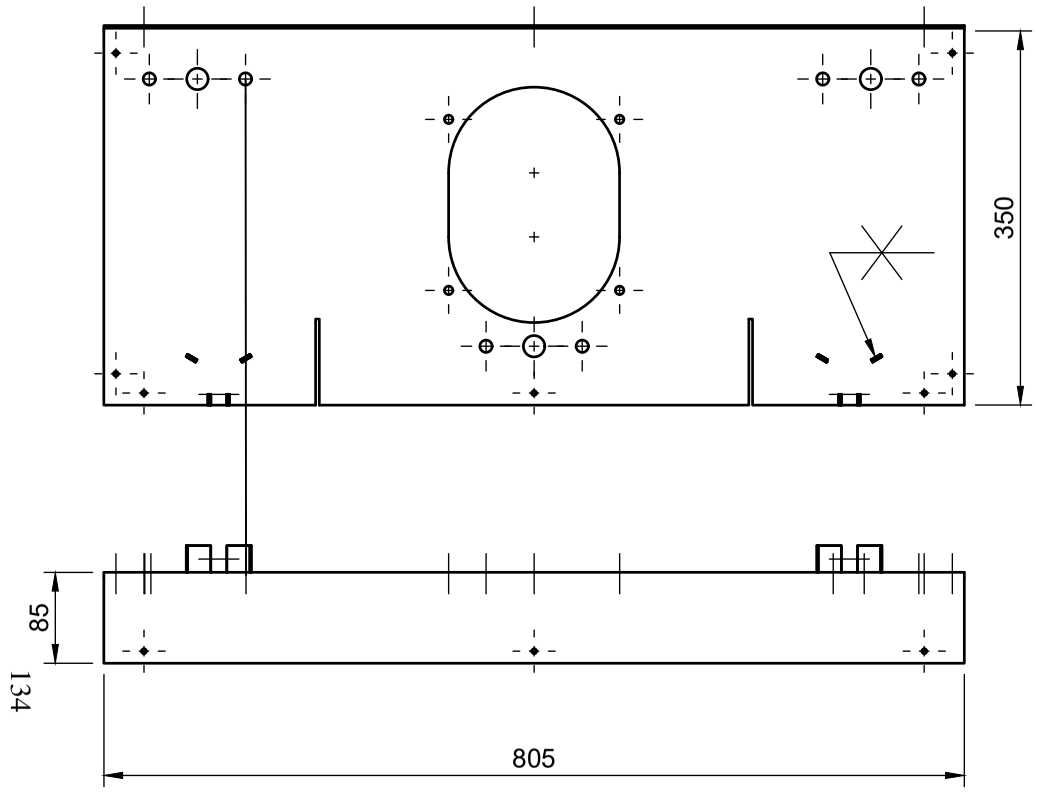

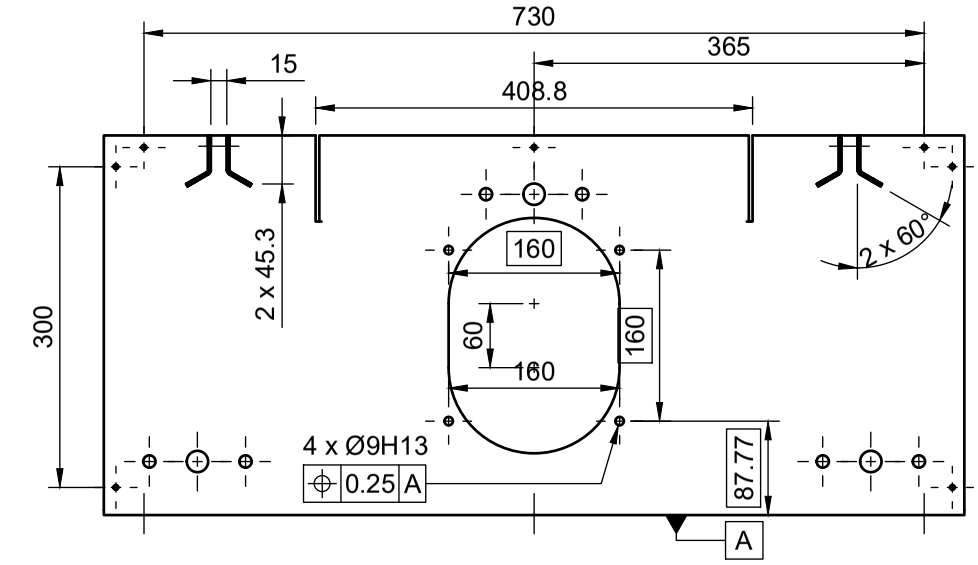

Tolerances and dimensions of the holes not referrenced in the present drawing are to be done in accordance to the holes in the Box component for correct mounting.

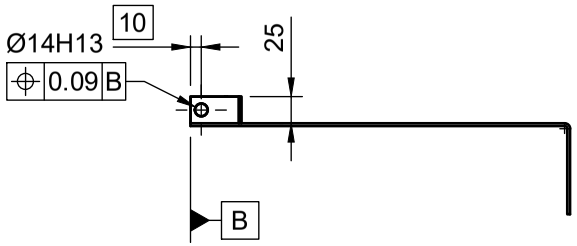

ISO 2378-mK
ISO 8015
ISO 13920-BF

Dept.	Technical reference	Created by	Material
DeMec		Ricardo Carvalho 11/09/2023	AISI 304 sheet metal
		Document type	Scale 1:5
		Title: Cutting Tool Lid, Appendages and Trapezium	Paper Size A3
			Qty. / Date of issue / Sheet 11/16

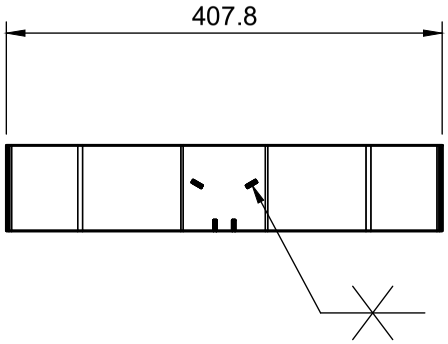

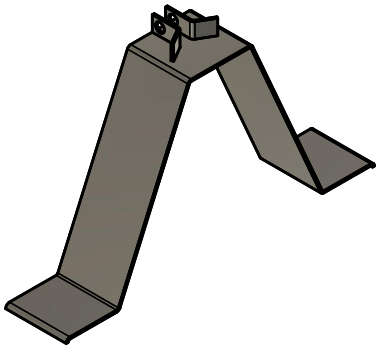

Isometric View

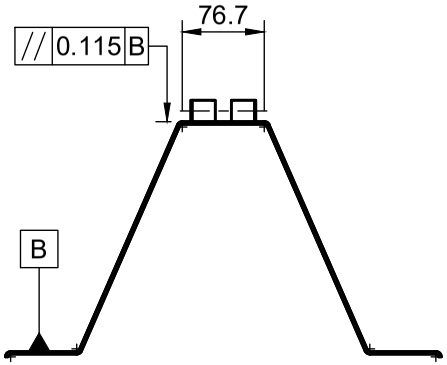

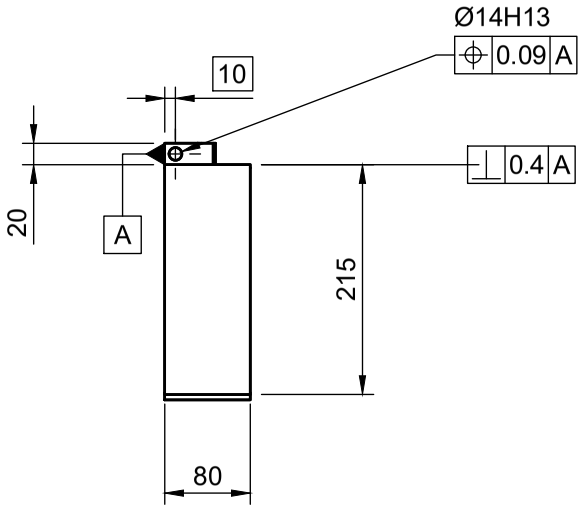

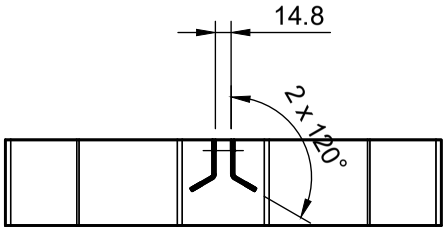

135

ISO 2378-mK
ISO 8015
ISO 13920-BF

Dept. DeMec	Technical reference	Created by Ricardo Carvalho 11/09/2023	Material AISI 304 sheet metal
		Document type	Scale 1:5
		Title: Cutting Tool Trapezium and Top Appendage	Paper Size A3
			Qty. / Date of issue / Sheet 12/16

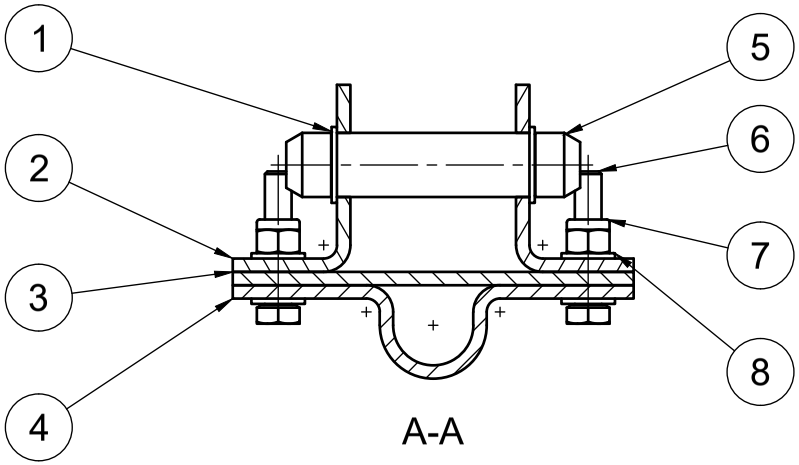

A-A

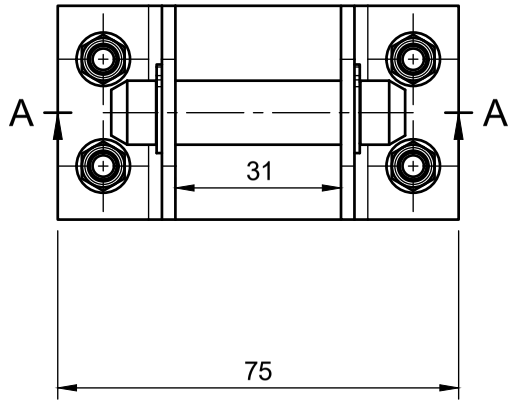

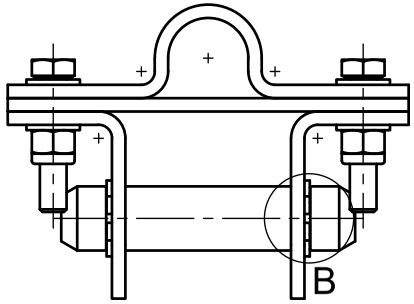

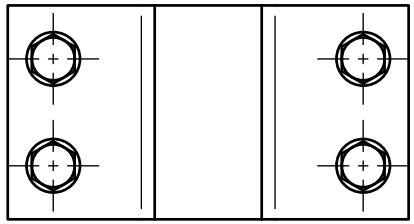

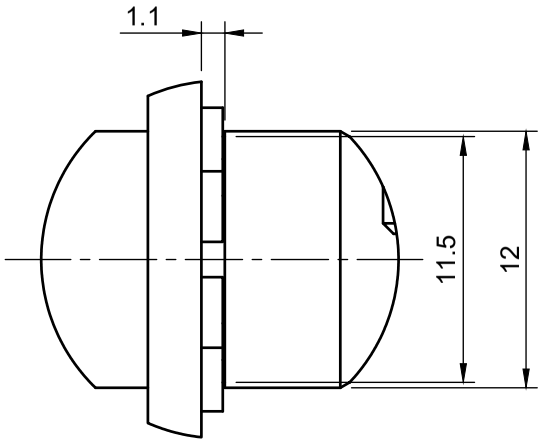

B (4:1)

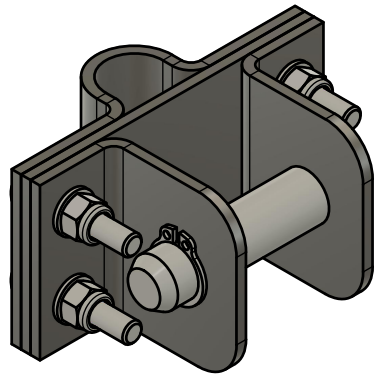

Isometric View (1:1)

Item	Qty	Part Number	Description
8	8	Washer	ISO 7089 5-A2
7	4	Hexagon nut	DIN 982 M5-A2
6	4	Hexagon head bolt	ISO 4014 (DIN 931) M5x25-A2
5	1	Clevis pin without head	ISO 2340 A 12x55-A2
4	1	Bottom Piece	AISI 304 sheet metal
3	1	Middle Piece	AISI 304 sheet metal
2	1	Top Piece	AISI 304 sheet metal
1	2	Elastic Ring	DIN 471 V2 12x1-A2

Parts List

Dept.: DeMec	Technical reference:	Created by: Ricardo Carvalho 11/09/2023	Material: AISI 304 sheet metal
		Document type:	Scale: 1:2
		Title: Cutting Tool Fixation Device	Paper Size: A3
			Qty.: / Date of issue: / Sheet: 13/16

136

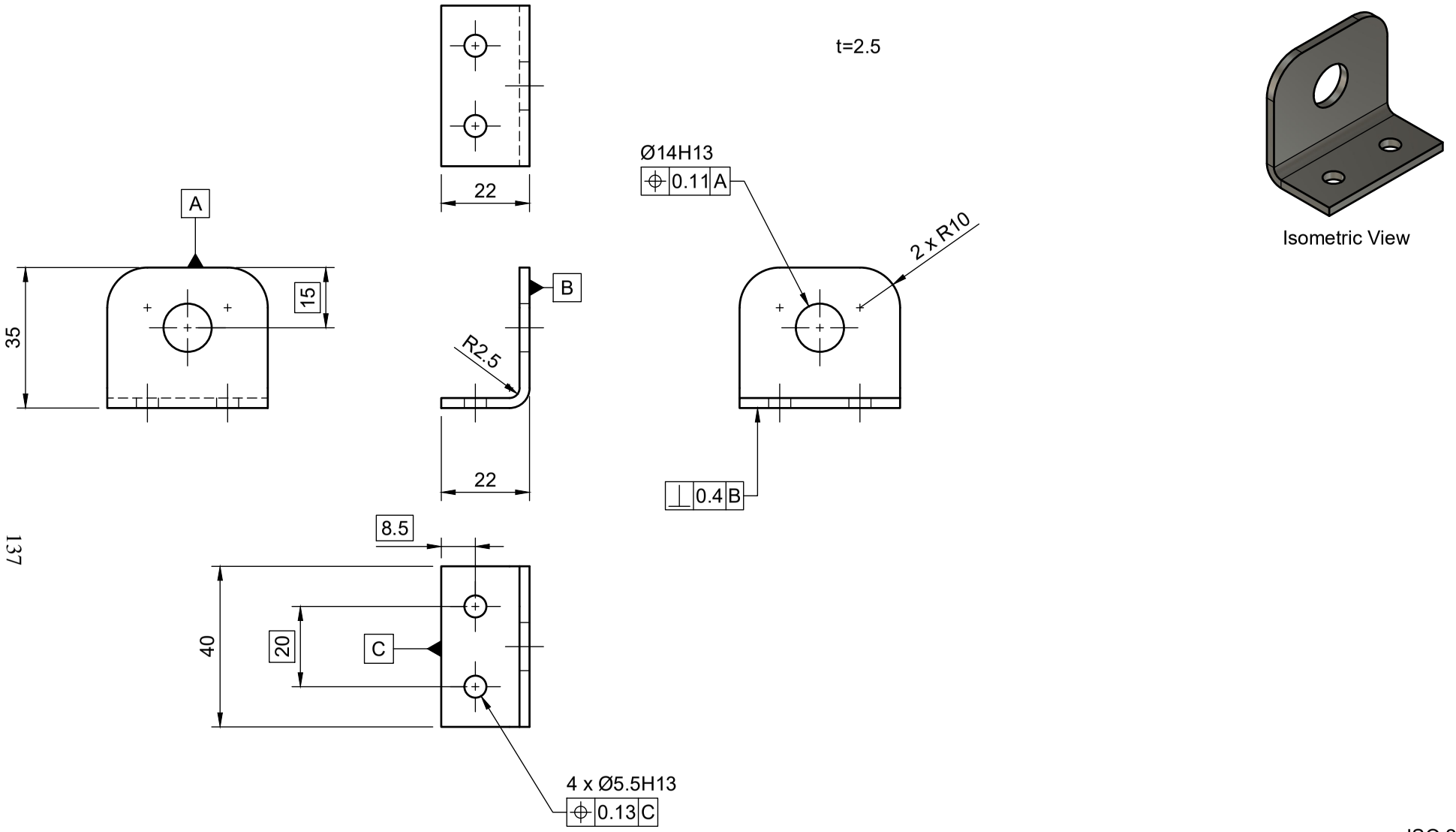

Isometric View

ISO 2378-mK
ISO 8015

Dept. DeMec	Technical reference	Created by Ricardo Carvalho 11/09/2023	Material AISI 304 sheet metal
		Document type	Scale 1:1
		Title: Cutting Tool Fixation Device Top Piece	Paper Size A3
			Qty. 2 / Date of issue / Sheet 14/16

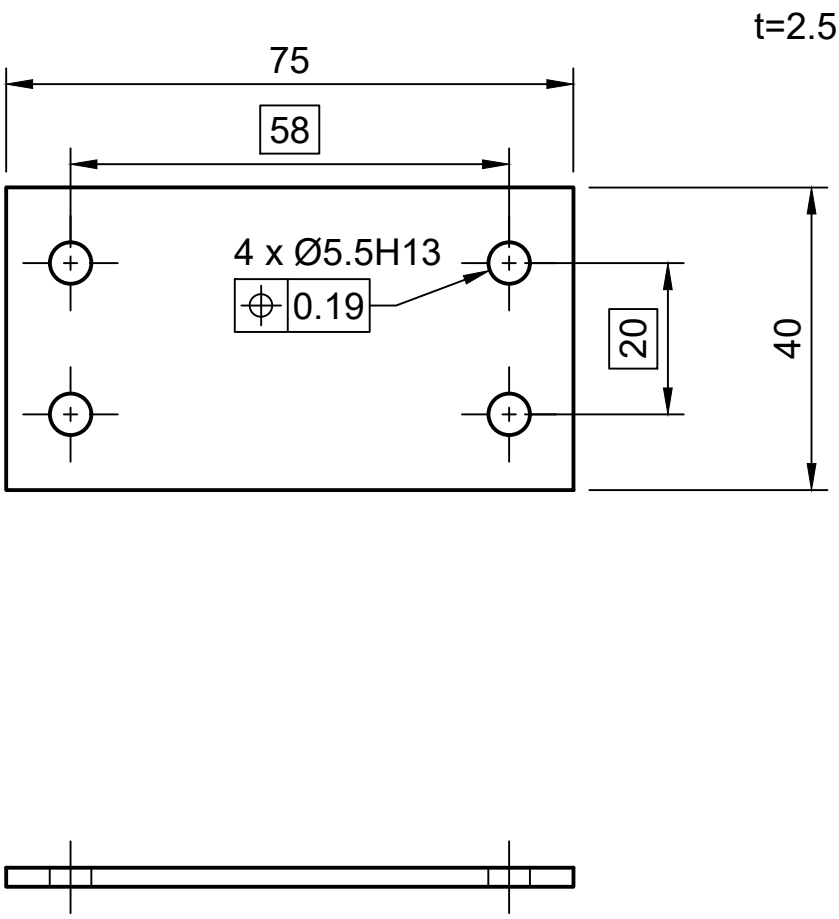

ISO 2378-mK
ISO 8015

Dept.	Technical reference	Created by	Material
DeMec		Ricardo Carvalho 11/09/2023	AISI 304 sheet metal
		Document type	Scale
			1:1
		Title	Paper Size
		Cutting Tool Fixation Device Middle Piece	A4
			Qty. 1 / Date of issue / Sheet 15/16

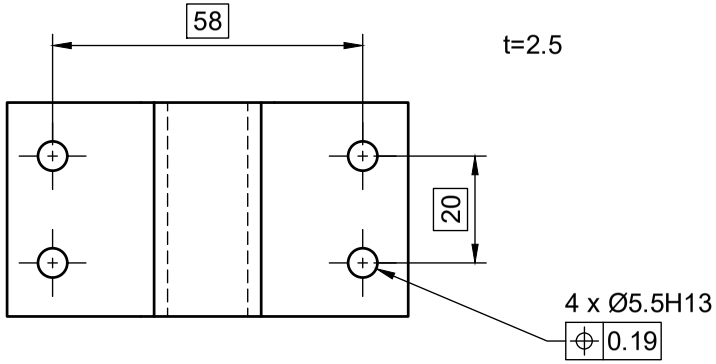

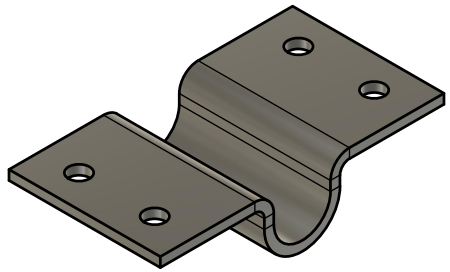

Isometric View

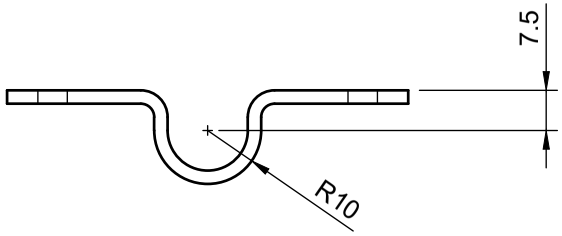

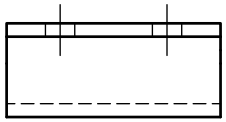

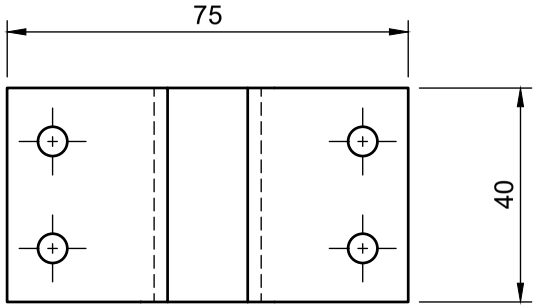

ISO 2378-mK
ISO 8015

Dept.	Technical reference	Created by	Material
DeMec		Ricardo Carvalho 11/09/2023	AISI 304 sheet metal
		Document type	Scale 1:1
		Title: Cutting Tool Fixation Device Bottom Piece	Paper Size A3
			Qty. 1 / Date of issue / Sheet 16/16

H.2 Cutting Solution

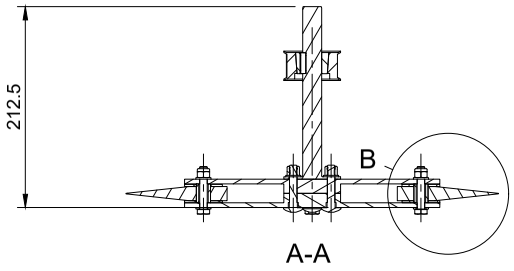

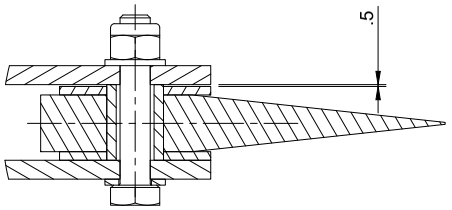

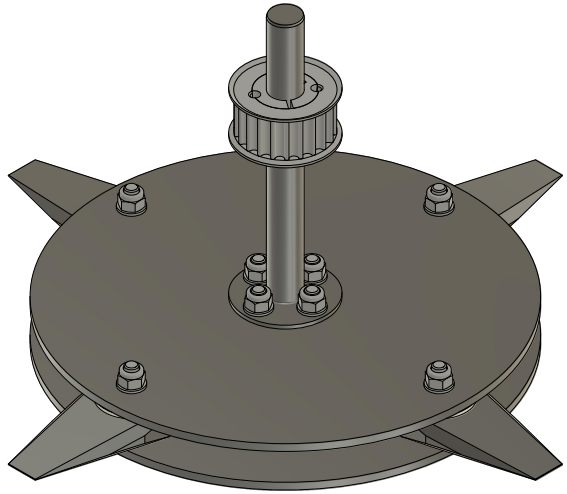

Isometric View (1:2)

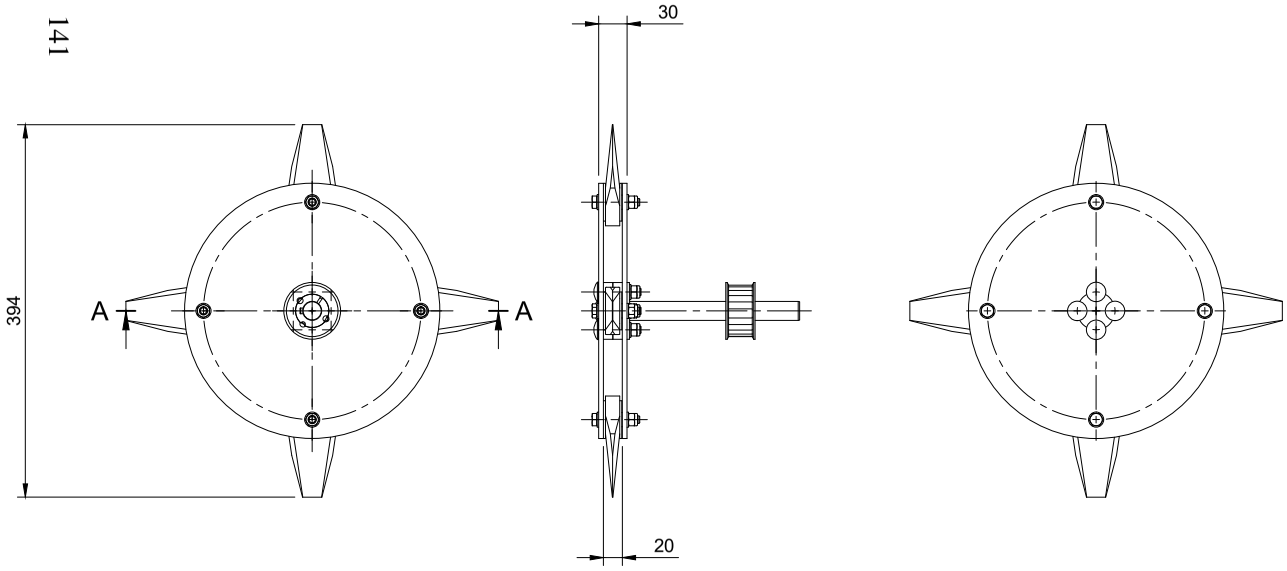

Item	Qty	Part Number	Description	Material
14	4	Cup square neck bolt	DIN 603 M8x45-8.8	Steel
13	1	Top Holding Disk	C45 Steel	Steel
12	1	Bottom Holding Disk	C45 Steel	Steel
11	1	Parallel key	DIN 6885-1 A 6x6x22-8.8	Steel
10	1	Taper lock bushing	1008-20	Steel
9	1	Pulley	TB 22 8M 20-1008	Steel
8	4	Washer	POM with PTFE filling	Acetal Resin, White
7	4	Hexagon head screw	ISO 4014 (DIN 931) M8x45-8.8	Steel
6	4	Blade	C45 Steel	Steel
5	8	Hexagon nut	DIN 982 M8-8.8	Steel
4	12	Washer	ISO 7089 8-200HV	Steel
3	4	Internal Bushing	POM with PTFE filling	Acetal Resin, White
2	4	Washe	POM with PTFE filling	Acetal Resin, White
1	1	Shaft	C45 Steel	Steel

Parts List

Dept. DeMec	Technical reference	Created by Ricardo Carvalho 11/09/2023	Approved by
		Document type	Scale 1:4
		Title Cutting Subsystem	Paper Size. A2
			Rev. / Date of issue / Sheet 1/7

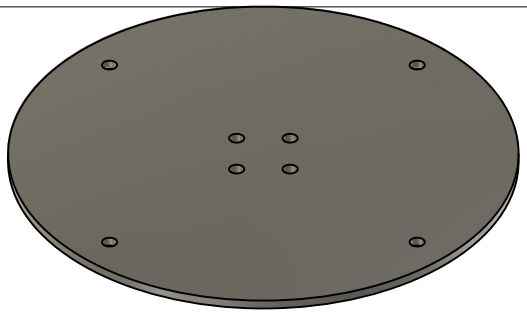

Isometric View

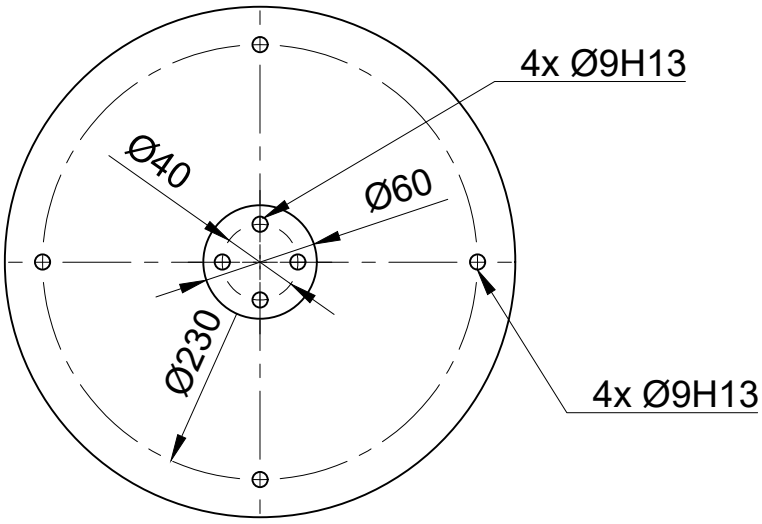

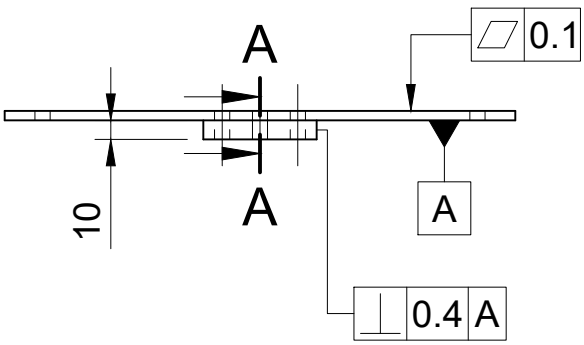

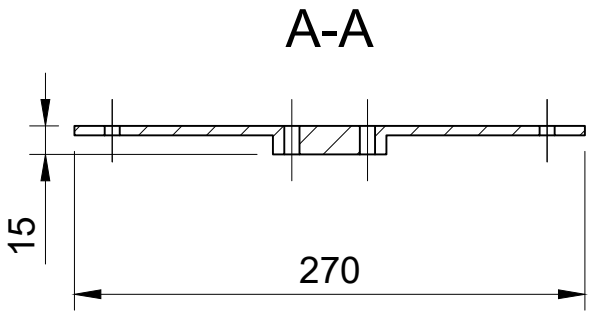

ISO 2378-mK
ISO 8015

Dept.	Technical reference	Created by	Approved by		
DeMec		Ricardo Carvalho 11/09/2023			
		Document type	Scale		
			1:4		
		Title	Paper Size		
		Cutting Subsystem Top Holding Disk	A4		
			Rev.	Material	Sheet
				C45 Steel	2/7

Same dimensions as
Top Holding Disk

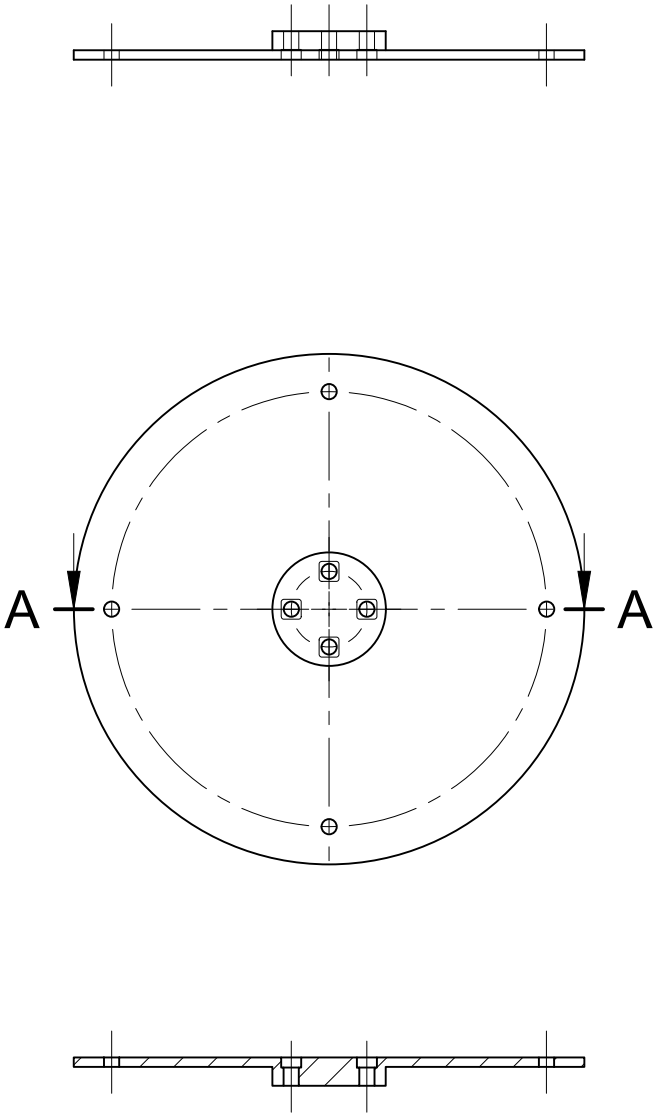

A-A

ISO 2378-mK
ISO 8015

Dept.	Technical reference	Created by	Approved by	
DeMec		Ricardo Carvalho 11/09/2023		
		Document type	Scale	
			1:4	
		Title	Paper Size	
		Cutting Subsystem Bottom Holding Disk	A4	
			Rev.	Material: C45 Steel / Sheet: 3/7

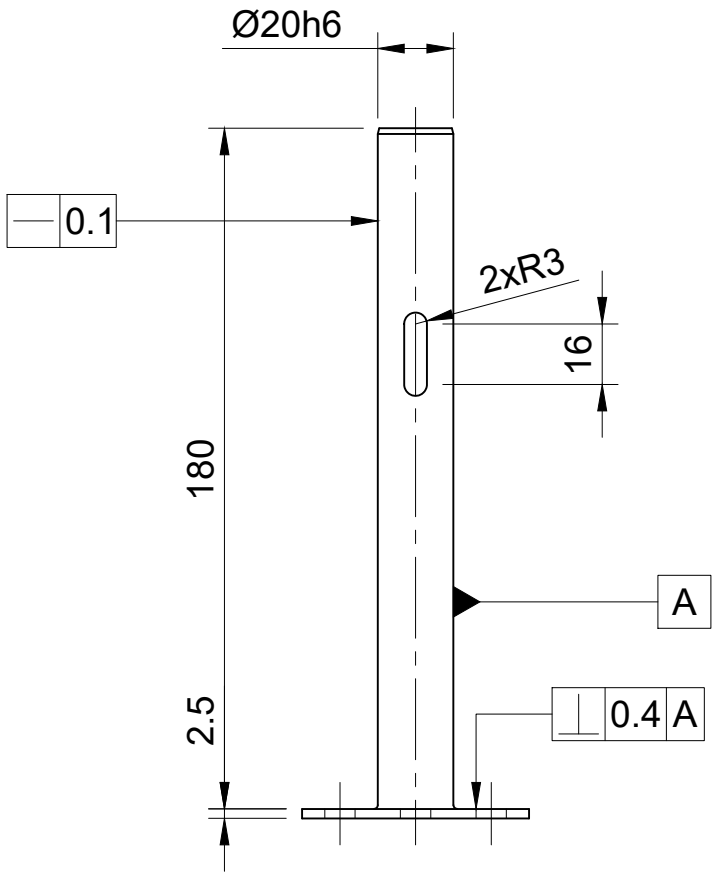

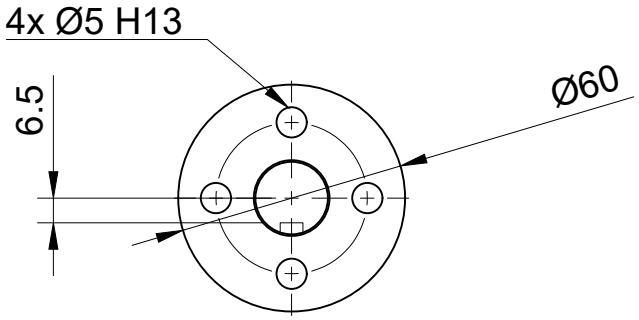

ISO 2378-mK
ISO 8015

Dept.	Technical reference	Created by	Approved by
DeMec		Ricardo Carvalho 11/09/2023	
		Document type	Scale 1:2
		Title: Cutting Subsystem Shaft 144	Paper Size: A4
			Rev. / Material: C45 Steel / Sheet: 4/7

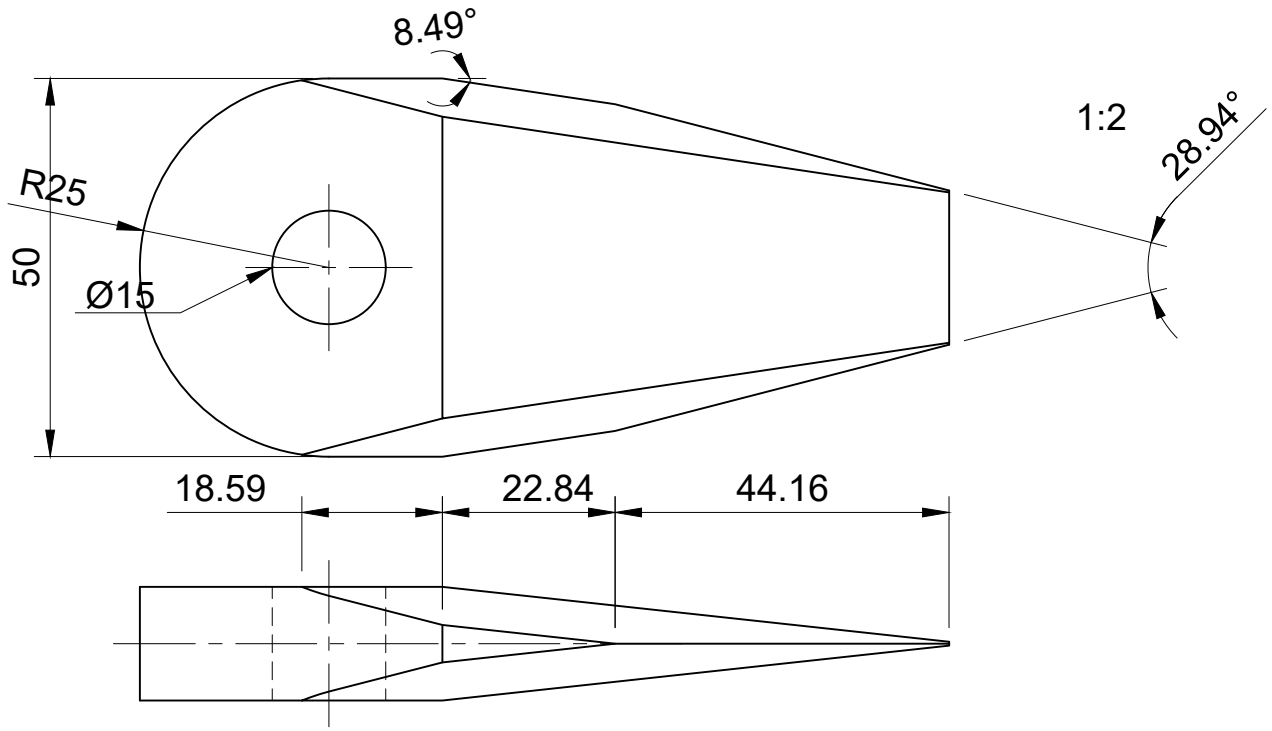

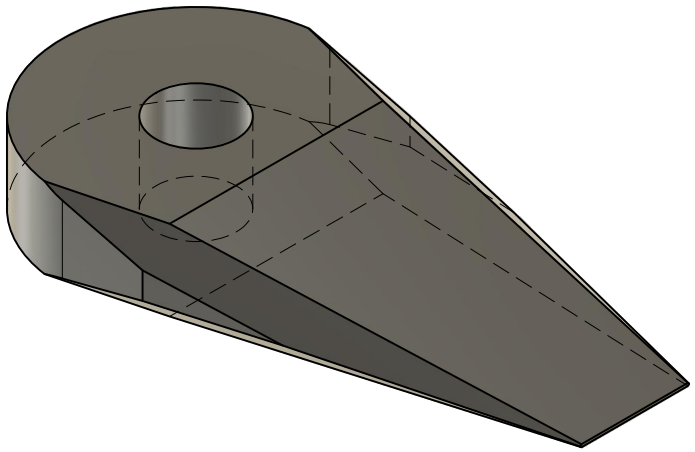

Isometric View

ISO 2378-mK
ISO 8015

Dept.	Technical reference	Created by	Approved by
DeMec		Ricardo Carvalho 11/09/2023	
		Document type	Scale 1:1
		Title: Cutting Subsystem Blade 145	Paper Size: A4
			Rev. / Material: W1 tool steel / Sheet: 5/7

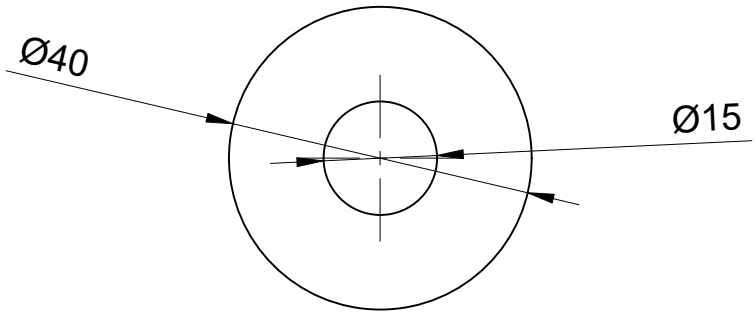

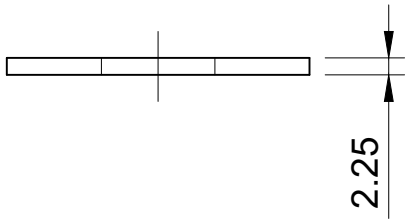

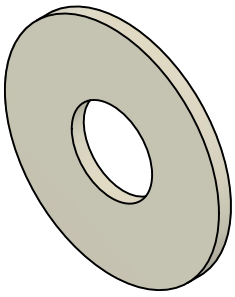

Isometric View

ISO 2378-mK
ISO 8015

Dept.	Technical reference	Created by	Approved by
		Ricardo Gomes de Carvalho 11/09/2023	
		Document type	Scale
			1:1
		Title	Paper Size
		Cutting Subsystem Washer 146	A4
			Rev. / Material: POM with PTFE / Sheet: 6/7

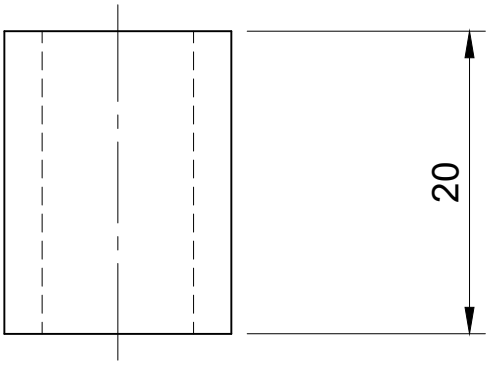

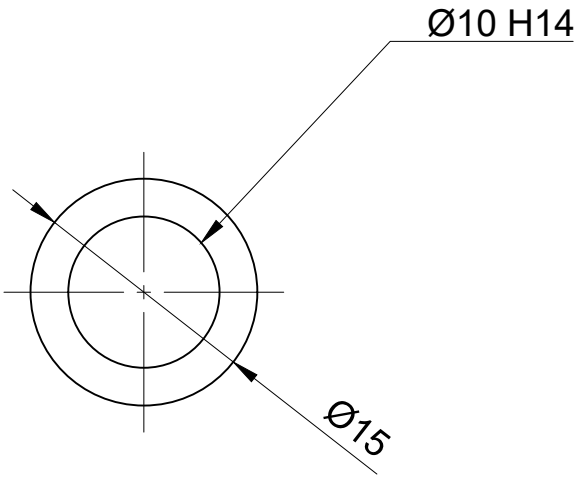

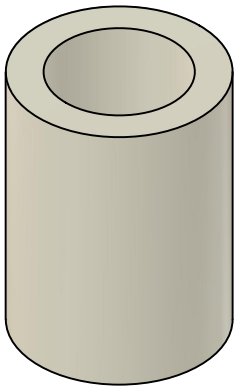

Isometric View

Dept.	Technical reference	Created by	Approved by
		Ricardo Gomes de Carvalho 11/09/2023	
		Document type	Scale
			2:1
		Title	Paper Size
		Cutting Subsystem Bushing 147	A4
			Rev. / Material: POM with PTFE / Sheet: 7/7

Appendix I

Cost Analysis

Table I.1: Cost of standardized components and branded components, in euros. Prices from Norelem unless specified on Observations column

Designation	**Quantity**	**Price (€/piece)**	**Total price (€)**	**Observations**
Cup square neck bolt DIN 603 M8x45-8.8	12	0.152	1.824	[1]
Hexagon nut DIN 982 M8-8	24	0.29	6.96	
Washer ISO 7089-8-200HV	48	0.13	6.24	
Hexagon Bolt ISO 4014 M8x45-8.8	12	0.26	3.12	
GM HPM3000B	1	268.32	268.32	[2]
TB 40-8M-20	1	22.87	22.87	[3]
TB 22-8M-20	3	15.38	46.14	[3]
TB taper bush 1610	1	6.47	6.47	[3]
TB taper bush 1008	3	4.5	13.5	[3]
Optibelt OMEGA 1728 D8M-HP 20 special belt	1	93.94	93.94	[4]
Parallel key A ISO/R 773 6x6x22	4	0.37	1.48	
Hexagon Bolt ISO 4017 M4x14-A2	8	0.18	1.44	[5]
Washer ISO 7089-4-A2	8	0.13	1.04	
Spring washer DIN 127 B V2 4-A2	8	0.0033	0.0264	[6]
Rivet nut with small countersunk head M4-A2	8	0.2545	2.036	[7]
Clevis pin with small head DIN 1434 A 12x35-A2	6	2.22	13.32	[8]
Spring cotter DIN 11024 2.5-1-A2	6	0.58	3.48	
Eye bolt DIN 444 B M12x50-A2	6	10.65	63.9	[9]
Hexagon bolt ISO 4014 M8x30-A2	24	0.52	12.48	[10]
Washer ISO 7089-8-A2	44	0.13	5.72	
Hexagon nut DIN 982 M8-A2	24	0.63	15.12	
TL Electrak GX D48N05A5-02M0NN-AMM	2	565.23	1130.46	[11]
Clevis pin without head ISO 2340 A 12x55-A2	4	2.22	8.88	[12]
Elastic ring DIN 471 V2 12x1-A2	8	0.45	3.6	
Elastic ring DIN 471 V2 15x1-A2	4	0.66	2.64	
Hexagon bolt ISO 4014 M5x30-A2	4	0.33	1.32	
Washer ISO 7089-5-A2	8	0.13	1.04	
Hexagon nut DIN 982 M5-A2	4	0.29	1.16	
Screw ISO 7380-1 V2 M8x10-A2	4	0.47	1.88	
Hexagon bolt ISO 4014 M10x35-A2	12	0.75	9	
Spring washer DIN 127 B V2 10-A2	12	0.0183	0.2196	[6]
Washer ISO 7089-10-A2	24	0.15	3.6	
Hexagon nut DIN 982 M10-A2	12	0.9	10.8	
Bearing Unit SKF FYTB 20 TF	6	23.44	140.64	[13]
Cover SKF ECY 204	3	3.71	11.13	[14]
		Total (€)	1915.8	

[1] Al Metal, Lda, minimum order 100 pieces https://www.parafusos-online.com/

[2] https://www.goldenmotor.com/

[3] Not from Optibelt, but from Norelem as standard components

[4] Rough estimate since it is a special length, from SLS bearings https://shop.slsbearings.com/sg/optibelt-1800-d8m-20-omega-double-timing-belt.html

[5] M4x14 not found, but the sizes above and below cost the same and M4x12 can also be used

[6] AI Metal, Lda, minimum order 500 pieces https://www.parafusos-online.com/

[7] AI Metal, Lda, minimum order 250 pieces https://www.parafusos-online.com/

[8] Stainless steel outside Fabory not found, normal steel price inserted

[9] Length not available, longer of 75 mm can be used

[10] Length not available, length of 35 mm used

[11] Price on Appendix F

[12] Not found online, assumed as the same price as DIN 1434

[13] Taken from SP-Spare Parts' website https://www.sp-spareparts.com/en/p/fytb20-tf-skf?_q=FYTB%2020%20TF

[14] Taken from RS's website https://pt.rs-online.com/web/p/rodamientos-de-insercion/3398849?gb=s